THE THERAPEUTIC POTENTIAL OF RHO GTPASE INTERVENTION

BY

AMY FRIESLAND

JULY, 2013

DIRECTOR: DR. QUN LU

DEPARTMENT OF ANATOMY AND CELL BIOLOGY

Small GTPases of the Rho family are well established regulators of critical cellular functions including cytoskeletal remodeling, motility, vesicle trafficking and cell cycle control. Additionally, aberrant signaling and/or regulation of Rho proteins have been implicated in various human pathologies. For these reasons, there is increasing interest in Rho GTPases as targets for therapeutic intervention. In the current study, we aim to understand Rho GTPase involvement in neuronal degeneration associated with clinical cisplatin use. Using a mouse model of cisplatin-induced peripheral neuropathy (CIPN) and a primary neuronal culture system we investigated how RhoA pathway suppression concomitant with cisplatin could prevent neuronal damage. Additionally, in order to fill a large gap in the field of Rho GTPase study and to allow us to further understand Rho GTPase cross regulation, we sought to identify and characterize novel small-molecule inhibitors of the Rho family member Cdc42.

Using our CIPN mouse model, we examined RhoA pathway suppression with LM11A-31, a p75 neurotrophin receptor ligand mimetic, on both RhoA signaling and neuronal damage associated with cisplatin application. We determined that cisplatin-induced decreases in peripheral nerve sensitivity and abnormal peripheral nerve morphologies could be prevented with concurrent use of LM11A-31 and cisplatin. Additionally, cisplatin-induced increases in RhoA activity and expression could be inhibited by LM11A-31. Furthermore, *in vivo* and *in*

vitro studies demonstrate that cisplatin can also reduce SHP2 phosphorylation, which in turn, can be alleviated by LM11A-31. These studies demonstrate the importance of RhoA signaling in the development of CIPN and highlight its usefulness as a potential therapeutic target.

To discover potential specific Cdc42 inhibitors, we applied high-throughput screening to identify compounds that are able to target the interaction between Cdc42 and its specific guanine nucleotide exchange factor, intersectin. ZCL278 was found to inhibit Cdc42 activity, expression, and directly bind to Cdc42. Additionally, ZCL278 inhibits Cdc42-mediated microspike formation, and disrupts GM130-docked Golgi structures. ZCL278 also suppresses Cdc42-mediated neuronal branching as well as cell motility and migration without disrupting cell viability. Therefore, ZCL278 is a novel small-molecule modulator of Cdc42 that will open the door to further study of Cdc42-mediated signaling pathways.

THE THERAPEUTIC POTENTIAL OF RHO GTPASE INTERVENTION

A Dissertation
Presented to
The Academic Faculty of the Department of
Anatomy & Cell Biology

by

Amy Michelle Friesland

In Partial Fulfillment
of the Requirements for the Degree
Doctor of Philosophy in Anatomy & Cell Biology

East Carolina University
July, 2013

THE THERAPEUTIC POTENTIAL OF RHO GTPASE INTERVENTION

by

Amy Michelle Friesland, B.S.

APPROVED BY:

DIRECTOR OF DISSERTATION: _____
Qun Lu, Ph.D.

COMMITTEE MEMBER: _____
Yan-Hua Chen, Ph.D.

COMMITTEE MEMBER: _____
Ann O. Sperry, Ph.D.

COMMITTEE MEMBER: _____
John P. Smith, Ph.D.

COMMITTEE MEMBER: _____
Art Rodriguez, Ph.D.

CHAIR OF THE DEPARTMENT OF ANATOMY & CELL BIOLOGY:

_____
Cheryl B. Knudson, Ph.D.

DEAN OF THE GRADUATE SCHOOL:

_____
Paul Gemperline, Ph.D.

DEDICATION

To my parents Cindy and Dwayne Laws

and Johnnie and Leslie Friesland

ACKNOWLEDGEMENTS

First and foremost, I would like to express my immeasurable gratitude for the unwavering love, support and encouragement from my wonderful family. I consider myself the luckiest girl in the world to have been born to such amazing parents, Johnnie Friesland and Cindy Laws, but even luckier to have them bring the best "bonus" parents, Leslie Friesland and Dwayne Laws, into my life. My grandparents Ned and Billie Callahan and Lou Jane and John Friesland have also done so much to shape me into the person I am today. I will forever be grateful for all the memories we have made together and all the important lessons they have taught me through the years. I am incredibly grateful for my great-grandmother Verdie Elliot, whose kindness, love and independence are an inspiration.

I would also like to thank my mentor, Qun Lu for allowing me to be a part of his laboratory for the past five years. He has taught and inspired me so much both inside and outside the realm of science. I have learned not only the importance of patience, perseverance and collaboration but also developed a passion for science and mentorship that I will carry with me always.

The faculty and staff of the Department of Anatomy and Cell Biology have contributed greatly to my experience as a graduate student and I will always look back fondly at all the camaraderie and time we spent together at departmental functions. I would like to thank Ann Sadler and Crystal Hooper for all their hard work and help through the years. Also, I appreciate all the conversations and scientific expertise of Joani Zary Oswald, Beverly Jeansonne, and Christi Boykin. I would like to thank my precandidacy committee: Dr. David Terrian, Dr. Jian Ding, Dr. Ann Sperry, and Dr. Donald Fletcher for their support in the early days of my graduate

career. To my candidacy committee: Dr. Qun Lu, Dr. Yan-Hua Chen, Dr. Art Rodriguez, Dr. John Smith, and Dr. Ann Sperry I truly appreciate all of your support and time spent advising and encouraging me to think critically and scientifically. I would like to thank Dr. Cheryl Knudson for her advice and encouragement throughout the years.

I also wish to acknowledge Drs. Kori Brewer and Jitka Virag in the Department of Physiology for recognizing my potential when I was an undergraduate and encouraging me to pursue my Ph.D. Additionally, I really appreciate the time and experience of working with Dr. Daniel Moore, Dr. John Norbury, and Dr. Claire Ruffin from the Department of Physical Medicine and Rehabilitation on nerve conduction studies. I really value the collaborative spirit of Dr. Kathyrn Verbanac, Dr. Yaxue Zhao, and Dr. Huchen Zhou, and my experience working with them has shown me importance of combining skills and minds to meet important scientific goals.

Finally, to all the past and present graduate students in the Department of Anatomy and Cell Biology I am so glad that I can call you my friends. Dr. Sarah James, Dr. Sonja Bareiss, Dr. Kristjan Thompson, and Dr. Lilliana Mellor thanks for all the encouragement in the early days. To Dr. Wendy Lu, June Nopparat, and Nicole Devaul you all have been some of the best friends anyone could ask for, and I wish you all the best in all that you do.

TABLE OF CONTENTS

LIST OF FIGURES

LIST OF TABLES

LIST OF SYMBOLS AND ABBREVIATIONS

Aβ	Amyloid-beta
AD	Alzheimer's disease
AML	Acute myeloid leukemia
AngII	Angiotensin II
APP	Amyloid precursor protein
ApoE	Apolipoprotein E
AT1	Angiotensin II receptor type 1
BSA	Bovine serum albumin
CA	Constitutively active
CAD	Coronary artery disease
Cdc42	Cell division cycle 42
CIPN	Chemotherapy induced peripheral neuropathy
Cisplatin	*Cis*-diamminedichloroplatinum(II) (CDDP)
CLIP-170	Cytoplasmic linker protein 170
CNF	Bacterial cytotoxic necrotizing factor
CNS	Central nervous system
CSPG	Chondroitin-sulfate proteoglycans
d	Doublet

dd	Doublet doublet
DAD	Diode array detector
DIC	Differential interference contrast
DH	Dbl-homology domain
DHR	DOCK homology region domain
DIV	Days *in vitro*
DLC	Deleted in lung cancer
DMF	Dimethylformamide
DMSO	Dimethyl sulfoxide
DN	Dominant negative
DNA	Deoxyribonucleic acid
DRG	Dorsal root ganglion
DTT	Dithiothreitol
EB1/APC	End binding protein 1/adenomatous polyposis coli
EDG	Endothelial differentiation gene
EGF	Epidermal growth factor
EMT	Epithelial to mesenchymal transition
ENaC	Epithelial Na^+ channel
eNOS	Endothelial nitric oxide synthase

ERK	Extracellular-signal-regulated kinase
ERM	Ezrin/radixin/moesin
FGD1	Faciogenital dysplasia 1 protein
GAP	GTPase activating protein
GEF	Guanine nucleotide exchange factor
GDI	Guanine nucleotide dissociation inhibitor
GDP	Guanosine-diphosphate
GM130	Golgi matrix protein of 130 kDa
GTP	Guanosine-triphosphate
HPLC	High performance liquid chromatography
HTVS	High-throughput virtual screening
IQGAP	IQ motif containing GTPase activating protein
IRSp53	Insulin receptor substrate p53
ITSN	Intersectin
JNK	c-Jun N-terminal kinase
K_d	Dissociation constant
kDa	Kilodalton
KO	Knock-out
LARG	leukemia-associated Rho GEF

LDL	Low-density lipoprotein
LIMK	LIM(**L**in11, **I**sl-1 & **M**ec-3) kinase
LPA	Lysophosphatidic acid
MAG	Myelin-associated glycoprotein
mDia	Mammalian Diaphanous
MKL1	Megakaryoblastic leukemia 1
MLC	Myosin light chain
MLCP	Myosin light chain phosphatase
MLL	Mixed lineage leukemia
MTOC	Microtubule-organizing center
NCI-CTC	National Cancer Institute-Common Toxicity Criteria
NGF	Nerve growth factor
NMR	Nuclear magnetic resonance
NO	Nitric oxide
OCT	Optimal cutting temperature compound
OMgp	Oligodendrocyte-myelin glycoprotein
$P75^{NTR}$	P75 neurotrophin receptor
PAK	P21-activated kinase
Par	Partitioning defective

PBS	Phosphate-buffered saline
PDGF	Platelet-derived growth factor
PIP-5	Phosphatidylinositol 4-phosphate 5 kinase
pKa	Acid dissociation constant
PKN	Protein-kinase N
PLC	Phospholipase C
PMSF	Phenylmethanesulfonylfluoride
PNS	Peripheral nervous system
pRhoA	Phosphorylated RhoA
proNGF	Precursor to nerve growth factor
pSHP2	Phosphorylated SHP2
PVDF	Polyvinylidene difluoride
q	Quartet
Rac1	Ras-related C3 botulinum toxin substrate 1
RhoA	Ras homolog gene family, member A
ROCK	Rho-associated coiled-coil containing protein kinase, Rho kinase
ROS	Reactive oxygen species
s	Singlet
S1P	Sphingosphine -1-phosphat

SHP2	src homology 2 domain containing a non-transmembrane protein tyrosine phosphatase
SMC	Smooth muscle contraction
SP	Standard precision
SPR	Surface plasmon resonance
SRE	Serum response element
SRF	Serum response factor
t	Triplet
TNS	Total neuropathy score
tRhoA	Total RhoA
UV	Ultraviolet
VCA	Verprolin-homology central and acidic motif
VSMC	Vascular smooth muscle contraction
WASP	Wiskott-Aldrich syndrome protein
WAVE	WASP family verprolin-homologous protein

CHAPTER I: INTRODUCTION

A. The Rho Family of Small GTPases

Rho GTPases comprise a family of small GTPases (α subunits of G-proteins) within the larger Ras superfamily. RhoA, the first member of this subfamily, was identified in 1985 in an effort to identify Ras-related genes in Aplysia (Madaule and Axel, 1985). Since that time, at least 20 different proteins that belong to this family have been discovered (as reviewed by Vega and Ridley, 2008). Rho GTPases are present in all eukaryotic cells, typically small in size (20-30 kDa) and perform regulatory functions due to their intrinsic GTPase activity (as reviewed by Ellenbroek and Collard, 2007; Etienne-Manneville and Hall, 2002). Acting as a molecular switch, Rho GTPases cycle between an active GTP-bound state and an inactive GDP-bound state. Once bound by GTP, specific downstream effector proteins can transduce extracellular signals through a wide variety of membrane receptors including integrins, ion channels, G-protein coupled receptors, or growth factor receptors. Such signaling result in changes in a variety of cellular processes such as gene transcription, cell morphogenesis, vesicular trafficking, migration, and cell cycle control (as reviewed by Jaffe and Hall, 2005; Ellenbroek and Collard, 2007; Lu et al., 2009).

The activity of small GTPases is tightly controlled by both positive and negative regulators specific for each GTPase (Fig. 1.1). Guanine nucleotide exchange factors (GEFs) facilitate the exchange of GDP for GTP, thus activating the protein and allowing it to bind to effector molecules (as reviewed by Bustelo et al., 2007). To date, two families of GEFs (including over 70 total members) have been identified that activate Rho GTPases; these possess

either a Dbl-homology domain (DH) or a Dock Homology Region domain (DHR) (as reviewed by Cherfils and Zeghouf, 2013). On the other hand, GTPase-activating proteins (GAPs) maintain a basal level of protein activity by catalyzing GTP hydrolysis and returning the GTPase to its GDP-bound (inactive) conformation through a RhoGAP catalytic domain (as reviewed by Cherfils and Zeghouf, 2013; Lu et al., 2009; Ridley, 2006). Finally, guanine nucleotide dissociation inhibitors (GDIs) prevent GTPase cycling by either binding to the GTP-bound form and preventing hydrolysis or to the GDP-bound form thereby preventing activation by GEFs. Additionally, GDIs are also able to sequester Rho proteins in the cytosol by binding to the post-translationally added C-terminal isoprenyl lipids (geranylgeranyl or farnesyl) of the Rho GTPase, which are responsible for membrane anchoring (as reviewed by Cherfils and Zeghouf, 2013; Dransart et al., 2005). Due to the host of functions of Rho proteins and their presence in various cell types, their activation likely depends on a balance between the actions of the three types of regulators at specific cell sites (as reviewed by Ellenbroek and Collard, 2007).

Our current understanding of the biological functions of the most highly conserved Rho GTPase family members: RhoA, Rac1 and Cdc42, has been supported by several methods including the use of constitutively active (CA) and dominant negative (DN) Rho GTPase mutants. Early studies by Paterson et al. (1990) and Nobes and Hall (1995) in Swiss 3T3 fibroblasts revealed the critical importance of these proteins to cell morphology, an actin-mediated function. Those studies showed that constitutive activation of RhoA, Rac1, and Cdc42 resulted in the formation of stress fibers, lamellipodia, and filopodia, respectively (Fig. 1.2). Actin stress fibers consist of long actin filament bundles that extend across the cell and are linked to the extracellular matrix (as reviewed by Hall, 1998). Lamellipodia and filopodia/microspikes, on the other hand, are found in motile cells as either an actin meshwork at the leading edge or

protrusions of actin filament bundles from the cell surface, respectively (as reviewed by Ladwein et al., 2008). Importantly, the generation of several specific Rho GTPase knock-out (KO) mice has greatly contributed to our knowledge of the functions of these proteins *in vivo*. Both Rac-1 and Cdc42 knockout mice do not survive birth and demonstrate defective germ-layer formation and gross brain abnormalities, respectively (Sugihara et al., 1998; Garvalov et al., 2007). These models have illuminated crucial roles of Rho proteins in embryonic development and solidified their importance for cell migration and neuronal development.

B. RhoA

RhoA, a ubiquitously expressed member of the RhoA subfamily of Rho proteins, which also includes the highly homologous RhoB and RhoC, was the first described and is the most characterized. Primarily a cytosolic protein, RhoA interacts with a variety of downstream effectors including ROCK, PIP-5, citron, PKN, and rhotekin (Fig.1.3; Michaelson et al., 2001). The most prominent and understood targets of RhoA signaling include the serine/threonine kinases Rho-associated coiled-coil containing protein kinases I and II (ROCK I, also known as p160ROCK or ROKβ and ROCK II, also known as ROCKα; Matsui et al., 1996; Ishizaki et al., 1996). When activated, Rho-kinases can phosphorylate a variety of substrates including myosin light chain (MLC) phosphatase (Amano et al., 1996; Kawano et al., 1999), LIM kinases (LIMK) (Amano et al., 2001; Maekawa et al., 1999) and ezrin/radixin/moesin (ERM; Matsui et al., 1998) which facilitate actin-myosin contractility, stress fiber formation, and interaction with the plasma membrane, respectively. Additional roles of ROCK signaling include cell-cell adhesion, motility, and cell cycle regulation (Amano et al., 2000; Croft and Olson, 2006; Redowicz, 1999). Demonstrating the importance of the RhoA-Rho kinase pathway, deletion of either ROCK I or

ROCK II in mice is embryonic lethal and leads to a variety of pathological phenotypes including growth retardation, omphalocele, and open eyelids (Shimizu et al., 2005; Thumkeo et al., 2003).

An additional RhoA effector mDia1 (mammalian Diaphanous 1), a formin protein, is essential for nucleation and polarization of actin filaments (Fig. 1.3A). The formin family of proteins aid in actin polymerization by binding to the barbed ends of elongating filaments, protecting them from capping proteins, delivering monomers to growing filaments and producing long, unbranched, actin filaments (Evangelista et al., 2003; Goode and Eck, 2007; Zigmond, 2004). Additionally, mDia1 can bind microtubules through its association with microtubule end capping protein EB1/APC and promote stabilization (Wen et al., 2004). Due to its influence on both actin filament nucleation and microtubule stabilization RhoA is, therefore, able to coordinate and modulate cytoskeletal rearrangements to facilitate stress fiber formation in migrating cells.

Currently, our understanding of RhoA signaling has been significantly aided by the discovery, development and utilization of activators and inhibitors (Table 1.1). For instance, the soluble serum factor lysophosphatidic acid (LPA), one of the earliest described activators of RhoA (Ridley and Hall, 1992) is a G-protein coupled receptor agonist that facilitates RhoA activation through the $G_{\alpha 12/13}$ subunits (Fromm et al., 1997; Gohla et al., 1998; Kranenburg et al., 1999) and leads to gene transcription involving serum response factor (SRF) and its co-activator megakaryoblastic leukemia 1 (MKL1). Sphingosine-1-phosphate (S1P), another serum lysophospholipid, also promotes RhoA activation via the EDG receptor (EDG 3 or EDG 5) which also couples to $G_{\alpha 12/13}$ to regulate serum response element (SRE) mediated transcription (Hill et al., 1995; Buhl et al., 1995; Lee et al., 1998). However, a major drawback of use of LPA or S1P lies in their lack of specificity, as both promote activity of other proteins such as Ras, c-

Jun N-terminal kinase (JNK), extracellular-signal-regulated kinase (ERK), and phospholipase C (PLC) (as reviewed by Takabe et al., 2008). Although still indirect, calpeptin has emerged as a more specific method to induce RhoA activation. Through SHP2 (src homology 2 domain containing a non-transmembrane protein tyrosine phosphatase) tryosine phosphatase inhibition, calpeptin maintains negative RhoA regulator p190RhoGAP in an inactive state thus promoting accumulation of GTP-RhoA (Schoenwaelder et al., 2000).

Importantly, a variety of inhibitors have been identified that allow further dissection of signaling both upstream and downstream of RhoA activation (Table 1.2). In early studies of Rho GTPase signaling the exoenzyme C3 transferase from *Clostridium botulinum*, which ADP-ribosylates asparagine 41 in the RhoA effector binding domain, was frequently employed as a specific and direct inhibitor of Rho activation (Kumagai et al., 1993). However, C3 transferase has poor cell permeability which results in the need for higher concentrations and longer incubation times, which in turn can disrupt basic cellular functions. Since then, several indirect, but specific, inhibitors such as the ROCK antagonists fasudil (Nagumo et al., 2000) and Y-27632 (Ishizaki et al., 2000; Narumiya et al., 2000) have been developed. Both Y-27632 and fasudil target the ATP-dependent kinase domains of ROCK, are cell permeable, and have high affinities for ROCK with K_i's of 200-300 nM (Ishizaki et al., 2000; Narumiya, Ishizaki and Uehata, 2000) and 330 nM (Uehata et al., 1997), respectively. Interestingly, Evelyn et al. (2007) identified the small molecule CCG-1423 as a potent inhibitor of MKL/SRF-dependent transcription that is stimulated by $G_{\alpha 12/13}$. Upstream of RhoA, p75 neurotrophin receptor ($p75^{NTR}$) signaling facilitates the release of prenylated RhoA from Rho-GDI, thus inducing its activation (Yamashita and Tohyama, 2003). LM11A-31, a $p75^{NTR}$ ligand mimetic of the nerve growth factor (NGF) loop 1 in the $p75^{NTR}$ binding domain, has recently been shown to be an inhibitor of RhoA-

mediated signaling pathways and will be further discussed in this dissertation (James et al., 2008; Massa et al., 2006).

Aberrant RhoA activity has been implicated in a wide variety of human diseases and disorders. Extensive clinical and experimental studies have provided compelling evidence for the importance of RhoA/ROCK pathways in cardiovascular disease. First, vasoactive agonists such as angiotensin II (Ang II) can activate RhoA/ROCK signaling pathways and modulate both contractility and vascular tone (Funakoshi et al., 2001; Guilluy et al., 2010). Specifically, ROCK regulates phosphorylation of MLC, a key event in the regulation of vascular smooth muscle cell (VSMC) contraction, by both inhibition of MLC phosphatase (MLCP) and direct phosphorylation of MLC (Kimura et al., 1996). Moreover, through MLCP inhibition, ROCK is able to contribute to Ca^{2+} sensitization of smooth muscle contraction (SMC) (Amano et al., 1996).

Due to these roles within VSMCs, ROCK signaling in arterial hypertension has been widely studied and targeted therapeutically. Hypertension is characterized by increased arterial pressure resulting from increases in contractility and vascular tone as well as remodeling within the arterial wall. In addition to the aforementioned roles within VSMC's, Rho kinase has been shown to inhibit production of the potent vasodilator, nitric oxide (NO), by negatively regulating endothelial nitric oxide synthase (eNOS) expression through disrupted eNOS mRNA stability during hypertensive states (Laufs and Liao, 1998; Takemoto et al., 2002). Clinically and experimentally, RhoA/ROCK pathways have been demonstrated to be upregulated as a result of hypertension in human patients (Masumoto et al., 2001) and animal models (Moriki et al., 2004; Mukai et al., 2001). Importantly, Uehata et al. (1997) showed that Y-27632 administration to renal hypertensive, deoxycorticosterone-acetate/salt treated and spontaneously hypertensive rats

could lower blood pressure. Since those early studies, researchers have begun to take a more in depth look at events upstream of RhoA using angiotensin II-induced hypertensive rats. Results showed that Y-27632 could potently promote vasodilation in hypertensive animals verses non-hypertensive animals (Chitaley et al., 2001). Additionally, blockade of the Ang II receptor, receptor type 1 (AT1), could prevent RhoA/ROCK upregulation in experimental models of hypertension (Kataoka et al., 2002). In humans, fasudil infusion was shown to be able to decrease vascular resistance and increase forearm blood flow in hypertensive patients, further implicating ROCK in clinical hypertension (Kishi et al., 2005).

Atherosclerosis, a progressive and chronic process that is characterized by vascular wall inflammation and fibrosis as well as lipid and macrophage accumulation, has also been critically linked to ROCK activity. First, ROCK has been implicated in the inflammatory process of atherosclerosis due to its ability to downregulate eNOS. Interestingly, in a porcine IL-1β-induced atherosclerosis model, long-term oral administration of fasudil was able to promote regression of coronary stenosis (Shimokawa et al., 2001). Additional work in mice with defective LDL-receptors that were administered a high cholesterol diet showed that Y-27632 could limit atherosclerotic plaque development (Mallat et al., 2003). Other mouse models of accelerated atherosclerosis, specifically apolipoprotein E (ApoE)-deficient mice, showed increased ROCK-mediated smooth muscle contraction within the aorta as well as increased phosphorylation of ERM, a major effector of ROCK activation, in atherosclerotic plaques (Rekhter et al., 2007). Fasudil treatment, within ApoE-deficient mice, was able to decrease both arterial thickness and macrophage accumulation in atherosclerotic lesions (Wu et al., 2009). In human patients with coronary artery disease (CAD), correlations between impaired endothelial cell function and increased ROCK activity have been documented (Nohria et al., 2006). Oral administration of

Rho kinase inhibitor fasudil in these patients resulted in significant reduction in both Rho kinase activity (~59%) and endothelium-dependent vasodilation, but not in healthy patients. Such findings further support RhoA/ROCK signaling as a significant therapeutic target in cardiovascular disease, and impart more strength for their clinical use.

In addition to the cardiovascular system, RhoA has clearly been demonstrated to play a critical role in neurological problems. RhoA is highly expressed throughout the nervous system and is present in both glial and neuronal cell populations (Suidan et al., 1997). RhoA/ROCK signaling has been established as a negative regulator of neuritogenesis (Da Silva et al., 2003; Kozma et al., 1997) and synaptic plasticity (Govek et al., 2004; Van Aelst and Cline, 2004). Due to these negative effects on neuronal development and stability, many studies support RhoA pathway inhibition to promote recovery for traumatic brain and spinal cord injury, stroke, and even Alzheimer's disease. Specifically, in rats with experimental spinal cord injuries, the significantly increased RhoA mRNA and protein expression in neurons, astrocytes, and oligodendrocytes (Dubreuil et al., 2003) due to injury could be reduced by both Y-27632 and fasudil administration (Hara et al., 2000; Sung et al., 2003). Although the precise role that RhoA plays remains elusive, we do know that during the secondary phase of neuronal injury many growth inhibitory signals converge on RhoA/ROCK and inhibit the regenerative ability of damaged neural tissue. Some of these factors include the myelin-associated inhibitors Nogo (Chen et al., 2000b), myelin-associated glycoprotein (MAG; McKerracher et al., 1994) and oligodendrocyte-myelin glycoprotein (OMgp; Wang et al., 2002) as well as chondroitin-sulfate proteoglycans (CSPGs); the glial scar-associated inhibitors which are up-regulated in reactive astrocytes (Gopalakrishnan et al., 2008). In addition, other studies suggest inflammatory events including leukocyte and endothelial T-cell migration can occur through Rho-dependent

mechanisms (Etienne et al., 1998; Adamson et al., 1999) and contribute to secondary injury. Furthermore, work by Honing et al. (2004) demonstrated that Y-27632 treatment could prevent RhoA-mediated migration and adhesion of monocytes across brain endothelial cell monolayers (Honing et al., 2004).

Interestingly, previous work in our laboratory has suggested a novel role of RhoA in chemotherapy-induced neurotoxicity. Clinically, neuropathy associated with platinum-based anti-neoplastic drug use is a common, debilitating and dose limiting problem. However, because neurons are not a mitotic population, cell cycle-dependent apoptotic mechanisms do not explain platinum-based neurotoxicity. *In vitro* studies showed distinct and significant neurite retraction in primary cortical/hippocampal cultures treated with cisplatin (James et al., 2008). Additionally in these cultures, upstream inhibition of RhoA with LM11A-31 prevented cisplatin-induced increases in GTP-bound RhoA and neurodegeneration. James et al. (2010) also demonstrated that ROCK inhibition with Y-27632 could successfully promote recovery in a mouse model of cisplatin-induced peripheral neuropathy (CIPN). A more precise role of RhoA in a CIPN model focusing on prevention rather than recovery, will be addressed in greater detail in Chapter II.

Although no specific mutations have been identified in any Rho protein in association with cancer, RhoA has been shown to be deregulated in leukemia, breast, lung, colon, gastric, bladder and testicular cancers. Considering that the cellular functions of RhoA correspond to several processes required for tumor formation and progression including cell survival, proliferation, and regulation of migration, it is not unexpected to find aberrant Rho protein activity in human cancers. Often this deregulation occurs at the level of activation or expression and is often due to alterations in the expression or activity of downstream effectors or other regulators of RhoA. For example, the specific RhoA GEF LARG (leukemia-associated Rho

GEF), originally isolated from a patient with acute myeloid leukemia (AML), has been identified as a fusion partner of the MLL protein (mixed lineage leukemia; Kourlas et al., 2000; Reuther et al., 2001). Through the MLL and LARG fusion, LARG becomes truncated upon chromosomal translocation which can then promote RhoA signaling pathways and leukemia development (Reuther et al., 2001). Another RhoA GEF, GEFH1, has been shown to be transcriptionally activated by induction of mutant p53 proteins. Through this activation, GEFH1 then promotes accelerated tumor cell proliferation in several cancer cell lines (Mizuarai et al., 2006). Such results suggest that increased RhoA activity may contribute to both invasion and metastasis, as well as promote growth of p53 tumors. GAPs, such as DLC-1 and DLC-2 (deleted in lung cancer 1 and 2), which are known to promote GTP hydrolysis in RhoA, have been found to be genomically deleted in primary breast tumors (Yuan et al., 2003) or downregulated in hepatocellular carcinomas (Ching et al., 2003). Reduction in RhoA-specific GAP activity would then lead to increased overall levels of RhoA activity. Downstream RhoA effectors such as ROCK have also been demonstrated to be altered in several cancer types. For example, ROCK has been demonstrated to be overexpressed in osteosarcoma (Liu et al., 2011), hepatocellular carcinoma (Wong et al., 2009), breast (Lane et al., 2008), testicular (Kamai et al., 2004), colon (Vishnubhotla et al., 2007) and bladder (Kamai et al., 2003) cancers and is highly correlated with increased tumor grade, progression and poor survival.

Thus, it is clear that proper regulation and activity of RhoA is vital to normal cellular function and that aberrant regulation and/or signaling to a variety of effectors can result in a wide array of pathology. Importantly, abundant data support pharmacological intervention of the RhoA pathway as a plausible method to hinder RhoA-mediated dysfunction in both *in vitro* and *in vivo* models.

C. Rac1

Rac1, a second prominent Rho protein, is ubiquitously expressed as compared to its other family members Rac2 and Rac3, which are predominately expressed in hematopoietic cells and neurons, respectively (Didsbury et al., 1989; Malosio et al., 1997). Like RhoA, Rac1 is localized mainly within the cytoplasm until activation induces its translocation to the plasma membrane where interaction with effector proteins and induction of subsequent downstream signaling cascades can occur (Wennerberg and Der, 2004). Through its primary downstream effectors P21-activated kinase 1 and 2 (PAK1/2), WASP family verprolin-homologous protein (WAVE) and to a lesser extent IQGAP, Rac1 can modulate cytoskeletal rearrangements which results in the formation of the motile structures known as lamellipodia or membrane ruffles as well as promotes cell adhesion, proliferation, and survival (Fig. 1.3B). PAK1/2 has an N-terminal GTPase binding domain which, when bound by activated (GTP-bound) Rac1, relieves autoinhibition and enhances kinase activity (Frost et al., 1996). PAK1/2 can then affect cytoskeletal organization by phosphorylating various proteins including MLCK, LIMK, cortactin, and components of Arp2/3 actin nucleation complex (Edwards et al., 1999; Vadlamudi et al., 2004). Regulation of actin polymerization through the Arp2/3 complex also occurs via mDia2 (Lammers et al., 2008) and WAVE, which lacks a GTPase binding domain and requires a complex of Rac1 and an adaptor molecule, IRSp53, to be activated (Miki et al., 2000). The C-terminal verprolin-homology central and acidic (VCA) motif of the WAVE/Rac1/IRSp53 complex can then promote binding to the Arp2/3 complex and subsequent actin network formation (Suetsugu et al., 2006). IQGAP, a Rac1 effector and actin-binding protein, is enriched at the leading edge of migrating cells (Bashour et al., 1997). In addition to its interaction with actin, IQGAP also binds cytoplasmic linker protein 170 (CLIP-170) which accumulates at the

plus ends of growing microtubules at the polarized leading edge of lamellipodia in migrating cells (Fukata et al., 2002).

Unlike RhoA, where a multitude of activators and inhibitors are available to study related signaling pathways, much of our understanding of Rac1 has come from *in vitro* studies using either dominant negative (DN) or constitutively active (CA) mutant cell lines or *in vivo* knockout models. Complete Rac1 knockout is lethal early in embryonic development (E8.5), displaying defective germ-layer formation and highlighting the importance of Rac1 signaling pathways in development (Sugihara et al., 1998). Inducible, cell-type-specific *rac1* gene knockouts have further expanded our knowledge and alleviated some of the limitations of DN/CA *in vitro* studies. Some of these studies have revealed the importance of Rac1 in central nervous system myelin sheath formation (Thurnherr et al., 2006), in hair follicle integrity (Chrostek et al., 2006), and in dendritic cell antigen presentation to T-cells (Benvenuti et al., 2004). The selection of Rac1 activators (Table 1.1) has been and remains limited to PDGF and EGF (Ridley et al., 1992), neither of which are specific nor direct stimulators of activity, making data resulting from their use difficult to interpret. However, a major step forward in studies of Rho GTPase signaling came with the development of NSC23766, a specific and direct Rac1 inhibitor (Gao et al., 2004). NSC23766 is a first-generation small molecule inhibitor which disrupts Rac1's ability to bind to Rac1-specific GEFs Trio and Tiam1 without interfering with RhoA or Cdc42 activity (Table 1.2). Importantly, this molecule has opened the door for the development of new small molecule inhibitors targeting the Rho GTPase pathway that could be used to target Rho proteins directly in various pathological situations.

As expected, due to its roles in a multitude of biological processes, Rac1 is known to contribute to pathological conditions such as hypertension, mental retardation, neurodegenerative

disorders, as well as several cancer types. Hypertension, a leading contributor to cardiovascular mortality, is characterized by increased sensitivity of blood pressure to salt. Interestingly, Shibata and colleagues (2011) recently showed that a high salt diet can activate Rac1 in the kidneys of a salt-sensitive hypertensive rat model. In addition, inhibition of Rac1 with NCS23766 prevented hypertension and renal damage associated with increased salt loading (Shibata et al., 2011). Also, Rac1/WAVE signaling has been implicated in the regulation of the epithelial Na^+ channel (ENaC), which is a major effector impacting systemic blood pressure and volume, and is responsible for Na^+ reabsorption in the aldosterone-sensitive nephron. Data revealed that Rac1/WAVE, but not Cdc42/WASP, was able to increase ENaC activity and these elevations could be decreased with the addition of NSC23766 (Karpushev et al., 2011). These results highlight the importance of Rac1 in cardiovascular disease as well as lend support to the use of NSC23766 for therapeutic intervention.

Rac1 is also gaining increasing attention for its involvement in several types of neurological problems. First, several studies have suggested important roles for Rac1 in the development of Alzheimer's disease (AD). In human patients, Rac1, along with increased cytoskeletal abnormalities, were shown to be increased in those with AD versus age-matched controls (Zhu et al., 2000). It has also been suggested that active Rac1, acting as a important component in amyloid - beta (Aβ) -induced reactive oxygen species (ROS) production, may aggravate AD (Lee et al., 2002). Other studies demonstrate that Rac1 may modulate Aβ levels by altering γ-secretase activity, a critical factor in amyloid precursor protein (APP) cleavage (Désiré et al., 2005; Gianni et al., 2003). Interestingly, dominant negative Rac1 mutants (COS-7 cells) or NSC23766-treated hippocampal neurons show reduced γ-secretase activity as well as decreased APP protein and mRNA levels (Boo et al., 2008; Wang et al., 2009).

Aside from AD, a possible role for Rac1 in depression and stress-related disorders has recently emerged. In rodent models, chronic stress (depression) induces functional and structural plasticity in several brain regions, specifically within the nucleus accumbens, the brain's reward center. As Rac1 is a well established modulator of synaptic structure, Golden and colleagues (2013) investigated its role in depression-induced synaptic remodeling in both animal models and post-mortem patients with clinically diagnosed major depressive disorder. Their work demonstrated a reduction in Rac1 expression following chronic stress in both animals and humans and, at least in rodents, stress resulted in the formation of immature stubby excitatory spines. Moreover, overexpression of constitutively active Rac1 could reverse depression-related behaviors and reduce the density of immature spines in animal models (Golden et al., 2013).

Like other Rho proteins, deregulation of Rac1 can promote initiation and/or progression of various types of cancer. Analysis of malignant breast, colon and lung tissue has revealed overexpressed Rac1 protein levels compared to benign tissue (Fritz et al., 1999). Rac1b, a splice variant of Rac1 which exhibits accelerated GDP/GTP exchange and does not interact with RhoGDI, is overexpressed and promotes cellular transformation in breast and colon cancers (Schnelzer et al., 2000; Singh et al., 2004). In addition, increased expression of Tiam1, a specific Rac1-GEF, is strongly correlated with invasiveness and poor prognosis in breast tumors (Adam et al., 2001; Minard et al., 2004). Specifically, Tiam1 can promote epithelial to mesenchymal transition (EMT) due to its ability to modulate E-cadherin based cell-cell adhesions (Hordijk et al., 1997). Interestingly, NSC23766, which competes with Tiam1 for the Rac1-GEF binding site, has been shown to inhibit migration (Zuo et al., 2006) and slow breast cancer cell growth through induction of G1 cell cycle arrest (Yoshida et al., 2010). In addition, data also reveals that Rac1 effector PAK is overexpressed or hyperactivated in more than 50% of

human breast tumors (Balasenthil et al., 2004). Such an increase in activity of either PAK or IQGAP has been shown to promote migration, invasiveness and anchorage-independent growth (Lozano et al., 2008; Noritake et al., 2004; Vadlamudi et al., 2000).

Clearly, Rac1 has tremendous biological significance for both normal cellular functioning and in the development of human pathology and, like RhoA, is becoming an important target for therapeutic intervention in a variety of human conditions.

D. Cdc42

Cell division cycle protein 42 (Cdc42) was first identified and characterized in the yeast species *Saccharomyces cerevisiae* as a major regulator of cell polarity and budding (Johnson and Pringle, 1990). Since that time, Cdc42 has been shown to be highly conserved across species and integrally involved in establishment of polarity as well as cellular morphogenesis (Boureux et al., 2007; Nobes and Hall, 1995). Functionally, when compared to RhoA and Rac1, the Cdc42 subclass is seemingly more diverse. In addition to its most characterized role in the formation of filopodia via actin cytoskeleton modulation, Cdc42 also plays important roles in gene transcription, cell cycle progression, vesicle trafficking, cell polarity, cell adhesion and motility (Cerione, 2004; Hall, 1998; Johnson, 1999; Lamarche et al., 1996).

In order to accomplish this multitude of tasks, Cdc42 signals through several major downstream effectors including partitioning-defective proteins (Par6, Par3, Par2), Wiskott-Aldrich syndrome protein (WASP) and its common effectors with Rac1, PAK and IQGAP (Fig. 3C). WASP and its neuronal isoform N-WASP interact with active (GTP-bound) Cdc42 to modulate actin polymerization in a similar manner as Rac1 effector WAVE. Specifically, WASPs directly interact with both profilin, an actin-binding protein, and the Arp2/3 complex to

promote actin assembly and filopodia formation (Ma et al., 1998; Machesky and Insall, 1998; Rohatgi et al., 1999). Par proteins are well known regulators of cell division and Cdc42-mediated cell polarity (Gotta et al., 2001; Kay and Hunter, 2001). When activated, Cdc42 can regulate the formation of the Par3-Par6-aPKC (atypical protein kinase C) complex which is important in the establishment of polarity of epithelial cells undergoing cell migration (Lin et al., 2000) as well as mediating microtubule stabilization at the cell front and orienting the Golgi and microtubule-organizing center (MTOC) in cells undergoing directional migration (Etienne-Manneville and Hall, 2003).

The study of Cdc42 has greatly lagged behind that of RhoA and Rac1 due to early embryonic lethality in genetic models and deficiencies in the molecular tools available to further dissect Cdc42 signaling pathways. Studies performed with constitutively active and dominant negative Cdc42 mutants revealed that Cdc42 is critical for actin-based filopodia formation in embryonic stem cells, fibroblasts and neurons (Chen et al., 2000a; Yang et al., 2006). Complete deletion of Cdc42 was found to be embryonic lethal very early in embryogenesis (E6.5) and severely disrupted actin cytoskeletal organization due to improper actin polymerization (Chen et al., 2000a). Several conditional KO mice of Cdc42 have since been generated and demonstrate that, physiologically, the function of Cdc42 depends upon cell type and stage of development. For example, conditional deletion of Cdc42 within the brain, aside from also being lethal, leads to decreases in axon numbers and brain size and malformed axonal tracts (Garvalov et al., 2007).

Like Rac1, small molecules specifically targeting Cdc42 have been lacking and have greatly limited our understanding and ability to manipulate Cdc42. Although Cdc42 activation can be induced by epidermal growth factor (EGF), bacterial cytotoxic necrotizing factor (CNF) toxins, or bradykinin, these methods are either nonspecific for Cdc42 (EGF and CNF) or indirect

and not well understood (bradykinin, Table 1.1) (Flatau et al., 1997; Kozma et al., 1995; Ridley, Paterson, Johnston, Diekmann and Hall, 1992). Until recently the only available Cdc42 inhibitors were the small molecules secramine B (Pelish et al., 2006) and Pirl1 (more recently known as CASIN; Peterson et al., 2006), which were identified from a large scale screening of compounds capable of inhibiting membrane traffic or PIP2-induced actin polymerization, respectively. Although these molecules have been available for a considerable time, they have not been extensively cited (Pirl/CASIN: 3 publications; secramine B: 9 publications). The primary reason for this is probably due to the fact that the mechanisms are not well understood and the molecules are not easily acquired. Both compounds, although structurally unrelated, appear to promote sequestration of RhoGDI-bound Cdc42 thereby preventing its association with membranes and subsequent GTP binding (Pelish et al., 2006). Importantly, our laboratory has undertaken a rigorous screening of small molecules that potentially fit into the Cdc42 binding pocket critical for association with GEF's. Specifically, we targeted the interaction between intersectin (ITSN), a Cdc42 specific GEF and adaptor molecule linking endocytosis to WASP-induced actin polymerization, and the GEF binding pocket of Cdc42 (Smith et al., 2005). From this screening, a compound designated as ZCL278 was identified as the first specific and direct small molecule inhibitor of Cdc42 (Table 1.2; Friesland et al., 2013). This molecule has filled a critical gap in the Rho GTPase field and will allow us to better understand Cdc42 signaling in general as well as how it correlates to the pathological condition. ZCL278 will be discussed in great detail in Chapter III of this dissertation.

Cdc42, like other Rho proteins, contributes to the formation of several pathological conditions. First, it is known to regulate cardiovascular and blood functions. Conditional KO of Cdc42 in the mouse heart resulted in hypertrophy in response to both physiological and

pathological stimulation (Maillet et al., 2009). Cdc42 may also play an important role in microvascular permeability. Constitutive Cdc42 activation has been shown to impede microvascular endothelial barrier function following thrombin insult, and increased permeability (Kouklis et al., 2004). Interestingly, some research also suggests that this reduction in permeability may result from destabilization of cadherin complexes which in turn may modulate Cdc42 activation (Broman et al., 2006). In addition, Cdc42 overexpression, due to genetic Cdc42GAP deletion, has been shown to promote anemia and blood progenitors demonstrate impaired F-actin assembly, migration and adhesion (Wang et al., 2006).

As Cdc42 is a well documented positive regulator of neuritogenesis, it is not unreasonable to suspect its involvement in neurological disorders (Govek et al., 2005). In fact, intersectin (ITSN), a prominent Cdc42-specific GEF, has been linked to Down syndrome. The intersectin gene, like Down syndrome, localizes to chromosome 21 (21q22) and when mutated, it is associated with damaged vesicle trafficking and endocytic function, which also happens to be characteristic of early endocytic anomalies that are reported in Down syndrome brains (Guipponi et al., 1998; Hussain et al., 2001). Furthermore, Down syndrome is frequently associated with early incidence of AD. Specifically, in AD, abnormal and enlarged early endosomes are located at the site of β-amyloid (Aβ) peptide generation and processing of several proteins involved in AD (Cataldo et al., 2000). Thus, there may be an important link between Rho GTPase signaling, Down syndrome, and AD. Additionally, mutations in FGD1, a Cdc42-specific GEF, results in faciogenital dysplasia or Aarskog-Scott syndrome. This syndrome is characterized by short stature, mental retardation, as well as facial, skeletal, and urogenital abnormalities (Pasteris et al., 1994; Zheng et al., 1996). More recent studies have also implicated aberrant Cdc42 signaling in schizophrenia. In post mortem human brain specimens of subjects with schizophrenia, Cdc42

protein and mRNA expression was found to be decreased as compared to that of non-schizophrenic patients. Furthermore, spine density, which has long been attributed to Cdc42-mediated pathways, were found to be lower in specific layers within the dorsaolateral prefrontal cortex (Ide and Lewis, 2010).

Deregulation of Cdc42, like other Rho proteins, has been increasingly implicated in various cancer types and in processes that promote cancer development and progression such as transformation and metastasis. Cdc42 overexpression has been described in melanoma (Tucci et al., 2007), non-small lung (Liu et al., 2009), colorectal (Gómez Del Pulgar et al., 2008), breast (Fritz et al., 2002), and testicular (Kamai et al., 2004) cancers. Loss of function/deregulation in several Cdc42 GAPs have been observed in several cancer types. Specifically, DLC-1, a GAP that modulates GTP hydrolysis in both RhoA and Cdc42, was demonstrated to be down regulated in breast and lung cancers and was associated with increased cell proliferation and tumor formation (Durkin et al., 2007). In addition, overexpression of the Cdc42 GEF, ARHGEF9, is correlated with increased epithelial to meschymal transition (EMT) due to increased Cdc42 activation and reduced E-cadherin expression (Chen et al., 2010). Importantly, cells that have undergone transformation lack proper polarity. Importantly, the Par3/Par6/aPKC complex, which is associated with tight junction structures, is required for the maintenance of cell polarity (Joberty et al., 2000; Qiu et al., 2000). This process implicates the Cdc42-dependent activation of the Par3/Par6/aPKC complex as a possible contributor to malignant cell transformations. Although the oncogenic capabilities of Cdc42 are still under investigation, its involvement in cell division, cell cycle progression, and proliferation support its role in cancer formation, invasion and metastasis (Gjoerup et al., 1998; Yasuda et al., 2006; Hill et al., 1995; Debidda et al., 2005).

As an extremely diverse Rho protein, Cdc42 subclass is a very important regulator of a multitude of critical cellular processes, and as such, it is an important component in many clinical and developmental problems. Identification of small molecule modulators of Cdc42 will be extremely important for furthering our understanding of Cdc42 signaling and/or its mechanisms in human pathology.

E. Rho GTPase cross-talk

Multiple studies, beginning with work done by Ridley and Hall (1992), have demonstrated that cross-talk regulation or Rho GTPase regulation by other Rho GTPases, does occur. Nobes and Hall (1995) demonstrated that a hierarchical relationship between RhoA, Rac1, and Cdc42 exists in quiescent fibroblasts. Studies revealed that active Cdc42 can stimulate Rac1, activated Rac1 can stimulate RhoA, Cdc42 and RhoA antagonize each other, and RhoA can antagonize Rac1 (as reviewed by Giniger, 2002; Lim et al., 1996; Nobes and Hall, 1995; Sander et al., 1999). According to Guilluy et al. (2011), this cross regulation can happen in several ways: (1) through RhoGEFs or RhoGAPs, (2) through RhoGDIs, or (3) through regulation of downstream signaling pathways (Guilluy et al., 2011).

The best documented and well understood example of Rho protein crosstalk is the antagonistic relationship between RhoA and Rac1. During cell migration, high Rac1 activity is found at the leading edge of cells, while RhoA activity is high at the opposite, retracting tail of the cell (Ridley et al., 2003). This activity has been shown to be maintained by the fact that Rac1 can alter RhoGAP activity, thereby inhibiting RhoA (Nimnual et al., 2003). Additionally, the Rac1 effector PAK can impair activation of ARHGEF1, a RhoA GEF, thus adding another avenue for RhoA suppression (Rosenfeldt et al., 2006). Alternatively, RhoA can antagonize

Rac1 activity. For example, ROCK, the major RhoA effector, can inhibit Rac1 activity by phosphorylating and activating the Rac1-specific GAP protein, FilGAP, thus promoting increased GTP hydrolysis (Ohta et al., 2006). Cdc42 and RhoA are also spatially exclusive from each other and modulate actin assembly and organization in different ways suggesting a similar antagonistic relationship as that of Rac1 and RhoA (Benink and Bement, 2005). Although the exact mechanism remains unclear, probably due to difficulties and deficiencies in specific Cdc42 activators and inhibitors, some studies suggest that Abr, a Bcr-related protein that contains both a GEF domain, specific for RhoA, Rac1, and Cdc42, and a GAP domain specific for Rac1 and Cdc42 (Chuang et al., 1995) could be involved. Recent work demonstrated that Abr regulates Cdc42 inactivation and RhoA activation during wound healing in *Xenopus* oocytes, although the precise mechanism still remains unclear (Vaughan et al., 2011). Novel roles of RhoGDIs have recently been described as important contributors to Rho protein crosstalk. Interestingly, RhoGDI1, one of the three conventional RhoGDIs that universally bind most Rho GTPases, can protect prenylated Rho proteins from proteosome-dependent degradation (Boulter et al., 2010). Moreover, RhoGDI1 is expressed at levels that reflect the sum of all Rho family members, indicating that it may create competition between family members for binding (Michaelson et al., 2001). In fact, Boulter (2010) demonstrated that overexpression of one Rho protein could displace another from RhoGDI1, and facilitate their inactivation. Thus, it is clear that Rho GTPase cross talk can complicate our understanding and interpretations of Rho protein function, but also is likely very important for fine tuning of Rho GTPase-dependent signaling cascades.

F. Cisplatin

First described by Rosenberg in 1965, cisplatin or *cis*-dichlorodiammineplatinum (II) is currently one of the most effective and widely used chemotherapeutic agents. Since its approval in 1978 for clinical use, cisplatin has been a successful oncological tool to treat various forms of cancer including testicular, ovarian, cervical, bladder, head and neck, lung, breast, prostate and colorectal (Boulikas and Vougiouka, 2003; Higby et al., 1974; Wozniak and Blasiak, 2002).

Cisplatin is the first member of a family of platinum-based drugs which also includes carboplatin and oxaliplatin. Structurally, the cisplatin molecule is composed of a platinum ion surrounded by four ligands (two amines and two chlorides) arranged in a square, where both chloride ligands and both amine ligands are beside each other in *cis* formation (Fig. 1.5). The *trans* isomer of this molecule is clinically ineffective. As depicted in Fig. 1.5, the cytotoxic mechanism of cisplatin relies on its ability to form inter- and intra-strand DNA cross-links (Eastman, 1990; Zwelling and Kohn, 1979) . Due to the high concentration of chloride ions outside a cell, the cisplatin molecule is relatively stable. However, as cisplatin diffuses into a cell where chloride concentrations are much lower, the chloride ions are lost and quickly replaced by water molecules, rendering them a positive, reactive species that can form bonds with DNA bases (as reviewed by Boulikas and Vougiouka, 2003). Due to its *cis* geometry, the newly aquated cisplatin molecule can easily form cross-links on the same strand of DNA or on adjacent sites between two strands of DNA. 1,2-intrastrand cross-links between purine bases are the predominate product of cisplatin administration. These include 1,2-intrastrand cross-links between guanine (GpG) bases which form nearly 90% of the adducts and the less common 1,2-intrastrand cross-link between adenine and guanine (ApG) bases (Fichtinger-Schepman et al., 1985; Kelland, 1993). The formation of DNA cross-links lead to major local distortions of DNA

structure, causing the helix to bend and/or unwind and ultimately initiates the process of apoptosis (as reviewed by Wozniak and Blasiak, 2002).

Typically, a cisplatin treatment regimen involves a series of intravenous injections that are administered to the patient every three to four weeks at a dose range of 20-120 mg/m^2 which depends on the condition of the patient, type of cancer being treated and whether other cytotoxic agents are co-administered (Boulikas and Vougiouka, 2003). Although cisplatin has greatly enhanced our ability to treat several types of cancer it's cytotoxic effects are not limited to neoplastic tissue. Thus, a variety of side effects can limit a chemotherapy patient's ability to tolerate appropriate cisplatin regimens. Like many other chemotherapeutics which target rapidly dividing cells, cisplatin patients exhibit hair and weight loss, nausea and vomiting, immunosuppression, as well as reduced blood and platelet production in bone marrow (myelosuppression). In addition, more specific side effects include hearing loss (ototoxicity), kidney damage (nephrotoxicity), and neuronal damage (neurotoxicity; Florea and Büsselberg, 2011). To date, the best management strategies for these side effects are to either increase cisplatin clearance with increased intravenous hydration with the option of osmotic diuretics or to reduce dosage (Tsang et al., 2009).

Peripheral neurotoxicity is the most common dose-limiting problem associated with cisplatin therapy. Chemotherapy-induced peripheral neuropathy (CIPN) develops in up to 50% of cisplatin patients (Gutiérrez-Gutiérrez et al., 2010; Strumberg et al., 2002; van der Hoop et al., 1990a) and has the tendency to be more prevalent and/or severe in patients with compromised immune systems, diabetes or alcoholism (Schloss et al., 2013). Onset of CIPN often begins after cumulative doses of 300 mg/m^2 or more (Gregg et al., 1992) and initially presents in a "glove and stocking" fashion whereby symptoms begin in distal extremities and progress proximally (Jaggi

and Singh, 2012; Kaley and Deangelis, 2009). Typical CIPN symptoms include loss of vibration sense, paresthesias, numbness, tingling and burning sensations, decreased reflexes, and decreased sense of vibration (Beijers et al., 2012; McWhinney et al., 2009). Importantly, CIPN incidence and severity is dose dependent (Gregg et al., 1992) and following dose reduction or treatment cessation, neurological symptoms may gradually improve, persist for a short time, or can be permanent (van der Hoop et al., 1990b). Clinical CIPN diagnosis has been somewhat complicated by the lack of a universal toxicity scale. For example, neurologists tend to prefer the Total Neuropathy Score (TNS) which compiles information pertaining to motor, sensory and autonomic signs and symptoms, determination of vibration perception thresholds and electrophysiological examinations, while oncologists prefer the National Cancer Institute-Common Toxicity Criteria (NCI-CTC) which provides a much less detailed description of clinical and pathological aspects of CIPN (Schloss, et al., 2013). Therefore, this lack of standardization may result in the under diagnosis of CIPN. Mechanistically, it remains unclear how CIPN develops, as neurons are not a mitotic population of cells and the primary cisplatin targets are rapidly dividing cells. CIPN and a potential mechanism will be further addressed in Chapter II.

G. Rationale for current studies

Given that Rho proteins are involved in a variety of regulatory functions within cells and implicated in a multitude of human pathological conditions, they are very attractive, exploitable targets for drug discovery and intervention. Our laboratory has become increasingly interested in understanding the mechanisms involved in cisplatin-induced peripheral neurotoxicities. More precisely, our studies aim to elucidate how Rho GTPase involvement in CIPN contributes to

neurodegeneration and how targeted Rho protein suppression may be used as a preventative or recovery measure from cisplatin-induced neuronal damage.

Initially, data derived from primary neuronal cultures treated with several anti-neoplastic agents known to lead to clinical neurotoxicity, showed marked morphological abnormalities in actin-based structures (James et al., 2008). Other unpublished work in PC-3 cells, metastatic human prostate cancer cells, and PZ-HPV-7 cells, non-cancer human prostatic epithelial cells, revealed that cisplatin could also induce actin-mediated process retraction and induction of morphological disruption prior to apoptosis in non neuronal cell populations (Fig. 1.4; unpublished work, Friesland and Lu, 2010). In addition, our other preliminary experiments sought to understand if cisplatin targeted other actin-mediated events such as cytokinesis. Flow cytometry was used to analyze the cell cycle in H522 lung cancer cells that were synchronized in G_1/S phase by aphidicolin (Fig. 1.6B) or G_2/M phase with nocodozole (Fig. 1.6C). When released from arrest both aphidicolin and nocodozole-treated cells were able to progress through the cell cycle (Fig. 1.6D-E). However, synchronized H522 cells treated with cisplatin displayed a G_1 to S phase block, closely resembling aphidicolin-induced arrest, in both treatment groups (Fig. 1.7A-B). Furthermore, this effect was only minimally recoverable following release from cisplatin (Fig. 1.7C-D), indicating that cisplatin preferentially targets a G_1 to S progression and not the actin-mediated cytokinesis process. Taken together, these preliminary results supported the actin cytoskeleton as an alternate target of cisplatin, aside from the widely accepted DNA-targeting cisplatin mechanism (Fig. 1.5; unpublished work, Friesland and Lu, 2010).

Moreover, work by James et al. (2008) showed that inhibition of Rho pathway signaling with LM11A-31 ($p75^{NTR}$ ligand mimetic) and Y-27632 (Rho kinase inhibitor) could not only decrease RhoA expression but also reverse cisplatin-induced neurodegeneration in primary

neuronal cultures. These results led James et al. (2010) to develop an *in vivo* model of CIPN in order to test the efficacy of using Y-27632-mediated ROCK suppression as a possible recovery method from cisplatin-induced neurodegeneration. Their data reveal that 15 weeks of cisplatin treatment could generate measureable reductions in peripheral nerve sensitivity as well as disruptions in axonal integrity. Finally, during a one-month recovery period following cisplatin injections, mice that received Y-27632 were able to demonstrate both functional recovery in hindpaw sensitivity and increased levels of myelination as compared to mice receiving only saline during recovery (James et al., 2010).

Although this work supported RhoA activation as a major contributor to the development of CIPN, it did not definitively confirm it. Furthermore, it would be more clinically relevant to patients undergoing cisplatin chemotherapy to focus on preventing CIPN from developing during treatment. Therefore, in the current study, we sought to modify the previous CIPN mouse model into a preventative *in vivo* study whereby we targeted RhoA signaling upstream with high and low doses of LM11A-31 concomitant with cisplatin treatment. From these studies we were able to address questions of RhoA activity and expression due to treatment with cisplatin alone and with cisplatin plus LM11A-31, as well as analyze the morphology of peripheral nerve fibers more closely. In addition, through protein analysis of peripheral nerve tissue and collected primary neuronal lysates we were able to generate data implicating SHP2 phosphatase, which modulates tyrosine dephosphorylation of p190-B RhoGAP to activate RhoA (Kontaridis et al., 2004; Sordella et al., 2003), in the CIPN mechanism.

Finally, as it has been well established that Rho proteins significantly influence each other, it is critical for the understanding of CIPN as well as other pathological conditions, to investigate cross-talk between Rho family members. However, to date this has been a difficult

task to accomplish as small molecules targeting the Cdc42 subclass of Rho proteins has lagged far behind those of RhoA and Rac1. Therefore, we undertook a similar strategy as was used to develop the Rac1 inhibitor, NSC23766 (Gao et al., 2004), in order to identify the first specific and direct Cdc42 inhibitor, ZCL278. Our studies have confirmed that this cell-permeable, easily synthesized compound could decrease GTP-bound Cdc42 and microspike formation as well as inhibit Cdc42-dependent cell migration and neuronal branching and disrupt Golgi organization (Friesland et al., 2013). Our identification of ZCL278 will allow further dissection of Cdc42-mediated signaling pathways and mechanisms by which Cdc42 can contribute to cancer, CIPN, and other neurodegenerative problems, in addition to investigations of how it is able to influence and modulate other Rho family members.

H. Statement of Hypothesis and Specific Aims

Hypothesis

RhoA pathway suppression in conjunction with cisplatin chemotherapy will prevent neurodegeneration and provide an effective combinatorial therapy in a mouse model of cisplatin-induced peripheral neuropathy.

Specific Aim I:

To investigate RhoA expression and activity in the sural nerve of the cisplatin-treated mouse as well as the effects of a $p75^{NTR}$ ligand mimetic and upstream RhoA inhibitor, LM11A-31 as a method to prevent cisplatin-induced neurotoxicity.

Pharmacological treatments: Age matched (3 months) C57/BL6 mice were treated with either saline or cisplatin every 14 days for 10 weeks. In addition, two additional groups of cisplatin-treated mice received either a high or low dose of LM11A-31.

Von Frey/Semmes-Weinstein sensory threshold testing: Von Frey/Semmes-Weinstein monofilaments were used to stimulate the hindpaw and evaluate a threshold force needed to elicit a sensory response in animals in all four treatment groups.

Immunofluorescent analysis of peripheral nerve tissue: Harvested sural nerves were removed from each animal following 10 weeks of treatment. Frozen cryosections of sural nerve cross-sections were prepared and immunolabeled with total (active and inactive) and phosphorylated (inactive) RhoA antibodies in order to compare RhoA activity due to treatment.

Morphological analysis of peripheral nerve tissue: Sural nerve cross-sections obtained from frozen cryosections were examined by phase-contrast microscopy. Axon, myelin, and total fiber (axon + myelin) areas and shapes were measured and compared between groups.

Protein analysis of peripheral nerve tissue: Harvested after 10 weeks of treatment, sciatic nerves were homogenized and subjected to Western blot analysis with antibodies against total and phosphorylated RhoA, total and phosphorylated SHP2, and GAPDH.

Primary neuronal cultures: Primary mouse cortical neurons were prepared and treated with either calpeptin, a known RhoA activator, or cisplatin. In addition, groups of neurons also received LM11A-31 in addition to both calpeptin or cisplatin.

Neuronal morphological analysis: Treated neurons were fixed and actin-based structures were visualized with phalloidin. Nuclei were stained with Hoescht 33258. Neuronal images

were captured using a Zeiss Axiovert S100 fluorescent light microscope (Carl Zeiss, Thornwood, NY) and branches and sprouts were counted and measured using MetaMorph™ 4.6 imaging software systems (Molecular Devices, Sunnyvale, CA).

Neuronal RhoA Immunofluorescence: Treated neurons were fixed and immunolabeled with total and phosphorylated RhoA antibodies.

Analysis of protein expression in neuronal lysates: Lysates were collected from drug-treated mouse primary neuronal cultures and subjected to Western blot analysis. Blots were probed for antibodies against phosphorylated RhoA and phosphorylated SHP2.

Statistical analysis: t-test analysis was performed and p-values were designated for each experiment, each of which were repeated a minimum of three times. Any null hypothesis with probability level less than 95% was rejected.

Specific Aim II: To identify and characterize small molecule inhibitors of Cdc42 activation for further determination of the roles of cross talk between Rho subfamilies in cisplatin-induced peripheral neurotoxicity.

Virtual screening: A database consisting of 197,000 compounds was virtually screened for small molecules that can disrupt the interaction of Cdc42 with its specific GEF intersectin (ITSN). The top ranked 50,000 molecules were then subjected to more stringent SP (standard precision) docking, after which the top ranked 100 molecules were manually inspected to select 30 compounds for *in vitro* and biological testing.

Synthetic procedures: Top ranking 100 compounds were synthesized and then purified by column and high performance liquid chromatography (HPLC).

Fluorescence titration: Lyophilized Cdc42 protein was reconstituted and placed in a quartz cuvette, to which aliquots of ZCL278 were added. The fluorescent wavelength of tryptophan (350 nm) was measured after each ZCL278 addition. Titration curves were generated to calculate K_d.

Surface plasmon resonance: In order to assess direct binding of ZCL278 and Cdc42, ZCL278 was covalently immobilized to purified Cdc42 on a CM5 chip and varying ZCL278 concentrations were added in order to determine K_d.

Determination of pKa values of ZCL278: The pKa of ZCL278 was calculated by dissolving ZCL278 in water and titrating with either HCl or varying DMSO concentrations.

Measurement of the solubility of ZCL278: Solubility of ZCL278 was determined by measures of UV absorption of saturated ZCL278 solutions.

p50RhoGAP or Cdc42GAP assay: Inorganic phosphate produced as a result of GTPase activity was measured using a p50RhoGAP or Cdc42GAP assay whereby Cdc42 was preloaded with either GTP or ZCL278, and then stimulated with Cdc42GAP.

Immunofluorescent characterization of ZCL compounds: Serum-starved Swiss 3T3 cells were treated with or without Cdc42 activator, RhoA activator, Rac activator, ZCL series compounds, Y-27632, or NSC23766. Cdc42-mediated microspike formation was then analyzed in phalloidin stained cells.

Western blot analysis of ZCL278: PC-3 were treated with a Cdc42 activator or a time course of ZCL278. Lysates were then collected, subjected to Western blot analysis, and probed with antibodies against phospho-Rac1/cdc42 (Ser71), phosphorylated WASP, and GAPDH.

G-LISA®: Cdc42 activation and inactivation was directly assessed in serum starved Swiss 3T3 cells which were treated with or without the Cdc42 activator, ZCL278 or NSC23766 using a G-LISA®, an ELISA-based assay that allows a quantitative determination of the levels of GTP-bound (active) Cdc42 in cellular lysates.

Active Cdc42 Immunofluorescence: Serum starved Swiss 3T3 cells were treated with ZCL278 or NSC23766 and then stimulated with a Cdc42 activator. Cells were then immunolabeled with an active Cdc42 and a phosphorylated RhoA antibody, in order to elucidate the effect of ZCL278 on Cdc42 activity *in vitro*.

GM130 Immunofluorescence: Serum starved Swiss 3T3 cells were treated with ZCL278 or NSC23766 and then stimulated with a Cdc42 activator. The influence of ZCL278 on Golgi organization was investigated by immunostaining for GM130, a *cis*-Golgi matrix protein.

Wound Healing Assay: Serum starved PC-3 cell monolayers were scratched and then treated with or without a Cdc42 activator, ZCL278, or NSC23766. After 24 hours, distance of migration was measured.

Primary neuron morphology: Mouse primary cortical neurons were harvested, cultured and treated with either DSMO or ZCL278. Cells were then fixed, probed with phalloidin, and branching was analyzed.

Primary neuron time-lapse imaging: Mouse primary cortical neurons were treated with either DSMO or ZCL278 for 10 minutes, during which they were recorded by time lapse light microscopy. Growth cones and filopodial dynamics were observed. Images were captured and analyzed with MetaMorph™ 4.6 imaging software systems (Molecular Devices, Sunnyvale, CA).

Statistical analysis: t-test analysis was performed and p-values were designated for each experiment, each of which were repeated a minimum of three times. Any null hypothesis with probability level less than 95% was rejected.

I. Significance

Rho GTPases are crucial regulators for a variety of cellular functions and aberrant activity or regulation of Rho proteins have been critically linked to a multitude of human pathologies. For these reasons, Rho proteins (including the major family members RhoA, Rac1 and Cdc42) have emerged as promising therapeutic targets. In the current study, we focus on Rho GTPase inhibition as a putative combinatorial therapy that could be used alongside traditional chemotherapeutic cancer treatment. Traditional chemotherapy is an effective method of cancer cell eradication; however, its cytotoxic effects are not limited to cancerous cells. Neurotoxicity is known to occur with use of several anti-neoplastic agents including the platinum-based compound cisplatin, and can be debilitating and dose-limiting for patients. Using a clinically relevant dose of cisplatin, our laboratory has developed a mouse model of cisplatin-induced peripheral neuropathy (CIPN). Using this model, we investigated the neuroprotective advantages of RhoA suppression in conjunction with cisplatin treatment as a possible method of CIPN prevention. In addition, this project focuses on filling a major gap in the understanding of Cdc42, through development of a novel small molecule inhibitor, ZCL278. Importantly, using ZCL278 we will be able to further dissect Cdc42 signaling pathways to understand the roles that Cdc42 plays in various diseases and disorders, including CIPN.

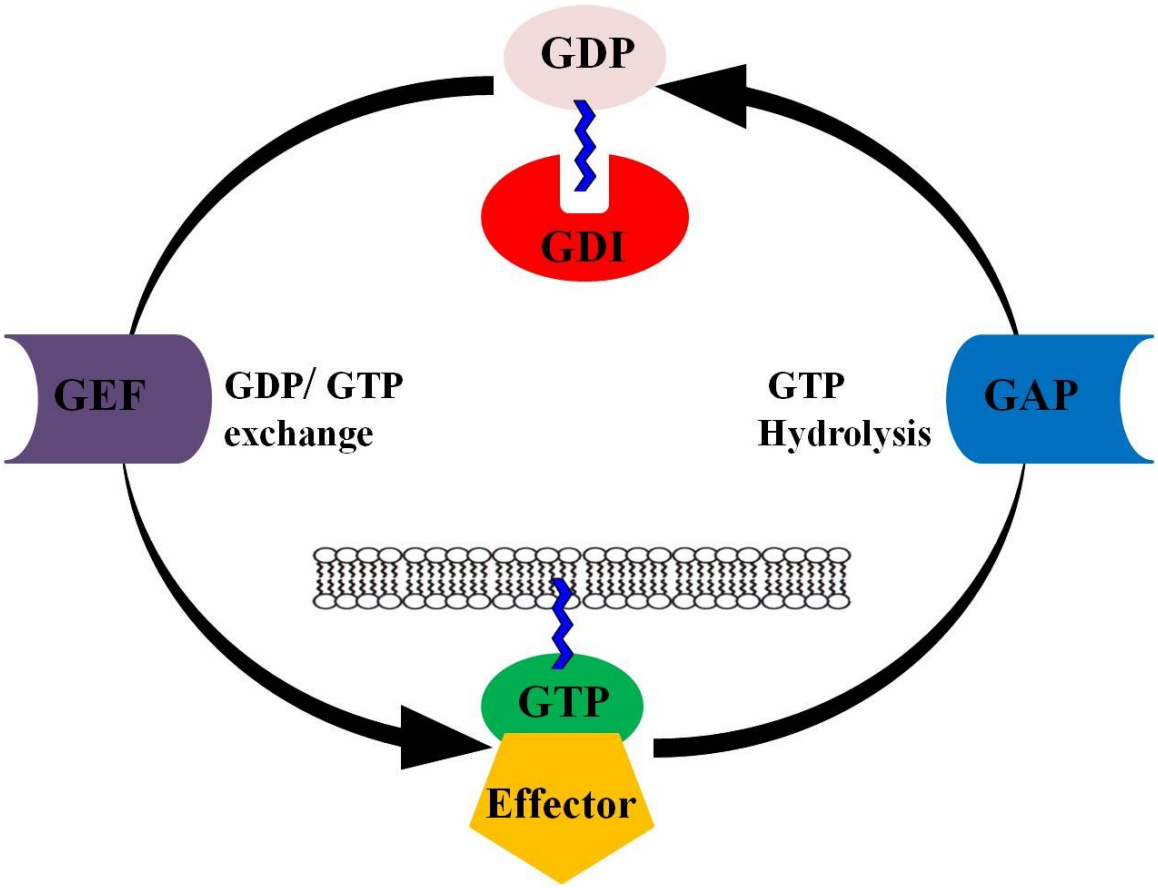
GDP
GDI
GEF
GDP/ GTP
exchange
GTP
Hydrolysis
GAP
GTP
Effector

Figure 1.1 ***The Rho GTPase Cycle.***

Rho GTPases cycle between an inactive GDP bound state and an active GTP bound state and are regulated by GTPase activating proteins (GAPs; inactivate), guanine nucleotide exchange factors (GEFs; activate) and guanine nucleotide dissociation inhibitors (GDIs), which bind to the inactive (GTP-bound) protein and prevent its activation.

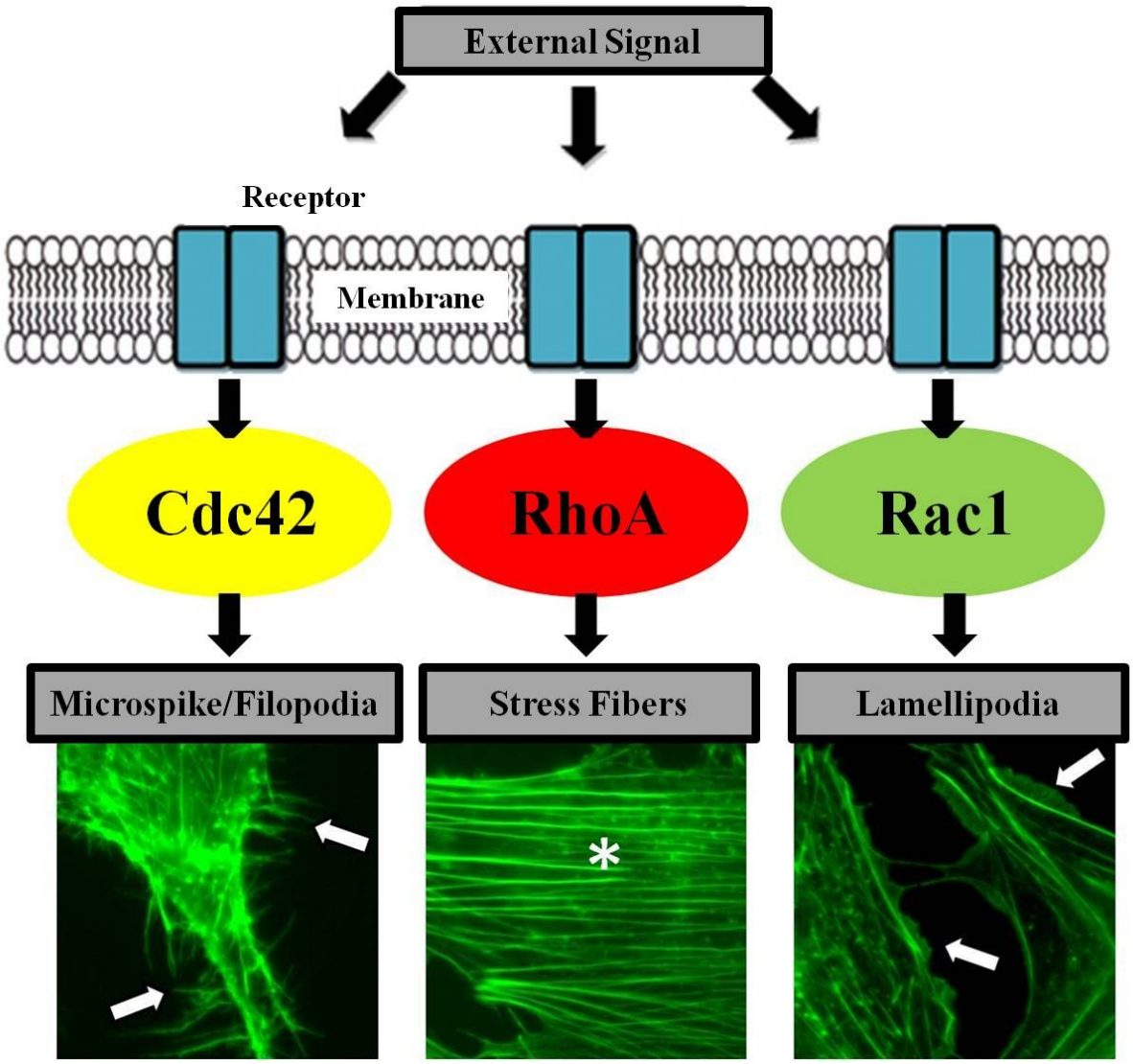
External Signal
Receptor
Membrane
Cdc42
RhoA
Rac1
Microspike/Filopodia
Stress Fibers
Lamellipodia

Figure 1.2 ***Rho GTPase signaling promotes characteristic actin-based structures.***

External signals transduced from membrane receptors (integrins, G-protein coupled receptors, ion channels, growth factor receptors) promote activation of RhoA, Rac1, and Cdc42 which can induce cytoskeletal rearrangements resulting in the formation of stress fibers, lamellipodia, and filopodia/microspikes, respectively.

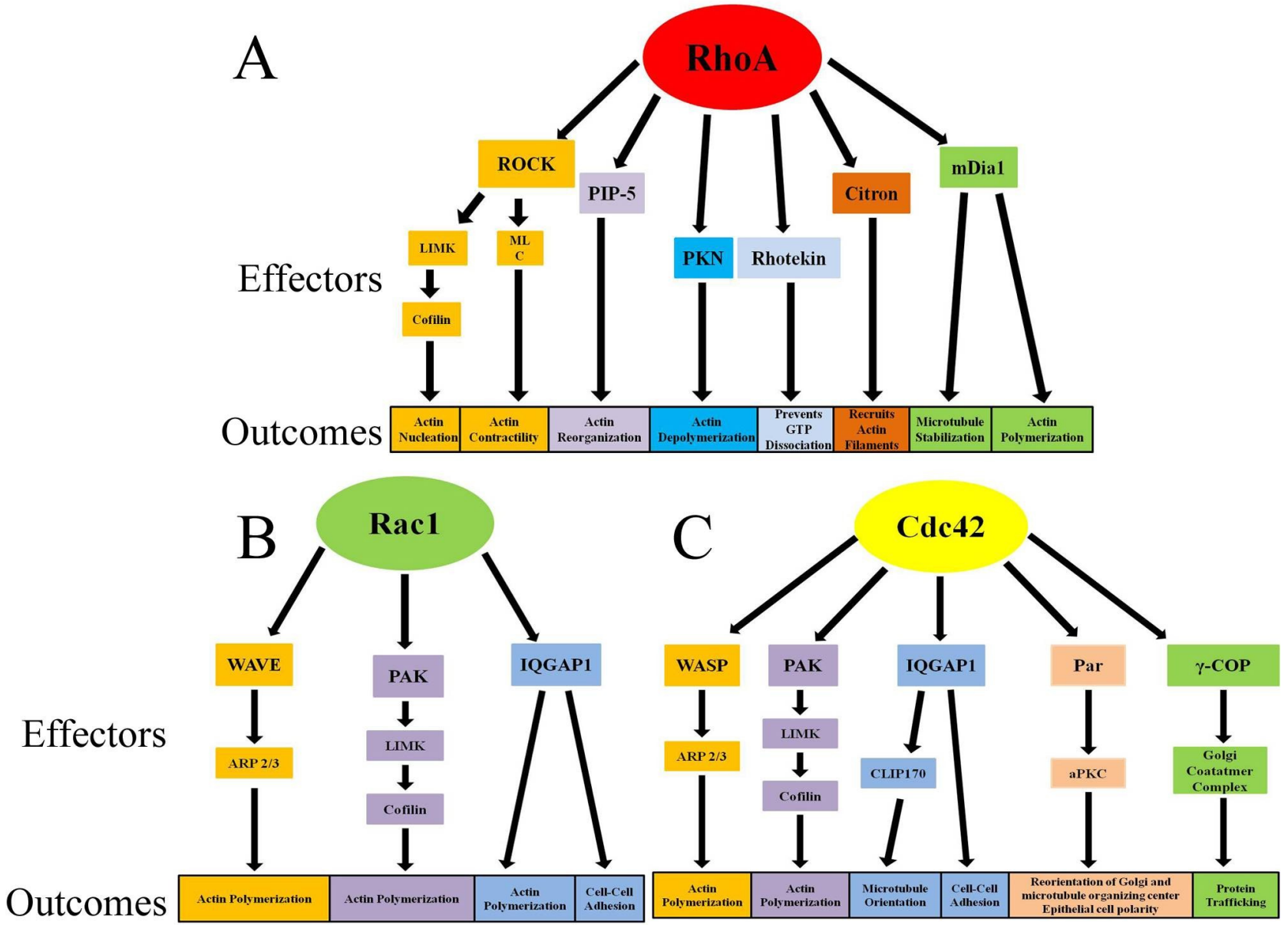
A
RhoA
ROCK
PIP-5
Citron
mDia1
LIMK
ML C
PKN
Rhotekin
Effectors
Cofilin
Outcomes
Actin Nucleation
Actin Contractility
Actin Reorganization
Actin Depolymerization
Prevents GTP Dissociation
Recruits Actin Filaments
Microtubule Stabilization
Actin Polymerization
B
Rac1
WAVE
PAK
IQGAP1
Effectors
ARP 2/3
LIMK
Cofilin
Outcomes
Actin Polymerization
Actin Polymerization
Actin Polymerization
Cell-Cell Adhesion
C
Cdc42
WASP
PAK
IQGAP1
Par
γ-COP
ARP 2/3
LIMK
CLIP170
aPKC
Golgi Coatatmer Complex
Cofilin
Actin Polymerization
Actin Polymerization
Microtubule Orientation
Cell-Cell Adhesion
Reorientation of Golgi and microtubule organizing center Epithelial cell polarity
Protein Trafficking

Fig 1.3 ***Rho GTPase effector proteins and outcomes.***

Overview of major downstream effectors of RhoA (A), Rac1 (B), and Cdc42 (C) and their resultant cellular outcomes.

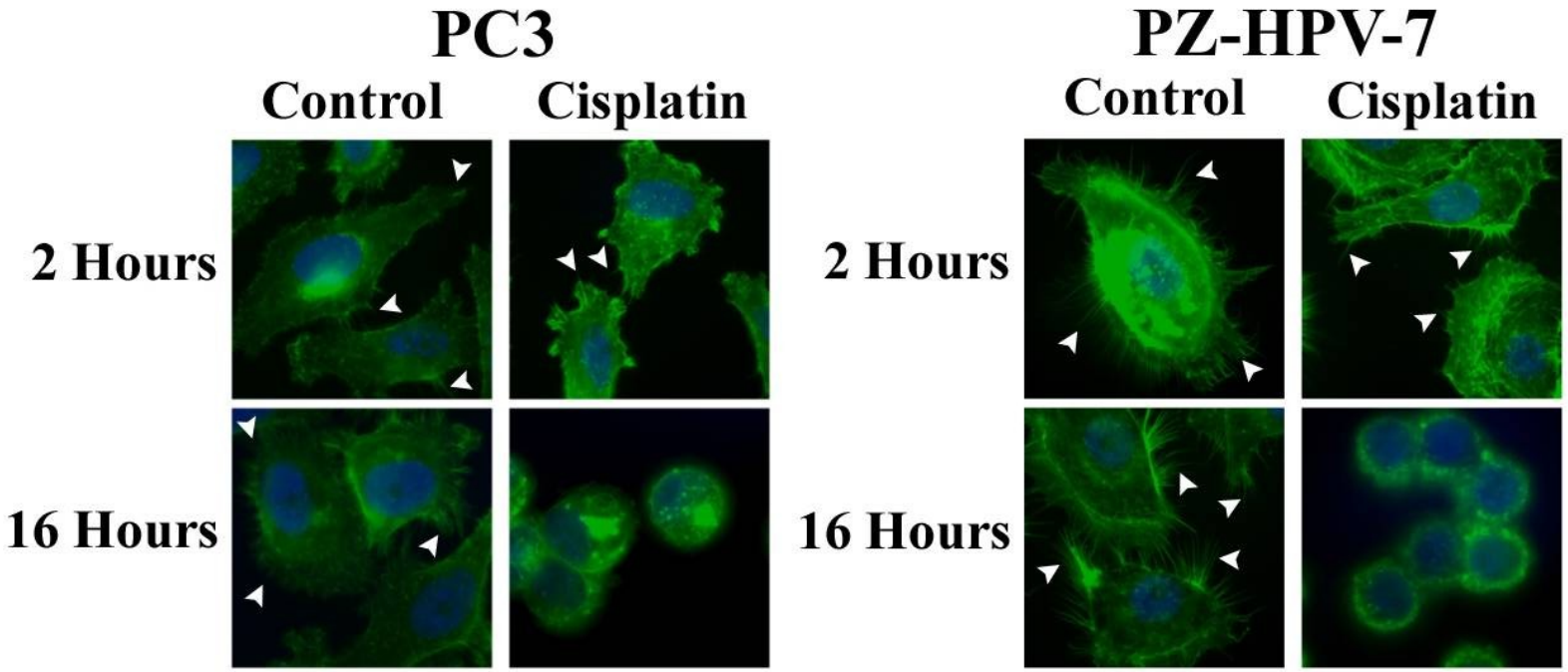
PC3
Control
Cisplatin
2 Hours
16 Hours
PZ-HPV-7
Control
Cisplatin
2 Hours
16 Hours

Figure 1.4 ***Cisplatin treatment leads to retraction of cellular processes in both PC-3 and PZ-HPV-7 cells.***

PC-3 cells, metastatic human prostate cancer cells, and PZ-HPV-7 cells, non-cancer human prostatic epithelial cells, were treated with DMSO (control) or 6μg/mL cisplatin for 2 or 16 hours. Fluorescein-phalloidin staining revealed many extended processes in control cells. Cisplatin treatment decreased the number and length of processes (white arrowheads) after 2 hours, which progressed to further retraction and rounded cell morphologies in both cell types after 16 hours.

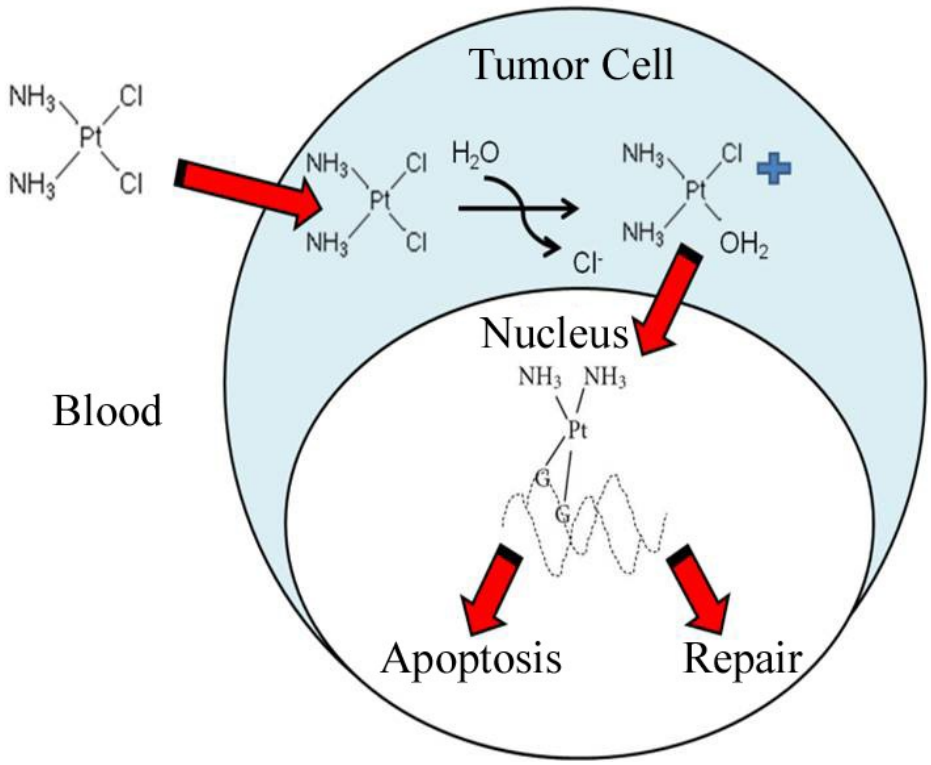
Tumor Cell
Blood
Nucleus
Apoptosis
Repair
H2O
Cl-

Figure 1.5 ***Structure and proposed cisplatin mechanism of action.***

Cisplatin is a platinum-based chemotherapeutic drug that is frequently used to treat various forms of cancer including testicular, ovarian, bladder, lung, and prostate cancer. Its primary mechanism of action is thought to occur as a result of spontaneous hydration reactions which lead to the displacement of the chloride ligands which then enables the platinum atom to bind nucleotide bases within the DNA. The most frequent adducts formed are the 1, 2 intrastrand cross-links between guanine bases. Ultimately, these distortions of the DNA will lead to one of two outcomes: (1) DNA repair or (2) apoptosis.

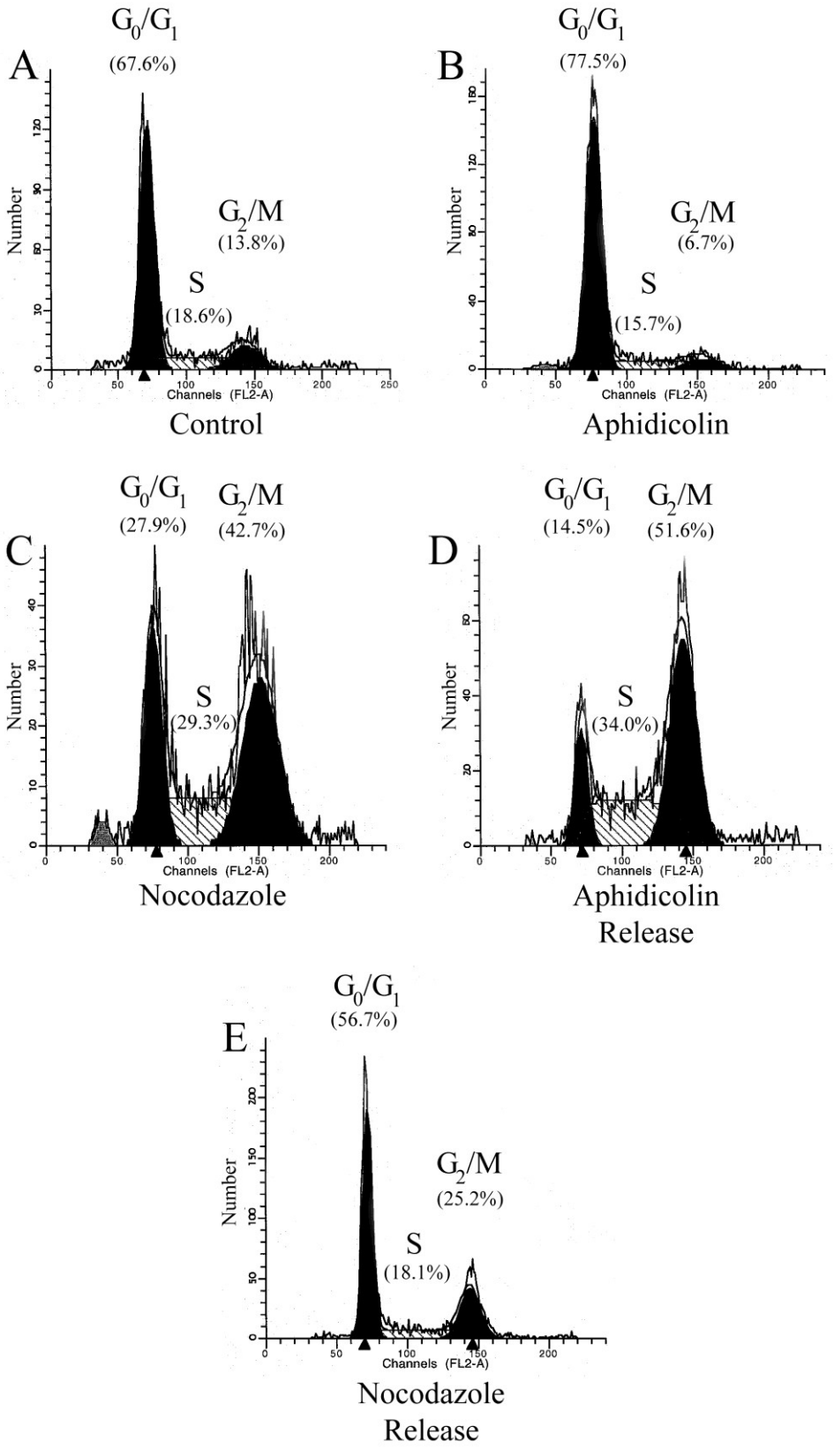
A
G0/G1
(67.6%)
G2/M
(13.8%)
S
(18.6%)
Number
Channels (FL2-A)
Control
B
G0/G1
(77.5%)
G2/M
(6.7%)
S
(15.7%)
Number
Channels (FL2-A)
Aphidicolin
C
G0/G1
(27.9%)
G2/M
(42.7%)
S
(29.3%)
Number
Channels (FL2-A)
Nocodazole
D
G0/G1
(14.5%)
G2/M
(51.6%)
S
(34.0%)
Number
Channels (FL2-A)
Aphidicolin
Release
E
G0/G1
(56.7%)
G2/M
(25.2%)
S
(18.1%)
Number
Channels (FL2-A)
Nocodazole
Release

Figure 1.6 ***Aphidicolin suppresses G1 to S transition while Nocodazole increases G2/M population in H522 lung cancer cells.***

Cultures of H522 cells were used to analyze the cell cycle by flow cytometry. Cells were maintained as non-treated controls (A) or treated for 20 hours with either 1μg/mL aphidicolin, which leads to G_1/S boundary arrest (B), or 0.1 μg/mL nocodazole, which arrests the cell cycle at the G_2/M boundary (C). Following 20 hours of 1 μg/ml aphidicolin (D) or 0.1 μg/ml nocodazole (E) treatment, H522 cells were released from blocks for 10 hours. Percentages reflect the proportion of cells within the population at each phase of the cell cycle.

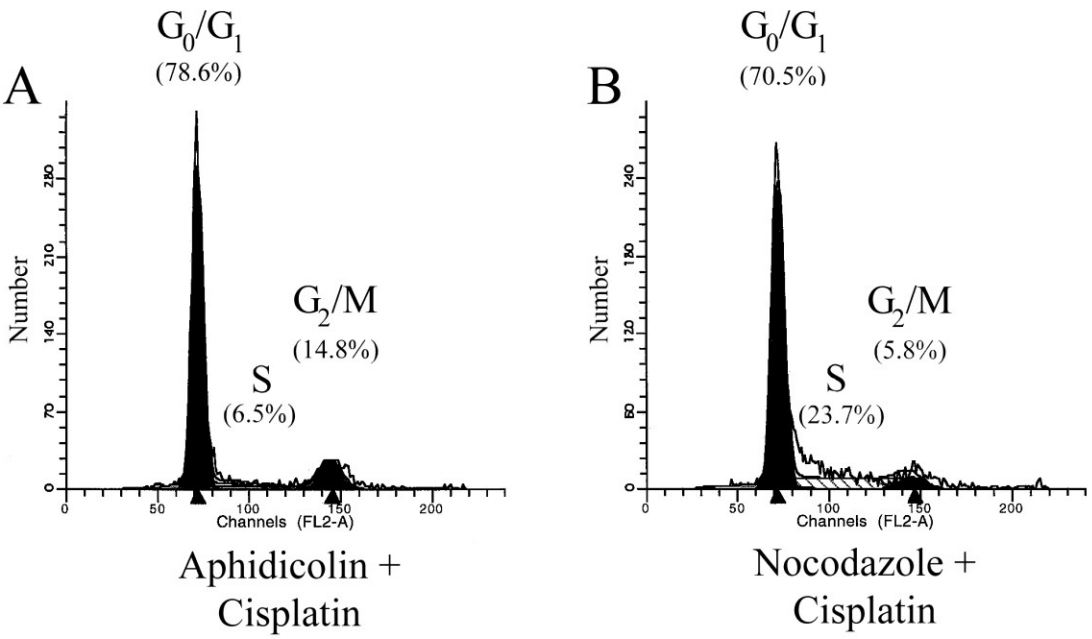
A
G_0/G_1
(78.6%)
G_2/M
(14.8%)
S
(6.5%)
Number
Channels (FL2-A)
Aphidicolin +
Cisplatin
B
G_0/G_1
(70.5%)
G_2/M
(5.8%)
S
(23.7%)
Number
Channels (FL2-A)
Nocodazole +
Cisplatin

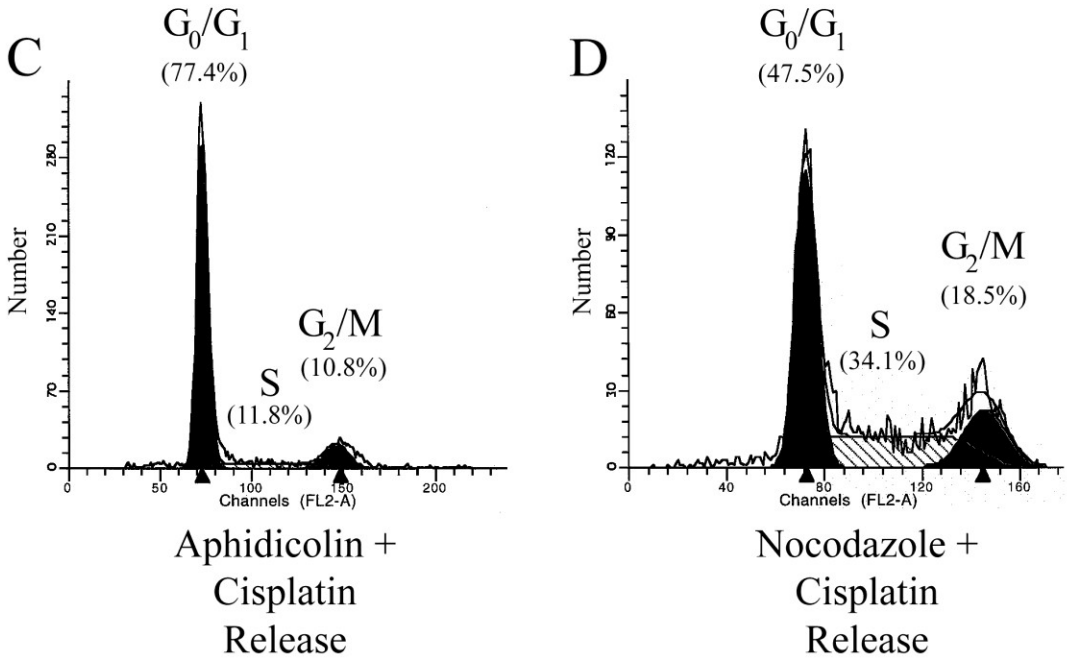
C
G_0/G_1
(77.4%)
G_2/M
(10.8%)
S
(11.8%)
Number
Channels (FL2-A)
Aphidicolin +
Cisplatin
Release
D
G_0/G_1
(47.5%)
G_2/M
(18.5%)
S
(34.1%)
Number
Channels (FL2-A)
Nocodazole +
Cisplatin
Release

Figure 1.7 ***Cisplatin blocks G_1 to S phase transition.***

H522 cells synchronized at either the G_1/S boundary (A) or G_2/M boundary (B) for 20 hours were then treated with 5 μg/mL cisplatin for 24 hours in order to further elucidate cisplatin's action within the cell cycle. H522 cells synchronized with 1 μg/ml aphidicolin (C) or 0.1 μg/ml nocodazole (D) for 20 hours followed by cisplatin treatment for 24 hours were then released from cisplatin for an additional 10 hours.

Table 1.1 Major Rho GTPase Activators

Rho GTPase	Activator	Method	Reference
RhoA	Lysophosphatidic Acid	Indirect, non-specific $G_{\alpha 12/13}$ agonist	(Ridley and Hall, 1992)
RhoA	Sphingosine-1-phosphate	Indirect, non-specific $G_{\alpha 12/13}$ agonist	(Hill, Wynne and Treisman, 1995)
RhoA	Calpeptin	Indirect, specific SHP2 tyrosine phosphatase -mediated p190RhoGAP inhibition	(Schoenwaelder et al., 2000)
RhoA, Rac1, Cdc42	Epidermal Growth Factor (EGF)	Indirect, nonspecific Stimulates tyrosine kinase receptor EGFR	(Ridley et al., 1992)
RhoA, Rac1, Cdc42	Bacterial cytotoxic necrotizing factor (CNF) toxins.	Direct, nonspecific deamidates glutamine-63 of Rho and glutamine-61 of Rac and Cdc42 in their Switch II regions	(Flatau et al., 1997; Schmidt et al., 1997)
Rac1	Platelet-derived growth factor (PDGF)	Indirect, nonspecific Acts through receptor tyrosine kinases	(Ridley et al., 1992)
Cdc42	Bradykinin	Indirect, nonspecific Acts through bradykinin receptor-linked G-proteins	(Kozma et al., 1995)

Table 1.2 Major Rho GTPase inhibitors

Rho GTPase	Inhibitor	Method	Reference
RhoA, Rac1, Cdc42	C3Transferase	Indirect, specific ADP-ribosylation on asparagine 41 in the effector binding domain	(Kumagai et al., 1993)
RhoA	Fasudil	Indirect, specific Selectively inhibits ROCK	(Nagumo et al., 2000) (Uehata et al., 1997)
RhoA	Y-27632	Indirect, specific Selectively inhibits ROCK	(Narumiya, Ishizaki and Uehata, 2000)
RhoA	CCG-1423	Indirect, nonspecific Targets MKL/SRF-dependent transcriptional activation	(Evelyn et al., 2007)
RhoA	LM11A-31	Direct, specific Blocks upstream activation of RhoA via the p75 neurotrophin receptor and prevents dissociation from RhoGDI	(Massa et al., 2006)
Rac1	NSC23766	Direct, specific Prevents Rac1 interaction with specific GEF's Trio and Tiam1	(Gao et al., 2004)
Cdc42	ZCL278	Direct, specific Targets Cdc42 interaction with Cdc42-specific GEF intersectin	(Friesland et al., 2013)
Cdc42	Pirl1	Indirect, specific Prevents dissociation from RhoGDI and GTP exchange	(Peterson et al., 2006)
Cdc42	Secramine B	Indirect, specific Prevents dissociation from RhoGDI and membrane association	(Pelish et al., 2006)

CHAPTER II: AMELIORATION OF CISPLATIN-INDUCED EXPERIMENTAL PERIPHERAL NEUROPATHY BY A SMALL MOLECULE TARGETING P75^{NTR}

A. Summary

Cisplatin is an effective and widely used first-line chemotherapeutic drug for treating cancer. However, many patients sustain cisplatin-induced peripheral neuropathy (CIPN), often leading to a reduction in drug dosages or complete cessation of treatment. Therefore, it is important to understand alternative cisplatin targets in peripheral nerve tissues and identify signaling pathways for potential intervention. Rho GTPase activation is increased following trauma in several models of neuronal injury. Thus, we investigated whether components of the Rho signaling pathway represent important neuroprotective targets with the potential to ameliorate CIPN and enhance current chemotherapy treatment regimens.

We have developed a novel CIPN model in the mouse. Using this model and primary neuronal cultures we examined the effects of LM11A-31, a small-molecule that blocks proNGF binding to the p75 neurotrophin receptor (p75^{NTR}), on Rho GTPase signaling and CIPN reduction. Von Frey filament analysis of sural nerve function showed that LM11A-31 treatment prevented decreases in peripheral nerve sensation seen with cisplatin treatment. Morphometric analysis of harvested sural nerves revealed that cisplatin-induced abnormal nerve fiber morphology and the decreases in fiber area were alleviated with concurrent LM11A-31 treatment. Cisplatin treatment increased RhoA activity accompanied by the reduced tyrosine phosphorylation of SHP2, which was reversed by LM11A-31. LM11A-31 also countered the effects of calpeptin, which activates RhoA by inhibiting SHP2 tyrosine phosphatase and reduces neuronal sprout numbers. Therefore, suppression of RhoA signaling by either blocking proNGF

binding to $p75^{NTR}$ or by activating SHP2 tyrosine phosphatase downstream of NGF receptor enhances neuroprotection in our experimental CIPN mouse model.

B. Introduction

Cisplatin (cis-diamminedichloroplatinum), a platinum-based compound, is a widely used and valuable tool to suppress cancer cell proliferation and promote remission of various solid tumors. The canonical cisplatin mechanism of action involves induction of inter- and intra-strand DNA cross-links which ultimately result in apoptosis of rapidly dividing cells (Huang et al., 1995). Unfortunately, cisplatin's cytotoxic effects are not limited to neoplastic tissue, as it frequently disrupts normal renal, gastrointestinal, hematologic, and peripheral nervous system function.

Peripheral neurotoxicity is the most common dose-limiting side effect of cisplatin, and often leads to dose reduction or complete cessation of effective treatment protocols. Current data estimates that up to 50% of patients receiving cisplatin develop some degree of peripheral neurotoxicity (Gutiérrez-Gutiérrez et al., 2010; Strumberg et al., 2002; van der Hoop et al., 1990) as a consequence of treatment. Additionally, patients with predisposing conditions, including alcoholism, diabetes, vitamin B12 deficiency, or HIV/AIDS seem to be more prone to the neurotoxic effects of cisplatin (Schloss et al., 2013). Neuropathies associated with cisplatin are predominately sensory in nature and tend to present in a "glove and stocking" fashion as numbness, tingling, and pain that initiates in the distal extremities (Jaggi and Singh, 2012; Kaley and Deangelis, 2009). Typically, cisplatin-induced neuropathies are predominately sensory in nature, with patients presenting with paresthesias, loss of vibration sense, and decreased reflexes (Beijers et al., 2012). Incidence and severity of cisplatin-induced peripheral neuropathy (CIPN)

is dose-dependent (Gregg et al., 1992) and may resolve or persist following treatment completion (van der Hoop et al., 1990). Cisplatin has been demonstrated to lead to the highest levels of tissue accumulation within the dorsal root ganglion (DRG) where it preferentially binds DNA (McDonald et al., 2005; Park et al., 2008). Although it is apparent that there must be additional targets aside from DNA replication, as neurons are not a proliferating population of cells and are affected by cisplatin, cisplatin's precise neurotoxic mechanism remains uncertain. Thus, it has become important not only to understand alternative cisplatin targets but to also explore signaling pathways for potential intervention.

In recent years, it has been well established that RhoA, a small GTPase, has increased activity following trauma in several models of neuronal injury (Brabeck et al., 2004; Cheng et al., 2008; Dergham et al., 2002; Dubreuil et al., 2003; Dubreuil et al., 2006). Additionally, inhibition of the RhoA pathway has been shown to effectively treat Alzheimer's disease, stroke, neuropathic pain and inflammatory reactions in experimental models (Tatsumi et al., 2005 ; Walters et al., 2002; Zhou et al., 2003). *In vitro* studies from our laboratory have demonstrated that Rho pathway inhibition, either upstream with a $p75^{NTR}$ receptor ligand mimetic (LM11A-31) or downstream with a selective $p160^{ROCK}$/ Rho kinase inhibitor (Y-27632), facilitates neuronal recovery in neuronal cultures treated with cisplatin (James et al., 2008). Subsequent *in vivo* studies, using a CIPN mouse model, demonstrated RhoA pathway inhibition with Y-27632 could facilitate recovery from peripheral neuropathy induced by cisplatin treatment (James et al., 2010). These findings highlight the importance of RhoA signaling in the development of neurological problems and the possibility that inhibition may enhance current clinical treatments.

Neuroprotective strategies that focus on prevention, rather than recovery, are more clinically desirable and important for patient well-being and treatment. In the current study, we

examined upstream suppression of the RhoA pathway with LM11A-31, which blocks proNGF binding to $p75^{NTR}$ (Massa et al., 2006), concurrent with cisplatin treatment in the CIPN mouse. Using this model, we show that cisplatin-induced decreases in peripheral sensory nerve function can be prevented with LM11A-31. Abnormal fiber morphologies and decreases in axon, myelin, and fiber area observed in peripheral nerves harvested from cisplatin-treated animals could also be alleviated with LM11A-31 pretreatment. In addition, simultaneous LM11A-31 treatment reversed cisplatin-induced increases in RhoA activity and decreases in tyrosine phosphorylation of SHP2. In primary neuronal cultures and peripheral nerve tissue, LM11A-31 countered the effects of calpeptin, which activates RhoA by inhibiting SHP2 tyrosine phosphatase and reduces neuronal sprout numbers. RhoA inhibition through LM11A-31 leads to longer, more branched neurites in comparison to cisplatin alone, highlighting the importance of RhoA in the development of CIPN and a potential site of intervention that could be exploited clinically for patients undergoing chemotherapy.

C. Experimental Procedures

C.1 Pharmacological treatments

Forty-four (22 male; 22 female) age-matched C57/BL6 mice (3 months; Charles River, Wilmington, MA) weighing an average of 24 g were obtained. Mice were treated with either 6 µg/g body weight cisplatin (Sigma Co, St. Louis, MO) or 200 µL 0.9% saline (Hospira, Lake Forest, IL) by intraperitonal injection every 14 days for a 10 week treatment period (n=10; 5 male & 5 female mice/ group). In addition to cisplatin (6 µg/g body weight), two additional groups of animals received either a low dose (25 µg/g body weight) or a high dose (50 µg/g body weight) of LM11A-31 (courtesy Dr. Frank Longo, Stanford, CA) by intraperitoneal injection

every 24 hours for the 10 week treatment period (n=12; 6 male & 6 female mice/ group). Mice were observed daily throughout the treatment for hair and weight loss. All animal experiments and testing were approved by the East Carolina University Animal Care and Use Committee (AUP:174a, see Appendix A).

C2. Von Frey/ Semmes-Weinstein sensory threshold testing of hindpaw

All animals were subjected to Von Frey/Semmes-Weinstein monofilament sensory threshold testing of the hind paws as previously described (James et al., 2010) every two weeks for the 10 week treatment period. Briefly, animals were placed within a clear plastic barrier upon an elevated screen and allowed to acclimate for 10 to 15 minutes. Von Frey/Semmes-Weinstein monofilaments (Stoeling Co., Wood Dale, IL) were applied to the point of bending onto the plantar surface of left and right hindpaws. Monofilament testing proceeded from the smallest diameter until the applied monofilament elicited response. Responses were recorded as positive when the animal responded 3 out of 5 applications. Differences between treatment groups were determined by *t*-test analysis using SigmaPlot 10.0 (Systat Software Inc., San Jose, CA).

C3. Tissue preparation

Animals were deeply anesthetized with 3% isoflurane vapor and euthanized by cervical dislocation. Tissues (dorsal root ganglion, sural and sciatic nerves) were rapidly removed and either fresh frozen on liquid nitrogen (for protein analysis) or fixed in Zamboni's fixative (2% paraformaldehyde, 0.5% picric acid, and 0.1% phosphate buffer) overnight. Tissue samples were then washed with phosphate-buffered saline and cryoprotected overnight in 30% sucrose in

PBS at 4°C. Tissues were then embedded in OCT and rapidly frozen with chilled isopentane. 5µm thick cryostat sections were affixed to Superfrost slides (Fisher Scientific, Pittsburgh, PA).

C4. Immunofluorescent analysis of peripheral nerve tissue

For immunostaining, sections were incubated with 0.2% Triton X-100 for 10 minutes at room temperature, 20 minutes at room temperature with 100mM glycine and blocked 30 minutes at 37 °C with 10% bovine serum albumin (BSA). Primary antibodies (rabbit total RhoA 1:100, Santa Cruz Biotechnology, Santa Cruz, CA; rabbit phosphorylated RhoA 1:100, Santa Cruz Biotechnology, Santa Cruz, CA) were all incubated overnight at 4°C. Immunofluorescent images were captured and analyzed with a Zeiss Axiovert S100 fluorescent light microscope (Carl Zeiss, Thornwood, NY). n= 3 sural nerves/ treatment group.

C5. Morphological analysis of peripheral nerve tissue

Morphometric evaluation of phase contrast images of sural nerve cross sections, captured at 63X with a Zeiss Axiovert S100 fluorescent light microscope (Carl Zeiss, Thornwood, NY), were conducted using MetaMorph™ 4.6 imaging software systems (Molecular Devices, Sunnyvale, CA). Due to natural size variation in sural nerves, morphometric analysis was carried out on three randomly selected 40 μm^2 regions in each nerve and averaged to obtain data for each sural nerve evaluated. Briefly, myelinated fiber (axon + myelin), axon, and myelin areas were measured with image analysis software. Based on the total area of the region counted (1600 µm) percentages of space occupied by axons, myelin, and total fibers were calculated. Additionally, after subtracting the total fiber area from the total area of the region, the percentage of endoneural space that was unoccupied by myelinated nerve fibers was determined. t-test

analysis was performed using SigmaPlot 10.0 (Systat Software Inc., San Jose, CA) to determine differences between drug treatment groups. n= 6 sural nerves/ treatment group. Any null hypothesis with the probability level less than 95 % was rejected.

C6. Protein analysis of peripheral nerve tissue

Due to the inability to obtain sufficient protein from sural nerves, flash frozen sciatic nerves were utilized for protein analysis. Harvested sciatic nerves were frozen on liquid nitrogen, crushed, and homogenized in a buffer consisting of 50mM Tris pH 7.4, 50mM sodium chloride, 5 mM magnesium chloride, 1 mM dithiothreitol (DTT), and 1% Triton X-100, and supplemented with protease inhibitors (1mM phenylmethanesulfonylfluoride (PMSF), 10mM sodium pyrophosphate, 20mM sodium fluoride, 1mM sodium orthovanadate, and a protease inhibitor cocktail (Roche Applied Science, Indianapolis, IN)). After determination of protein concentrations, equal amounts of protein were loaded onto an 18% tris-glycine gel (Invitrogen, Carlsbad, CA), transferred to PVDF membrane (Milipore, Billerica, MA) and subjected to Western blot analysis. Blots were blocked and probed with mouse total RhoA 1:400 (Cytoskeleton Inc., Denver, CO), rabbit phosphorylated RhoA 1:500 (Santa Cruz Biotechnology, Santa Cruz, CA), rabbit total SHP2 1:500 (Milipore, Billerica, MA), and phosphorylated SHP2 (Y542) 1:500 (Cell Signaling Technology, Danvers, MA). GAPDH (mouse, 1:2000; Calbiochem, San Diego, CA) was used as a loading control.

C7. Primary neuronal cultures

Primary cortical neurons were isolated from a 18-day timed pregnant mouse as previously described (James et al., 2008). Neurons were cultured for 5 days i*n vitro* (DIV) in B-

27 supplemented Neurobasal media (Invitrogen Carlsbad, CA) then selected neurons were treated for 24 hours with cisplatin (8 μg/mL). LM11A-31 was then applied to selected neurons at 6 DIV at a concentration of 100 nM for an additional 24 hours. Finally, at 7 DIV, selected cells were treated with calpeptin for 30 minutes (1 unit/mL; Cytoskeleton, Denver, CO). Neurons were then fixed for 15 minutes in 4% paraformaldehyde.

C8. Neuronal morphological analysis

Neuronal actin-based structures were identified with fluorescein-phalloidin (Molecular Probes, Eugene, OR) and nuclei were labeled with Hoechst. Neuronal images were captured using a Zeiss Axiovert S100 (Carl Zeiss, Thomwood, NY). Morphometric analyses were then performed using MetaMorph™ 4.6 imaging software systems (Molecular Devices, Sunnyvale, CA) as previously described (James et al., 2008; Jones et al., 2004). Briefly, branch numbers were determined by applying the MEASURE COUNT OBJECT function of the software system. Branches were scored when they were longer than 10 μm. Processes shorter than 10 μm were designated as sprouts, and not counted as branches. The imaging system was calibrated so that dendrite length measurements were true values. t-test analysis was performed using SigmaPlot 10.0 (Systat Software Inc., San Jose, CA) to determine differences between drug treatment groups. n= 3 representative neurons/ treatment group. Any null hypothesis with the probability level less than 95 % was rejected.

C9. Neuronal RhoA immunofluorescence

Primary cortical neurons on poly-L-lysine coated coverslips, treated as previously described, were incubated with 0.2% Triton X-100 for 10 minutes at room temperature, 20

minutes at room temperature with 100mM glycine and blocked 30 minutes at 37 ^{o}C with 10% bovine serum albumin (BSA). Primary antibodies (rabbit total RhoA 1:100 and rabbit phosphorylated RhoA 1:100, Santa Cruz Biotechnology, Santa Cruz, CA) were incubated one hour at room temperature. Immunofluorescent images were captured and analyzed with a Zeiss Axiovert S100 fluorescent light microscope (Carl Zeiss, Thornwood, NY). n= 3 representative neurons/ treatment group.

C10. Analysis of protein expression in neuronal lysates

Mouse primary cortical neurons were treated as previously described, lysed with RIPA buffer supplemented with protease inhibitors (1mM phenylmethanesulfonylfluoride (PMSF), 10mM sodium pyrophosphate, 20mM sodium fluoride, 1mM sodium orthovanadate, and a protease inhibitor cocktail (Roche Applied Science, Indianapolis, IN)), and subjected to Western blot analysis. Blots were blocked and probed with anti-phosphorylated RhoA 1:500 (Santa Cruz Biotechnology, Santa Cruz, CA) and anti-rabbit phosphorylated SHP2 (Y542) 1:500 (Cell Signaling Technology, Danvers, MA).

C11. Statistical analysis

t-test analysis was performed using SigmaPlot 10.0 (Systat Software Inc., San Jose, CA) and p-values were designated for each experiment, each of which were repeated a minimum of three times. Any null hypothesis with probability level less than 95% was rejected.

D. Results

D1. Cisplatin-induced decline in sensory function can be prevented with concurrent use of LM11A-31

CIPN was induced in age-matched C57/BL6 mice by intraperitoneal administration of 6 μg/g body weight (18 mg/m^2) cisplatin once every two weeks for a ten week treatment period (5 successive doses). Such doses are clinically relevant and represent a high, yet tolerable, dose successfully used to induce neuropathy in mice (James et al., 2010; Verdú et al., 1999). In addition to cisplatin, two additional, selective groups of mice received either a high (50 μg/g) or low (25 μg/g) dose of the p75^{NTR} receptor ligand mimetic, LM11A-31. This compound targets the p75^{NTR} receptor (Massa et al., 2006; Longo and Massa, 2008), which is known to lie upstream of RhoA activation and modulate Rho GTPase activity (James et al., 2008). Saline-treated mice were maintained as experimental controls. Mice were observed daily for clinical signs of chemotherapy treatment such as hair and weight loss. All mice receiving cisplatin showed consistent weight loss over the course of treatment, as well as increased hair loss. Any mice displaying any signs of discomfort, pain, or weight loss exceeding 20% of original body weight were euthanized in accordance with the East Carolina University Animal Care and Use Committee guidelines for animal use.

In order to assess peripheral nerve function in both control and experimental groups, Von Frey/Semmes-Weinstein monofilament testing was performed as previously described (James et al., 2010; Ta et al., 2009). Briefly, following a 10 minute acclimation period, Von Frey/Semmes-Weinstein monofilaments of varying diameters, which correspond to force, were sequentially applied to the plantar surface of the hindpaw until positive responses were elicited. Positive responses included both hindpaw withdrawal and licking and were recorded when

elicited at a specific force for 3 out of 5 monofilament applications. Clinically, similar testing is frequently employed to screen patients with suspected diabetic or chemotherapy-induced peripheral neuropathies (Grisold et al., 2012; Feng et al., 2009). In that case, the monofilaments are placed perpendicularly against the plantar surface of the great toe until bending, if a patient does not respond, monofilaments in ascending order are applied until a sensation is felt (Tanenberg, 2009).

In the current experiment, touch perception analysis with Von Frey/Semmes-Weinstein monofilaments showed a significant increase (p= 0.04, relative to saline) in force required to elicit a response, indicative of a decline in sensory nerve function, in the cisplatin treated group after 6 weeks (Fig. 2.1). However, addition of LM11A-31 at either high (50µg/g) or low (25µg/g) doses prevented these deficits in touch perception, as seen by significant reductions (p= 0.02, relative to cisplatin) in force applied to the hindpaw. Neither LM11A-31 doses alone showed responses that were significantly different from saline over the 10 week treatment period.

D2. LM11A-31 treatment reduces abnormal sural nerve fiber morphology induced by cisplatin

The rodent hindpaw, as well as the human foot, is innervated by branches of the sciatic nerve (tibial, common peroneal (fibular) and sural). The predominately sensory sural nerve provides innervation to the lower hind leg, heel, and plantar surface of the hindpaw or heal in the human foot. Therefore, sural nerves were harvested post treatment, Zamboni fixed, frozen and 5 µm cross-sections were subjected to further analysis. Through phase contrast microscopy, which highlights the myelin sheath as dark ring-like structures surrounding the inner axon, differences in nerve fiber morphologies can be seen between control and cisplatin-treated groups. As shown

in Fig. 2.2A, saline-treated nerve fibers display round morphologies that are well myelinated, as demonstrated by the dense black circles (red arrow). However, abnormally shaped nerve fibers (yellow arrows) and decreases in the degree of myelination (red arrows) were frequently observed in cisplatin-treated nerves, which is consistent with our previous data (James et al., 2010). Addition of 50 μg/g LM11A-31 to cisplatin treatment alleviated myelin sheath reduction (red arrow) and fibers maintained a rounded fiber morphology closely resembling that of saline. Interestingly, nerve fibers that received a lower dose of LM11A-31 maintained a high degree of myelination but, like cisplatin fibers, anomalous flattened and infolded morphologies were consistently observed (yellow arrows).

Due to natural variation in nerve sizes between animals, randomly selected 40 um^2 regions of sural nerve cross sections were used to collect and quantify morphological data (Fig. 2.2 B-F). All sural nerve sections were derived proximal to the sciatic bifurcation and displayed a single fascicle. Comparisons between the percentage of the total area occupied by axons, myelin and total fiber (myelin plus axon; Fig. 2.2B, C and D, respectively) showed a reduction in cisplatin nerves which was prevented by addition of either dose of LM11A-31 (p=0.05). Additionally, a 10% increase in percentage of the total area not occupied by fibers observed in cisplatin nerves (p=0.05) was diminished with either LM11A-31 doses (p=0.05; Fig. 2.2 E). Importantly, quantification of nerve fibers treated concurrently with LM11A-31 and cisplatin were not significantly different from saline. G-ratios, which describe the degree of myelination of a nerve fiber as a ratio between axonal diameter/fiber diameter (Rushton, 1951), were also calculated. Data revealed G-ratios within the optimal range (0.47-0.6) for the sural nerve in all four treatment groups (Chomiak and Hu, 2009; Fig. 2.2F). Cisplatin treatment alone did not alter the G-ratio significantly from saline. However, significant increases in the degree of myelination

were observed with both high and low LM11A-31 doses, further supporting data suggesting the $p75^{NTR}$ receptor plays an important role in myelin regulation (Cosgaya et al., 2002; Song et al., 2006).

D3. LM11A-31 inhibits cisplatin-induced increase in phosphorylated RhoA but promotes SHP2 phosphorylation in peripheral nerves

To determine and compare RhoA activity levels between treatment groups we performed immunofluorescent analysis of frozen sural nerve cross sections with antibodies detecting total levels of RhoA (tRhoA) and phosphorylated RhoA (pRhoA). Phosphorylation at serine 188 is an important site for negative regulation of RhoA by cAMP and cGMP-dependent kinases (Dong et al., 1998; Ellerbroek et al., 2003; Sawada et al., 2001). Therefore, decreases in pRhoA are indicative of an increase in the levels of active (GTP-bound) RhoA. Immunofluorescent data revealed only a slight increase in tRhoA activity in cisplatin nerves compared to controls, while both doses of LM11A-31 showed an overall reduction in tRhoA activity (Fig. 2.3A, top panel). Quantification of pixel intensity in Fig. 3B confirms the visual comparison and demonstrates LM11A-31 not only significantly reduces tRhoA activity compared to cisplatin (p=0.05), but also to saline (p=0.0001). pRhoA immunostaining (Fig. 2.3A, bottom panel), on the other hand, reveals a dramatic 32% pRhoA decrease in cisplatin versus saline nerves (p=0.0001, Fig. 2.3C), suggesting an increase in active RhoA levels. Addition of 50 μg/g LM11A-31 revealed a 40% pRhoA activity increase relative to cisplatin (p=0.0001) and closely resembled saline controls. However, the lower LM11A-31 dose was only minimally effective in preventing cisplatin-induced pRhoA decreases with only a 2% increase in pixel intensity versus cisplatin only nerves (Fig. 2.3C). Interestingly, this data implies that tRhoA activity can be inhibited similarly

regardless of high or low dose, but LM11A-31 is less sensitive at lower doses for pRhoA activity inhibition. When expressed as a ratio of pRhoA to tRhoA the pixel intensity quantification more clearly describes the activity level of RhoA due to treatment (Fig. 2.3D). These data demonstrate a significant 40% increase in RhoA activity due to cisplatin which could be significantly inhibited by the addition of high (65%; p=0.0002) and low (37% p=0.04) LM11A-31 doses. Such results not only support our hypothesis that RhoA activity is increased due to cisplatin treatment, but suggest that treatment with LM11A-31 could be employed as a preventative measure.

In order to further confirm RhoA's role in CIPN we assessed protein expression in fresh frozen sciatic nerve samples. Due to insufficient protein concentrations obtained from sural nerves, we utilized the larger sciatic nerve from which the sural nerve branches in the mouse. The tRhoA expression appeared to be unchanged in the sciatic nerve, regardless of treatment (Fig. 2.4, first panel). However, reflecting pRhoA immunofluorescent results, cisplatin decreased pRhoA expression and concurrent use of LM11A-31 lead to expression similar to controls (Fig. 2.4, second panel). SHP2 tyrosine phosphatase, downstream of NGF receptor tyrosine kinases, is known to modulate RhoA signaling. Additional analysis of both phosphorylated (Fig. 2.4, third panel) and total SHP2 phosphatase (Fig. 2.4, fourth panel) levels were performed. Results demonstrated decreased expression of phosphorylated SHP2, which is correlated with increased RhoA activity, due to cisplatin treatment. LM11A-31 treatment was able to abrogate this effect when used in conjunction with cisplatin. However, similarly to tRhoA levels (Fig. 2.4, first panel), total levels of SHP2 (Fig. 2.4, fourth panel) were not altered by either cisplatin or LM11A-31.

D4. LM11A-31 and SHP2 phosphatase modulation can inhibit cisplatin-induced neurodegeneration

RhoA has been well established as a negative regulator of neuronal branching (Ahnert-Hilger et al., 2004; Bito et al., 2000; Threadgill et al., 1997). In order to further analyze the effects of cisplatin and LM11A-31 on RhoA and RhoA-mediated processes *in vitro*, a primary neuronal culture system was established from E18 mouse cortical tissue. Typical neuronal development begins with axonal extension at 3 days *in vitro* (DIV) and establishment of dendritic processes from 5-7 DIV (Dotti et al., 1988; James et al., 2008). Therefore, cortical neurons were cultured for 5 DIV, treated with cisplatin (8 μg/mL), and after 24 hours, LM11A-31 (100 nM) was then applied for an additional 24 hours. At 7 DIV, RhoA was constitutively activated in selected cells with a SHP2 phosphatase inhibitor, calpeptin, for 30 minutes (1 unit/mL). Tyrosine dephosphorylation of p190-B RhoGAP modulated by SHP2 phosphatase has been shown to function as a constitutive RhoA activator (Kontaridis et al., 2004; Sordella et al., 2003).

As depicted in Fig. 2.5.A (upper panel) immunofluorescent analysis of actin-based structures reveals a distinct reduction in branching due to treatment with either calpeptin or cisplatin. Quantification of branch number (Fig. 2.5B), sprout number (Fig. 2.5C), and branch length (Fig. 2.5D) shows significant reductions due to cisplatin treatment. However, RhoA activation through SHP2 phosphatase resulted in less dramatic (not significant) reductions in both branch (Fig. 2.5B) and sprout (Fig. 2.5C) numbers. In contrast, addition of LM11A-31 to cisplatin treatment increased branch numbers (Fig. 2.5B), sprout numbers ($p<0.03$; Fig. 2.5C), and branch length ($p<0.02$; Fig. 2.5D). Concurrent treatment of LM11A-31 and calpeptin

resulted in a significant increase in branch number ($p<0.05$; Fig. 2.5B), while sprouting and branch length remained unchanged.

In order to elucidate RhoA activity in treated neurons, pRhoA immunostaining was performed. Total RhoA levels (Fig. 2.6A; upper panel) were shown to be similar in cisplatin and control neurons, while calpeptin treatment significantly increased the total level of RhoA (Fig. 2.6B; $p<0.005$). Addition of LM11A-31 to both cisplatin and calpeptin-treated cells resulted in significant decreases in tRhoA activity compared to each treatment alone (Fig. 2.6B). As shown in Fig. 2.6A (lower panel) and quantified and Fig. 2.6C, results revealed a significant increase in pRhoA activity due to both calpeptin ($p<0.01$) and cisplatin ($p<0.0006$) application relative to non-treated controls. The addition of LM11A-31 significantly inhibited these increases elicited by cisplatin ($p<0.003$). The same inhibitory trend from LM11A-31 can be observed for these increases elicited by calpeptin, although the inhibition was not significant. The ratio of pRhoA to tRhoA pixel intensity revealed expected increases in RhoA activity in both calpeptin ($p<0.0006$) and cisplatin-treated ($p< 0.002$) neurons that was attenuated with addition of LM11A-31 to cisplatin-treated ($p<0.009$) neurons, but not those treated with calpeptin (Fig. 2.6D). These results not only further support RhoA as a negative regulator of neurite branching, but confirm our *in vivo* results suggesting that LM11A-31-mediated RhoA inhibition can preserve neuronal structure during cisplatin treatment.

Additional analysis of protein expression in lysates prepared from primary neuronal cultures treated with cisplatin, calpeptin and LM11A-31 were performed. As depicted in Fig. 2.6E decreases in pRhoA expression, indicative of increased levels of active RhoA, were observed in cisplatin-treated lysates which could be countered by LM11A-31 application. However, calpeptin treatment did not result in major reductions in pRhoA expression.

Additionally, co-treatment of neuronal cultures with LM11A-31 and calpeptin did not display clear inhibitory actions on protein expression levels. Phosphorylated SHP2 (pSHP2) expression, which is indicative of inhibited SHP2 phosphatase activity and increased RhoA activation, was shown to be significantly decreased due to both cisplatin ($p<0.02$) and calpeptin-treatment ($p<0.03$; Fig. 2.6F). However, LM11A-31 was able to attenuate cisplatin-induced pSHP2 reductions but not calpeptin. These results indicate that at the neuronal culture level there are likely two independent mechanisms of RhoA activations through $p75^{NTR}$ and calpeptin-induced inhibition of SHP2 phosphatase.

E. Discussion

Peripheral neuropathy remains a debilitating, dose-limiting side effect of many platinum-based chemotherapeutics. To date, multiple avenues of neuroprotective intervention have been investigated with concurrent cisplatin use including Vitamin E (Pace et al., 2003; Pace et al., 2007; Pace et al., 2010), glutathione (Cascinu et al., 1995; Smyth et al., 1997) and Org 2766, an adrenocorticotrophic hormone analogue (Koeppen et al., 2004; van der Hoop et al., 1990a). However, clinical success has been minimal; leaving dose reductions or alterations in dose scheduling the only option for patients (Beijers et al., 2012; Pachman et al., 2011; Schloss et al., 2013).

In the current study, we show elevation of the small GTPase RhoA is correlated with increased incidence of peripheral neuropathy in a mouse model of CIPN. Additionally, upstream inhibition of RhoA with LM11A-31, a $p75^{NTR}$ receptor ligand mimetic, could not only suppress RhoA upregulation in cisplatin-treated mice, but prevent cisplatin-induced decline in peripheral nerve function seen using the Von Frey/Semmes-Weinstein monofilament testing. Importantly,

morphological analysis of sural nerve cross sections revealed that abnormal nerve fibers frequently seen due to cisplatin treatment could be thwarted with the addition of LM11A-31 at both high and low doses. Our *in vitro* studies also support data derived in our *in vivo* model of CIPN. For example, the increased RhoA activity and dramatic reduction in neurite branching and sprouting due to cisplatin application could be inhibited by addition of LM11A-31. Such results suggest a novel neuroprotective target that could be exploited during cisplatin chemotherapy.

$p75^{NTR}$ receptor acts as a displacement factor that releases RhoA from Rho GDP-dissociation inhibitor (Yamashita and Tohyama, 2003). This activation of RhoA has a key role in inducing inhibition of axon growth (Ahnert-Hilger et al., 2004; Kranenburg et al., 1997). Our studies support a model that in addition to its inhibitory action on DNA synthesis, cisplatin elicits cellular stress leading to $p75^{NTR}$ receptor dissociation from RhoA, thereby promoting RhoA activation and signaling to Y-27632-sensitive $p160^{ROCK}$/Rho kinase. Increased RhoA/ROCK signaling results in axon retraction and repulsion (Nakayama et al., 2000; Fig 2.7). Furthermore, cisplatin-induced cellular stress suppresses SHP2 tyrosine phosphatase, which also activates RhoA. Calpeptin-sensitive inhibition of SHP2 activates RhoA and attenuates neurite branching and extension, further supporting this model. Notably, cisplatin-induced increases in RhoA activity and decreases in tyrosine phosphorylation of SHP2 can be reversed by LM11A-31 treatment. LM11A-31 also countered the trends of calpeptin in activating RhoA and reducing neuronal sprout numbers. Therefore, LM11A-31 is a small molecule that can effectively reduce the impact of experimental CIPN.

Identification of RhoA signaling as a potential neuroproetctive target in CIPN has important implications. Studies showed that inhibition of RhoA downstream effector $p160^{ROCK}$/Rho kinase by Y-27632 attenuated tumor growth, indicating that suppression of RhoA

signaling may be used as an adjuvant to counteract negative side effectst of cisplatin chemotherapy (Routhier et al., 2010). Employment of RhoA inhibitor in the treatment regimen may also allow cisplatin to be effective at the lower dosages, further reducing the risks of peripheral neuropathy. The identification of the RhoA upstream modulator $p75^{NTR}$ and its inhibitor LM11A-31 provided yet additional important evidence that RhoA suppression is a potential site of intervention to circumvent CIPN. Interestingly, the nerve growth factor (NGF) receptor has also been implicated in cisplatin-induced neurotoxicity, and as shown by Aloe et al. (2000) that repeated administration of exogenous NGF can be an effective measure to combat cisplatin damage in the mouse (Authier et al., 2009). Future studies will determine the neuroprotective effects of LM11A-31 in tumor-bearing mouse models as a significant step towards its application clinically.

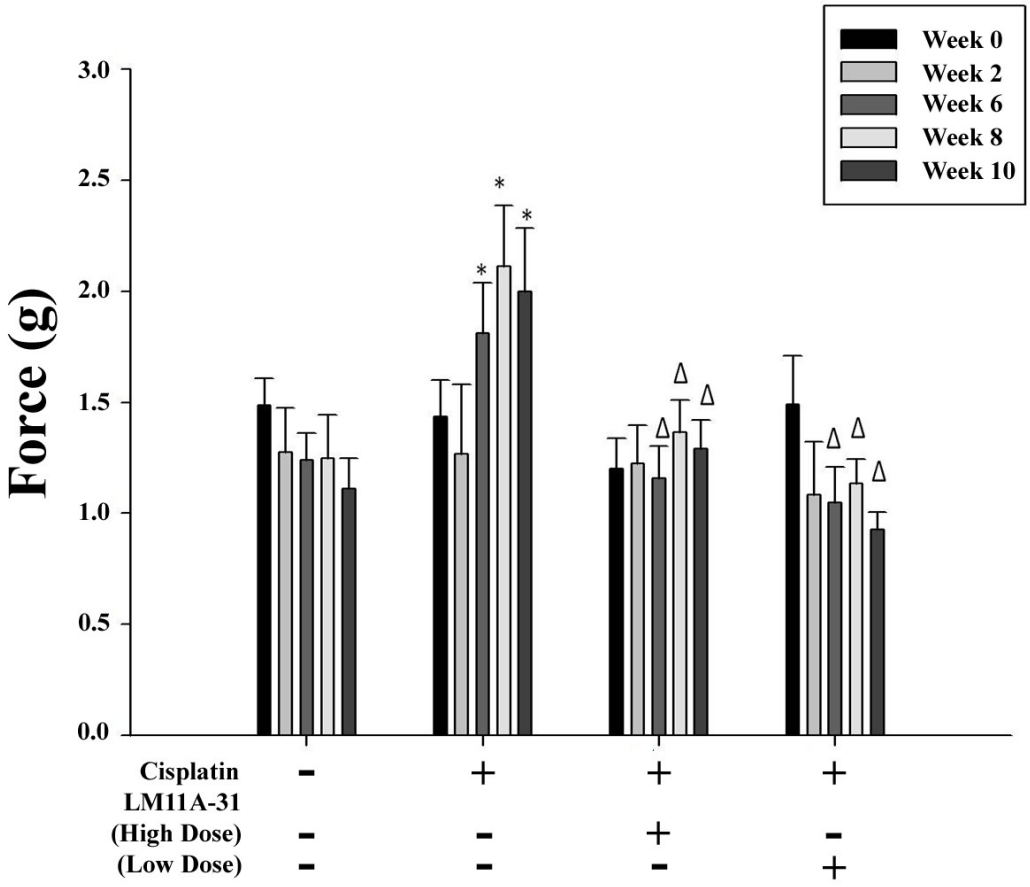
Week 0
Week 2
Week 6
Week 8
Week 10
Force (g)
3.0
2.5
2.0
1.5
1.0
0.5
0.0
Cisplatin
LM11A-31
(High Dose)
(Low Dose)
- + + +
- - + -
- - - +

Figure 2.1 ***Cisplatin-induced decline in sensory function can be prevented with concurrent use of LM11A-31.***

Peripheral nerve function was analyzed by mechanical (touch) stimulus perception using Von Frey/ Semmes-Weinstein monofilaments. Results showed that cisplatin induced a decrease in sensory function over the course of treatment that could be prevented by either high or low doses of LM11A-31. Values represent mean ± S.E.M. $p< 0.04$ *, relative to saline; $p<0.02$ $^{\Delta}$, relative to cisplatin. n= 10 animals/ treatment group saline and cisplatin; n=12 animals/ treatment group LM11A-31 high and low dose.

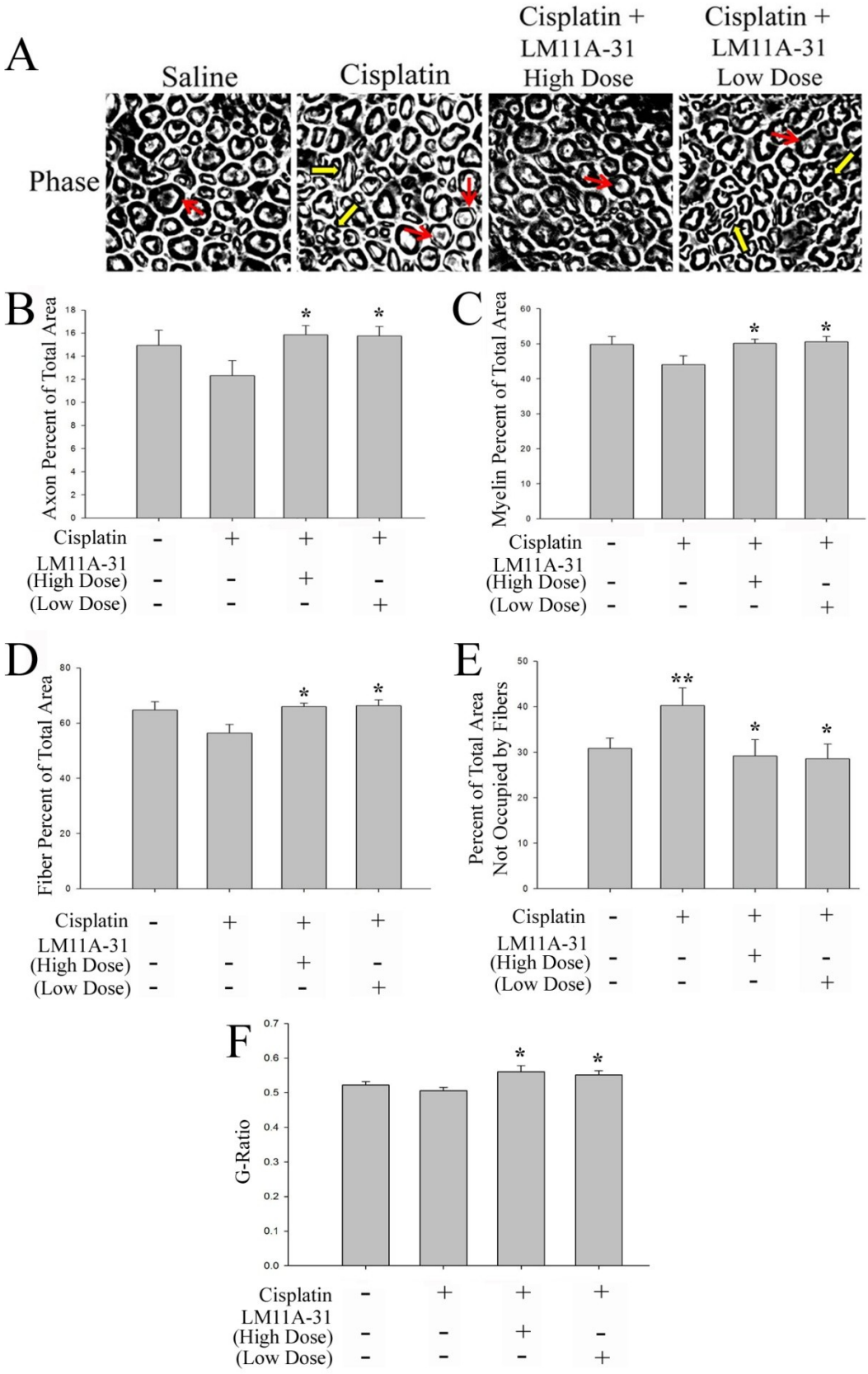
A
Saline
Cisplatin
Cisplatin + LM11A-31 High Dose
Cisplatin + LM11A-31 Low Dose
Phase
B
Axon Percent of Total Area
C
Myelin Percent of Total Area
D
Fiber Percent of Total Area
E
Percent of Total Area Not Occupied by Fibers
F
G-Ratio
Cisplatin
LM11A-31 (High Dose)
(Low Dose)

Figure 2.2 ***LM11A-31 treatment reduces abnormal sural nerve fiber morphology induced by cisplatin.***

Sural nerve cross sections were analyzed by phase-contrast microscopy (63X). (A) Cisplatin altered sural nerve morphology (yellow arrows) and myelination (red arrows) in comparison to saline treatment. LM11A-31 treatment reversed the cisplatin-induced abnormally shaped nerve and reduced myelination. Quantification of sural nerve axon (B), myelin (C), fibers (axon + myelin, D), unoccupied (E) percent of areas in randomly selected 40 um^2 regions, and G-ratio (ratio of axonal diameter to the total fiber diameter which then reflects the level of myelination of a nerve fiber, F) of sural nerve cross sections. Results indicate a reduction in the percent of area occupied by axons (B), myelin (C) and fibers (D) in the cisplatin treated group and a significant recovery with LM11A-31 treatment. Additionally, the percent of space unoccupied by nerve fibers (E) was significantly increased in cisplatin treated sural nerves, which could be prevented by addition of LM11A-31. G-ratio (F) calculations revealed the degree of myelination is significantly increased with addition of LM11A-31 relative to cisplatin. Values represent mean ± S.E.M. $p< 0.05$ **, relative to saline; $p<0.05$ *, relative to cisplatin. n=6 regions/ treatment group.

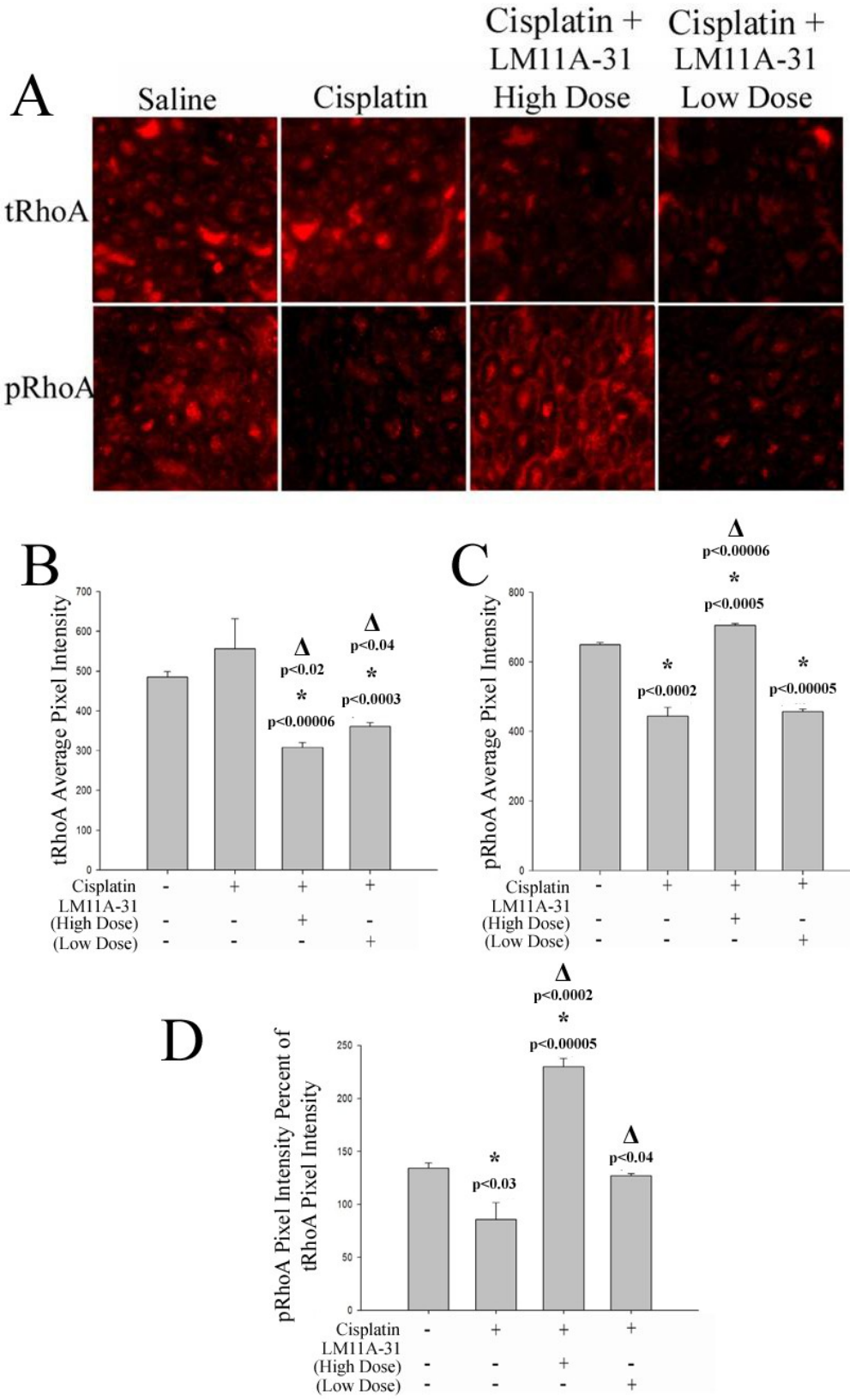
A
Saline
Cisplatin
Cisplatin + LM11A-31 High Dose
Cisplatin + LM11A-31 Low Dose
tRhoA
pRhoA
B
tRhoA Average Pixel Intensity
Δ p<0.02 * p<0.00006
Δ p<0.04 * p<0.0003
Cisplatin - + + +
LM11A-31 (High Dose) - - + -
(Low Dose) - - - +
C
pRhoA Average Pixel Intensity
* p<0.0002
Δ p<0.00006 * p<0.0005
* p<0.00005
Cisplatin - + + +
LM11A-31 (High Dose) - - + -
(Low Dose) - - - +
D
pRhoA Pixel Intensity Percent of tRhoA Pixel Intensity
* p<0.03
Δ p<0.0002 * p<0.00005
Δ p<0.04
Cisplatin - + + +
LM11A-31 (High Dose) - - + -
(Low Dose) - - - +

Figure 2.3 ***LM11A-31 inhibits cisplatin-induced increase in phosphorylated RhoA in the sural nerve.***

Total RhoA (tRhoA) and phosphorylated RhoA (pRhoA) immunofluorescent analysis of 5 um sural nerve cross sections. (A, lower panel) Results revealed an increase in the levels of active RhoA due to cisplatin treatment as indicated by a decrease in pRhoA immunostaining. However, cisplatin treatment did not alter the expression of total RhoA levels (A, upper panel). Concurrent treatment with LM11A-31 showed an increase in pRhoA and a decrease in tRhoA immunostaining which is indicative of RhoA inhibition. Quantification of pixel intensity of tRhoA (B), pRhoA (C) and the ratio of pRhoA pixel intensity to tRhoA pixel intensity (D) were determined. Values represent mean ± S.E.M; *, relative to saline; Δ, relative to cisplatin. n=4 nerves/ treatment group.

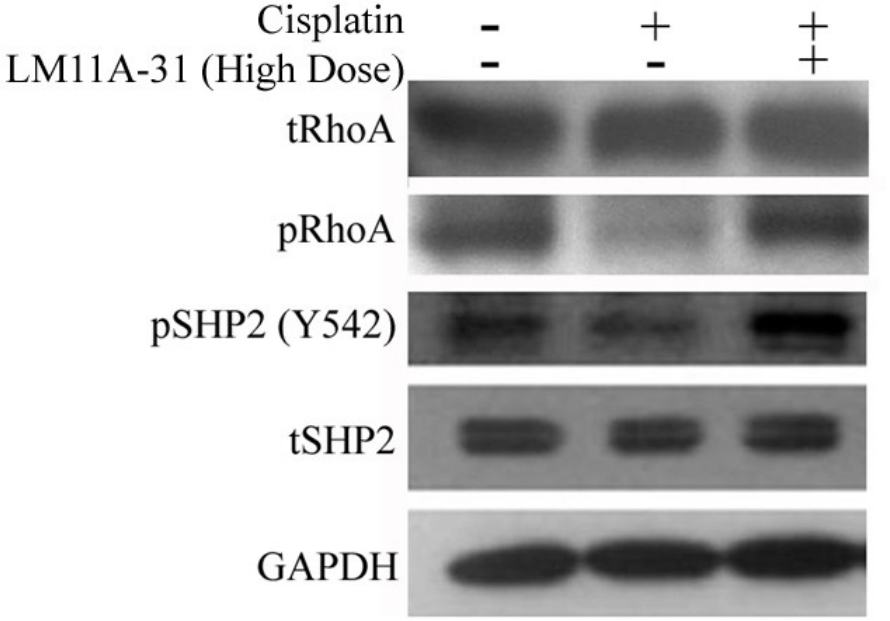
Cisplatin - + +
LM11A-31 (High Dose) - - +
tRhoA
pRhoA
pSHP2 (Y542)
tSHP2
GAPDH

Figure 2.4 ***Increased pRhoA and pSHP2 protein expression due to cisplatin treatment can be inhibited by a high dose of LM11A-31.***

Mouse sciatic nerves were harvested, homogenized and subjected to Western blot analysis. Blots were then probed with total RhoA (tRhoA), phosphorylated RhoA (pRhoA), phosphorylated SHP2 (pSHP2), and total SHP2 (tSHP2) antibodies. GAPDH was used as a loading control.

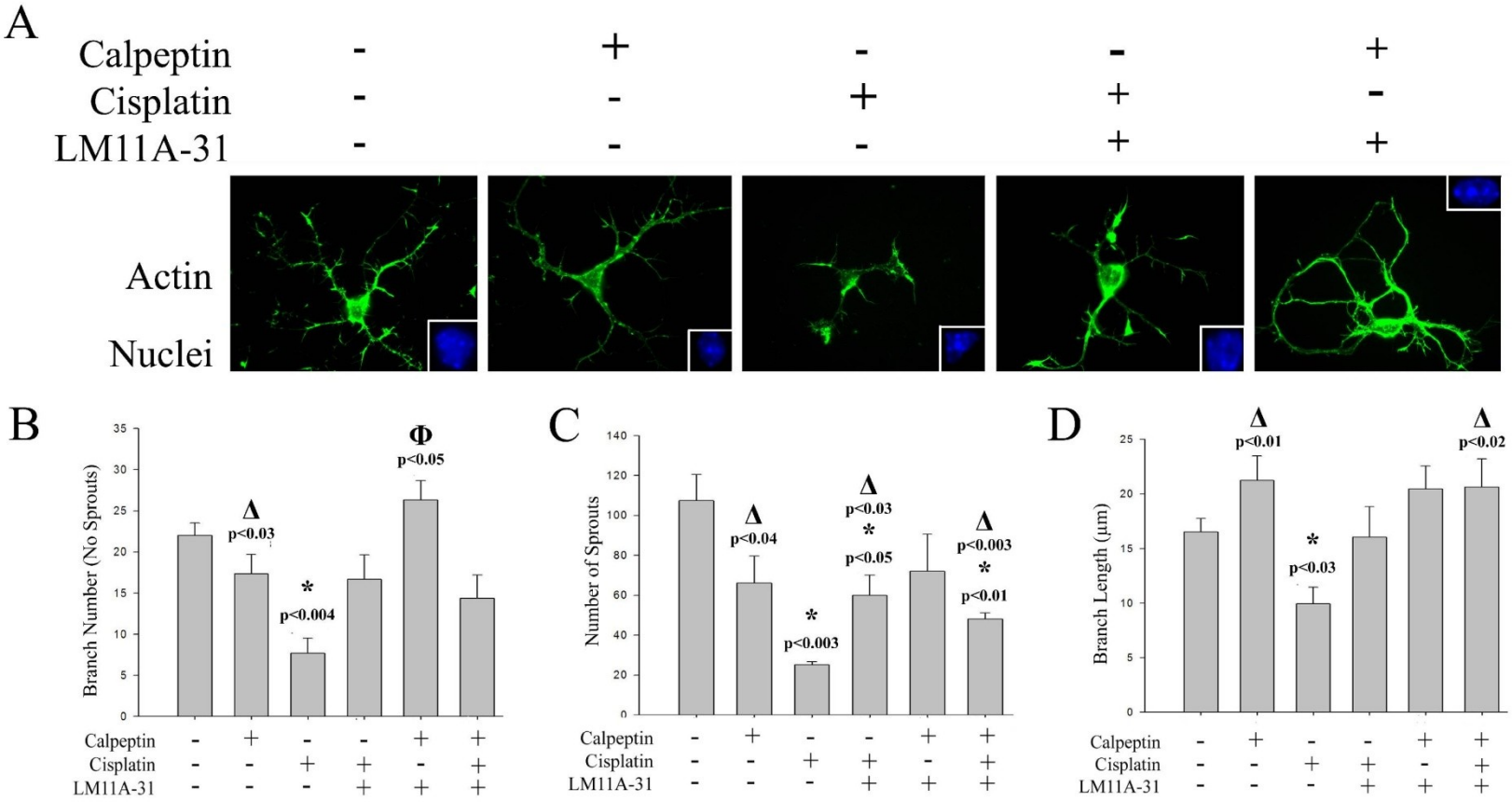
A
Calpeptin - + - - +
Cisplatin - - + + -
LM11A-31 - - - + +
Actin
Nuclei
B
Branch Number (No Sprouts)
Δ p<0.03
* p<0.004
Φ p<0.05
C
Number of Sprouts
Δ p<0.04
* p<0.003
Δ p<0.03
* p<0.05
Δ p<0.003
* p<0.01
D
Branch Length (μm)
Δ p<0.01
* p<0.03
Δ p<0.02
Calpeptin
Cisplatin
LM11A-31

Figure 2.5 *LM11A-31 inhibits cisplatin-induced neurodegeneration*.

Mouse cortical neurons grown for 5 days i*n vitro* (DIV) were treated for 24 hours with cisplatin (8 ug/μL), at 6 DIV with LM11A-31 for 24 hours (100nM), or at 7 DIV with calpeptin for 30 minutes (1 unit/mL). (A) Neurons were labeled with FITC-phalloidin (green); nuclei were labeled with Hoechst (inset, blue). Quantification of branch number (B), sprout number (C), branch length (D) and pRhoA pixel intensity (E). Values represent mean ± S.E.M. *, relative to saline; Δ, relative to cisplatin; Φ, relative to calpeptin. n= 3 representative neurons/ treatment group.

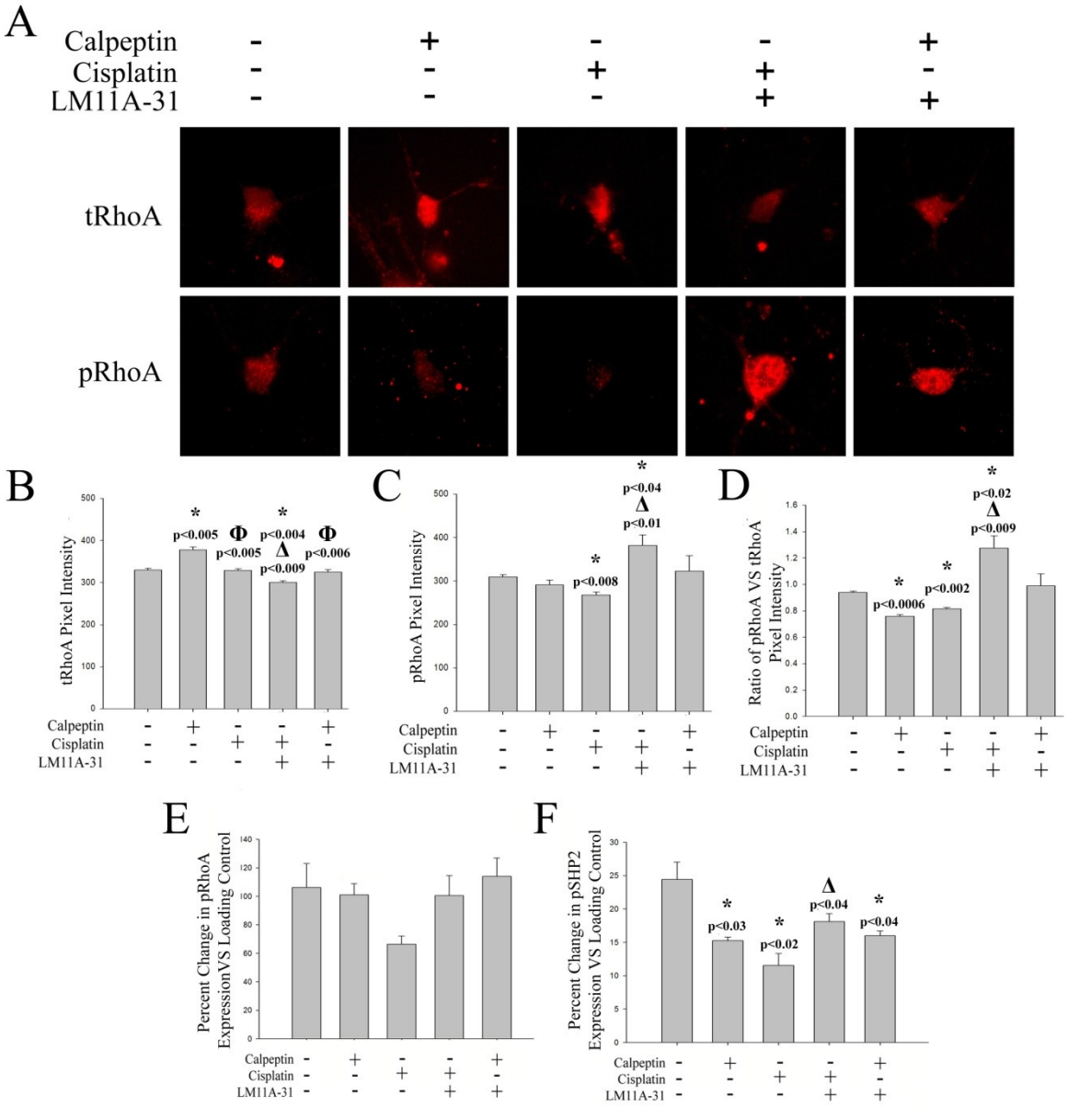
A
Calpeptin
Cisplatin
LM11A-31
tRhoA
pRhoA
B
tRhoA Pixel Intensity
p<0.005
Φ
p<0.005
p<0.004
Δ
p<0.009
Φ
p<0.006
C
pRhoA Pixel Intensity
p<0.008
p<0.04
Δ
p<0.01
D
Ratio of pRhoA VS tRhoA Pixel Intensity
p<0.0006
p<0.002
p<0.02
Δ
p<0.009
E
Percent Change in pRhoA Expression VS Loading Control
F
Percent Change in pSHP2 Expression VS Loading Control
p<0.03
p<0.02
Δ
p<0.04
p<0.04

Figure 2.6 ***LM11A-31 inhibits RhoA activity stimulated by cisplatin and calpeptin.***

Mouse cortical neurons grown for 5 days i*n vitro* (DIV) were treated for 24 hours with cisplatin (8 ug/mL), at 6 DIV with LM11A-31 for 24 hours (100nM), or at 7 DIV with calpeptin for 30 minutes (1 unit/mL). (A) Neurons were labeled with total RhoA (top panel) and phosphorylated RhoA (lower panel). Quantification of total RhoA pixel intensity (B), phosphorylated RhoA pixel intensity (C) and a ratio of the pixel intensity of phosphorylated RhoA to that of total RhoA(D) were calculated. n=3 representative neurons/ treatment group. Western blot analysis of phosphorylated RhoA (E) and phosphorylated SHP2 (F) were also performed and quantified. Values represent mean ± S.E.M. *, relative to saline; Δ, relative to cisplatin; Φ, relative to calpeptin.

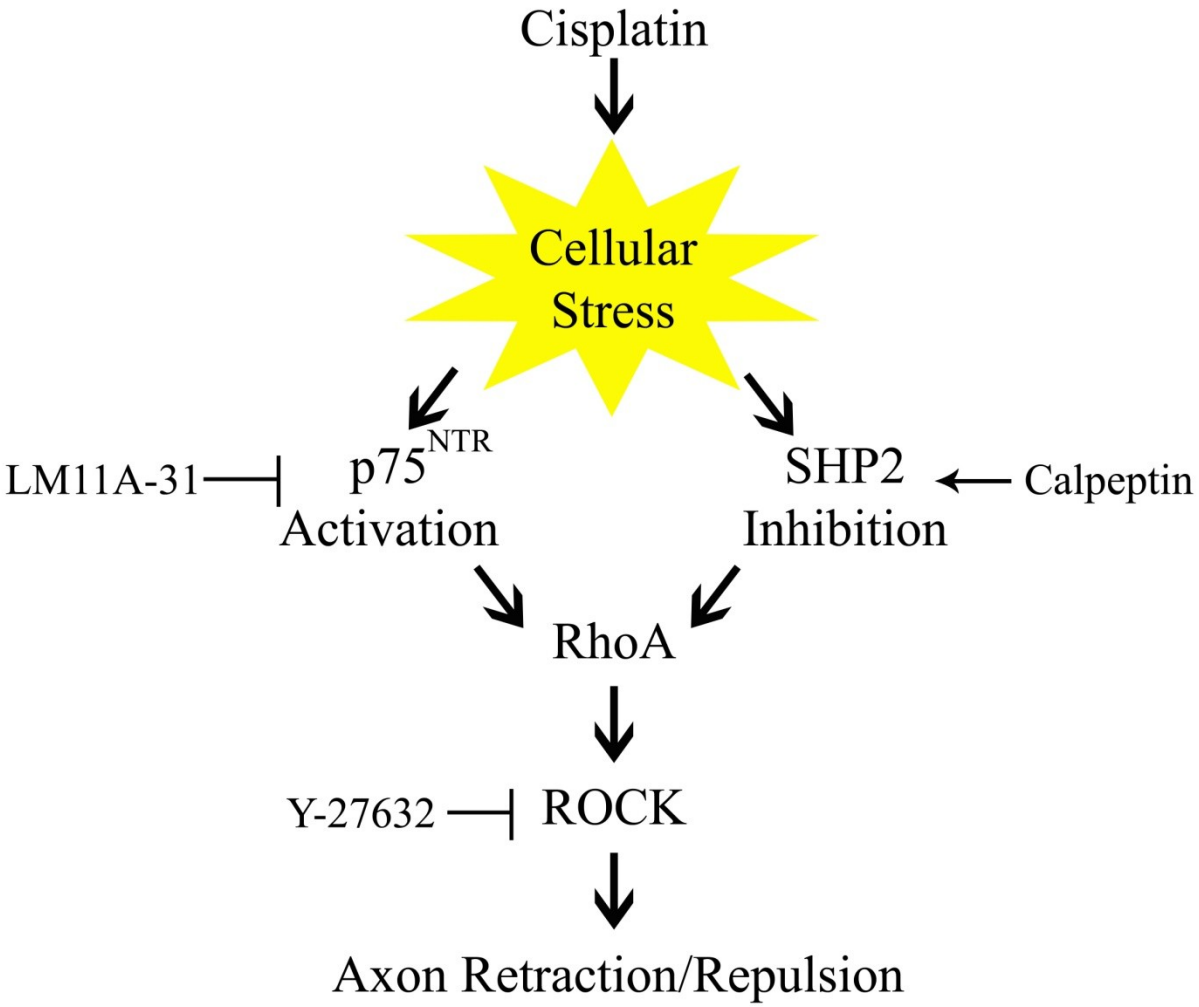
Cisplatin
Cellular Stress
LM11A-31
p75NTR
Activation
SHP2
Inhibition
Calpeptin
RhoA
Y-27632
ROCK
Axon Retraction/Repulsion

Figure 2.7 ***Proposed mechanism of cisplatin-induced peripheral neuropathy*****.**

Cisplatin-induced cellular stress (DNA and/or mitochondrial) may result in the activation of both the $p75^{NTR}$ receptor and SHP2 tyrosine phosphatase, through which RhoA can be activated, and resulting in neuronal retraction and repulsion can result.

F. Acknowledgements

We would like to acknowledge Jonathon Lee, Maria Duenas, and Zhiying Weng for their assistance performing Von Frey/Semmes-Weinstein monofilament testing. Western blots of pSHP2 and tSHP2 in Figure 2.4 were performed by Zhiying Weng.

CHAPTER III: SMALL MOLECULE TARGETING CDC42-INTERSECTIN INTERACTION DISRUPTS GOLGI ORGANIZATION AND SUPPRESSES CELL MOTILITY

This chapter is modified and reprinted from the Proceeding of the National Academy of Science, **110**, 1261-1266 (2013), see Appendix B.

A. Summary

Signaling through the Rho family of small GTPases has been intensely investigated for its crucial roles in a wide variety of human diseases. While RhoA and Rac1 signaling pathways are frequently exploited with the aid of effective small molecule modulators, studies on the Cdc42 subclass lagged due to lack of specific activator or inhibitors. In order to solve this problem and fill this important gap, we have applied high-throughput in silico screening and identified compounds that are able to fit into the surface groove of Cdc42, which is critical for guanine nucleotide exchange factor (GEF) binding. Based on the interaction between Cdc42 and intersectin, a specific Cdc42 GEF, we discovered compounds that rendered intersectin-like interactions in the binding pocket. By using *in vitro* binding and imaging as well as biochemical and cell-based assays, we demonstrated that ZCL278 has emerged as a selective Cdc42-small molecule modulator that directly binds to Cdc42 and inhibits its functions. In Swiss 3T3 fibroblast cultures ZCL278 abolished microspike formation and disrupted GM130-docked Golgi structures, two of the most prominent Cdc42-mediated subcellular events. ZCL278 reduces the peri-nuclear accumulation of active Cdc42 in contrast to NSC23766, a selective Rac inhibitor. ZCL278 suppresses Cdc42-mediated neuronal branching and growth cone dynamics as well as

actin-based motility and migration in a metastatic prostate cancer cell line (PC-3) without disrupting cell viability. Thus, ZCL278 is the first small molecule that specifically targets Cdc42-intersectin interaction and inhibits Cdc42-mediated cellular processes, therefore providing a powerful tool for research of Cdc42 subclass of Rho GTPases in human pathogenesis such as cancer and neurological disorders.

B. Introduction

Cdc42, a member of the Rho GTPase family of low molecular weight G-proteins, is an important regulator of many biological processes. First identified by its involvement in the establishment of polarity in *Saccharomyces cerevisiae*, Cdc42 has since been shown to play key roles in cytoskeletal organization, vesicular trafficking, cell cycle control, and transcription (Cerione, 2004; Johnson and Pringle, 1990; Stengel and Zheng, 2011). As with most GTPases, transduction of signals occurs through the exchange of GDP for GTP, thus activating Cdc42 (Sinha and Yang, 2008). The cycling between nucleotide-dependent conformation states of Rho family GTPases is supported by three regulatory proteins: guanine nucleotide exchange factors (GEFs), GTPase activation proteins (GAPs), and guanine nucleotide dissociation inhibitors (GDIs). GEFs facilitate activation of the GTPase by catalyzing the exchange of bound GDP for GTP, while GAPs promote the GDP-bound confirmation (Lu et al., 2009; Ridley, 2006). Additional negative regulation occurs through GDIs which sequester Rho proteins in the cytoplasm and prevent nucleotide exchange (Ellenbroek and Collard, 2007).

Recent studies have implicated aberrant Cdc42 activity in a variety of human pathologies including cancer and neurodegeneration (Auer et al., 2011; Stengel and Zheng, 2001). Interestingly, no mutations in the Cdc42 gene have been identified that can be attributed to

human cancer (Rihet et al., 2001). Abnormal phenotypes appear to be due to deregulation or overexpression of Cdc42 in an apparent tissue and microenvironment-dependent fashion (Stengel and Zheng, 2001). Cdc42 has been attributed to several aspects of cancer including cellular transformation (Lin et al., 1999) and metastasis (Chen et al., 2010; Johnson et al., 2010). As a key regulator of neurite morphogenesis, Cdc42 has also been shown to be crucial for normal brain development, as conditional Cdc42 knockout mice do not survive birth and show gross brain abnormalities (Auer et al., 2011; Garvalov et al., 2007).

However, among the three classical Rho subfamilies, studies on Cdc42 signaling lag behind those of RhoA and Rac1. This is partly due to the more rapid activation-inactivation cycles of Cdc42 in T-cells and the lack of selective small molecule tools to aid in capturing this process directly. In the current study, we have utilized computer-assisted virtual screening to identify compounds that are able to fit into the surface groove of Cdc42, which is critical for GEF binding. Based on Cdc42's interaction with intersectin (ITSN), a specific Cdc42 GEF, chemical compounds that rendered ITSN-like interactions in the binding pocket were preferentially selected for further investigation (Ahmad and Lim, 2010; Goreshnik and Maly, 2010; Snyder et al., 2002). We have now determined ZCL278 as a potent, cell permeable Cdc42-specific small molecule inhibitor that suppresses actin-based cellular functions, including Golgi organization and cell motility.

C. Experimental procedures

C1. Virtual screening

The Glide program (Schrodinger, New York, NY) was employed to screen the SPECS database consisting of 197,000 compounds for small molecules that can disrupt the interaction of

Cdc42 with ITSN. The crystal structure of Cdc42-ITSN complex (Protein Data Bank ID: 1KI1) (Synder et al., 2002) was used in the virtual screening. The ITSN residues that occupy the Cdc42 binding interface are Leu1376, Met1379, Gln1380, Thr1383, and Arg1384. The binding pocket on Cdc42 was created with residues of Cdc42 within 7.0 Å of the center of the above five ITSN residues. After the protein structure was prepared in Protein Preparation Wizard, the docking grid was generated in the Receptor Grid Generation module. After preparation in LigPrep (Schrodinger, New York, NY), the compounds were subjected to HTVS (high-throughput virtual screening) docking and the top ranked 50,000 molecules were subjected to more stringent SP (standard precision) docking. The top ranked 100 molecules were manually inspected to select 30 compounds for *in vitro* and biological testing.

C2. Compound synthesis

General procedures

NMR spectra were recorded on a Bruker Avance III at 400 MHz. Chemical shifts are expressed in parts per million (™) relative to residual solvent as an internal reference ($CDCl_3$: 7.26; MeOD: 3.31; DMSO-d_6: 2.50). High resolution mass spectra were obtained on Bruker micrOTOF II. Column chromatography was performed using Huanghai silica gel (45-75 μM). High performance liquid chromatography analysis was performed on an Agilent 1200 with a flow rate of 1 mL/min and a gradient of 20% v/v MeOH in H_2O (t = 0.0 min) to 100% MeOH (t = 20.0 min) using a DAD detector. A ZORBAX Eclipse XDB-C18 column (4.6 mm×150 mm, 5 μM) was used. Purity of compounds was based on the integrated UV chromatogram at 254 nm. All reagents and building blocks were commercially available unless otherwise indicated. Reactions were not optimized for maximum yields.

C3. Synthetic procedures

Ethyl 2-(4-bromo-2-chlorophenoxy) acetate (compound 2)

To a solution of 4-bromo-2- chlorophenol (**solution 1**) (5.2 g, 25.0 mM) and ethyl 2-bromoacetate (4.3 g, 25.7 mM) in 50 mL DMF, anhydrous K_2CO_3 (3.45 g, 25.0 mM) was added (Fig. 3.1D). After stirring overnight at 70 ^oC, the mixture was poured into 150 mL water and extracted with ethyl acetate (70 mL×4). The organic layer was combined, washed with brine (100 mL ×3) and dried over anhydrous Na_2SO_4. The residue after rotary evaporation was purified by column chromatography to give **compound 2** (6.18 g, 84.1% yield) as a light oil. ^1H NMR (400 MHz, $CDCl_3$): ™7.53 (singlet (s), 1H), 7.30 (doublet (d), 1H, J = 8.4 Hz), 6.72 (d, 1H, J = 8.4 Hz), 4.68 (s, 2H), 4.26 (quartet (q), 2H, J = 7.2 Hz) and 1.29 (triplet (t), 3H, J = 7.2 Hz).

2-(4-Bromo-2-chlorophenoxy) acetic acid (compound 3)

To solution of **2** (5.0 g, 17.0 mM) in 50 mL dioxane, 1 M NaOH (50 mL) was added. After stirring at room temperature overnight, the mixture was acidified with 1 M hydrochloric acid to pH = 3. After the reaction mixture was extracted with ethyl acetate (50 mL×4), the organic layer was washed with brine (50 mL), dried over anhydrous Na_2SO_4 and concentrated to give **compound 3** (4.69 g, 94.3% yield) as a white solid. ^1H NMR (400 MHz, DMSO-d_6): ™7.66 (s, 1H), 7.44 (d, 1H, J = 8.8 Hz), 6.97 (d, 1H, J = 8.8 Hz), 4.72 (s, 2H).

4-(3-(2-(4-Bromo-2-chloro-phenoxy)-acetyl)-thioureido)-N-(4,6-dimethyl-pyrimidin-2-yl)-benzenesulfonamide (compound 5)

Compound 3 (539 mg, 2.0 mM) in 25 mL $SOCl_2$ and a drop of DMF were heated to reflux. After **3** hours, $SOCl_2$ was removed by distillation and the residue was dried *in vacuo* for 5 minutes to give crude acyl chloride **compound 4**. The solution of **4** in 10 mL dry acetone was added dropwise into sodium thiocyanate (326.8 mg, 4.0 μM) in 10 mL acetone at 0 ^oC. The mixture was stirred at 30 ^oC for 2 hours before 4-amino-*N*-(4,6-dimethyl-2- pyrimidinyl) benzenesulfonamide (556 mg, 2.0 mM) was added at 0 ^oC. After stirring at room temperature overnight, it was filtered and washed with water and acetone to give **compound 5** (276 mg, 23.6% yield) as a yellow powder. ^1H NMR (400 MHz, DMSO-d_6):

™12.19 (s, 1H), 11.68 (s, 1H), 11.52 (br s, 1H), 7.99 (d, 2H, J = 8.4 Hz), 7.86 (d, 2H, J = 8.4 Hz), 7.70 (d, 1H, J = 1.6 Hz), 7.49 (d, 1H, J = 8.8 Hz), 7.10 (doublet doublet (dd), 1H, J_1 = 8.8 Hz, J_2 = 1.6 Hz), 6.75 (s, 1H), 5.02 (s, 2H), 2.25 (s, 6H). HRMS (ESI): $[M+Na]^{+3}$ $C_{21}H_{19}BrClN_5NaO_4S_2$ calculated 605.9648, found 605.9632. HPLC: purity 95.9% (t = 18.4 min).

C4. Fluorescence titration

Lyophilized Cdc42 protein (Cytoskeleton Inc., Denver, CO) was reconstituted to 5 mg/mL in a buffer consisting of 50 mM Tris, 0.5 mM $MgCl_2$, 50 mM NaCl, 3% sucrose, and 0.6% dextran. The stock solution was then diluted to 1 μM in 5 mM phosphate buffer pH 7.4. Into a quartz cuvette containing Cdc42 solution, aliquots of ZCL278 were added and incubated for 5 minutes before each fluorescent measurement (Varian Cary Eclipse). The excitation wavelength was 275 nm and the fluorescence of tryptophan at 350 nm was measured after each

addition. The titration curve was fitted using the equimolar specific binding model in GraphPad and the K_d was calculated.

C5. Surface plasmon resonance

SPR experiments were performed on a Biacore T100 using CM5. All solutions used in the experiment were prepared with Milli-Q water, filtered with a 0.22 μm membrane filter, and degassed before use. Cdc42 solution in PBS (5 mM, pH 7.4) at a concentration of 1 mg/mL was diluted to 30 μg/mL with sodium acetate buffer (pH 4.0). The chip was activated with EDC/NHS (10 μL/min for 600 s). Then Cdc42 was loaded (5 μL/min for 400 s) and immobilized covalently. Roughly, 6000 RU of Cdc42 was immobilized on the chip. Any excess of unbound Cdc42 was removed by flowing PBS (5 mM, pH 7.4, with 2% DMSO) over the chip. ZCL278 was prepared as 2.5-30 μM solutions in PBS (5 mM, pH 7.4, with 2% DMSO), and injected (10 μL/min for 100 s). After each loading, data was collected and analyzed with the Biocore3000 software and GraphPad.

C6. Determination of pKa values of ZCL278

A Gemini Profiler was used for pKa measurement. First, 0.607 mg of ZCL278 was dissolved in 8 mL water (with 15 M KCl and DMSO). The solution was titrated with 0.5 M HCl in the pH range of 3.0 to 11.0, and the response was recorded. The measurement was repeated with different concentrations of DMSO (60, 49.2, 41.1, 31.8 wt%) and the collected pKa values were plotted and extrapolated to 0 wt% DMSO to give the pKa values of ZCL278 in water: 3.48 ± 0.04, 6.61 ± 0.02, 7.45 ± 0.01. There are four nitrogen atoms that are potentially associated with the apparent pKa values: pyrimidine N (N_a), sulfonamide N (N_b), aryl side of thioureido N

(N_c), and carbonyl side of thioureido N (N_d). The N_a, corresponding to a pKa of 3.48, should be deprotonated and stay in a neutral form at the pH of 7.4. The NH groups with pKa values of 6.61 and 7.45 should be partially deprotonated and give a population of charged species in solution.

C7. Measurement of the solubility of ZCL278

First, the standard linear plot was obtained by measuring the UV absorption (315 nm) of ZCL278 at the concentrations of 20, 30, 40, 50, 65 μM. A linear equation of y = 0.0119x + 0.0101 was obtained. Next, excess amount of ZCL278 powder was dissolved in 10 μL DMSO, then dispersed into 3 mL PBS buffer (pH 7.4). More ZCL278 powder was added to ensure the solution reached complete saturation. The solution was sonicated, kept at room temperature for 5 min, and filtered through 0.22 μm membrane to obtain the saturated solution A for measurement. At the same time, 10 μL of DMSO in 3 mL PBS was prepared as the blank control. Solution A was diluted by 5 times to give solution B. The UV absorption of solution B was measured and fitted into the linear equation to give a concentration of 36.24 μM (R^2 = 0.9995). Thus the concentration of solution A of 181.18 μM was obtained as the solubility of ZCL278.

C8. p50RhoGAP or Cdc42GAP assay

Inorganic phosphate produced as a result of GTPase activity was measured using a p50RhoGAP or Cdc42GAP assay (Cytoskeleton Inc., Denver, CO), an absorbance-based detection method (Moskwa, et al., 2005). Briefly, Cdc42 was preloaded with either GTP or ZCL278 and incubated in the reaction buffer (provided in kit) for 20 minutes at 37°C. GAP was then added for an additional 20 minutes at 37°C. Following a 10-minute incubation in CytoPhos Reagent (Cytoskeleton Inc., Denver, CO) inorganic phosphate was detected at 650 nm. n=3

independent experiments/ treatment group. Any null hypothesis with the probability level less than 95 % was rejected.

C9. Immunofluorescence

Serum starved Swiss 3T3 fibroblasts treated with or without Cdc42 activator (CN02, Cytoskeleton, Inc. Denver, CO), RhoA activator (CN01, Cytoskeleton, Inc. Denver, CO) , Rac activator (CN02, Cytoskeleton, Inc. Denver, CO), ZCL series compounds, Y-27632 (ROCK inhibitor; Tocris Bioscience, Bristol, UK) or NSC23766 (Rac1 inhibitor; Tocris Bioscience, Bristol, UK) were fixed in paraformaldehyde and subjected to immunostaining. For labeling of active Cdc42 and phosphorylated RhoA, cells were probed with mouse monoclonal antibody against an active Cdc42 (NewEast Biosciences, Malvern, PA) or rabbit anti-phosphorylated RhoA (Santa Cruz Biotechnology, Santa Cruz, CA). For GM130 immunofluorescent staining, cells were probed with mouse monoclonal antibody against GM130 (BD Biosciences, Franklin Lake, NJ). After appropriate secondary antibody labeling, rhodamine- or FITC-phalloidin (Molecular Probes, Eugene OR) were applied to stain filamentous actin. Immunofluorescent images were then analyzed using a Zeiss Axiovert S100 (Carl Zeiss, Thornwood, NY). Pixel intensity was measured at five random points of five cells and averaged to generate average pixel intensity for each treatment group using MetaMorph™ 4.6 imaging software systems (Molecular Devices, Sunnyvale, CA). Details of active Cdc42 immunostaining were demonstrated by presenting each image in the pseudocolor setting with MetaMorph software.

C10. Western Blot

Serum starved PC-3 cells were treated with or without Cdc42 activator or ZCL278 and lysed in a buffer containing 50mM Tris pH 7.5, 10mM $MgCl_2$, 0.5M NaCl, and 1% Triton X-100 plus a protease inhibitor cocktail (Roche Applied Science, Indianapolis, IN). Western blotting were performed with a phospho-Rac1/cdc42 (Ser71) antibody (Milipore, Billerica, MA), a phospho-WASP antibody (Assay Biotech, Sunnyvale, CA) or GAPDH (Calbiochem, San Diego, CA), followed by secondary antibodies conjugated to horseradish peroxidase. The membrane was then developed by chemiluminesence (Amersham, Buckinghamshire, UK).

C.11 G-LISA®

G-LISA® Cdc42 Activation Assay Kit (Cytokeleton Inc., Denver, CO) was used to measure Cdc42 activity. Serum starved Swiss 3T3 cells were treated with or without the Cdc42 activator, ZCL278 or NSC23766. Cell lysates were then processed according to the manufacturer's protocol using 0.15 mg/mL total protein/sample. Positive controls included cells activated with the Cdc42 activator and with a constitutively active Cdc42 protein (Cytoskeleton Inc., Denver, CO), while negative controls included untreated cells lysates and buffer-only controls. Samples were developed using a colorimetric substrate (Cytoskeleton Inc., Denver, CO) and the absorbance was read at 490 nm (Biotek, Winooski, VT). n=3 independent experiments/ treatment group. Any null hypothesis with the probability level less than 95 % was rejected.

C.12 Wound Healing Assay

Serum starved PC-3 cell monolayers were scratched at three distinct sites per well. Cells were then treated with or without the Cdc42 activator, ZCL278, or NSC23766. Phase contrast images were obtained at 0 and 24 hours of treatment using a Zeiss Axiovert S100 (Carl Zeiss, Thomwood, NY). The distance of migration was determined by measurement of the leading edge of the migrating cells using MetaMorph™ 4.6 imaging software systems (Molecular Devices, Sunnyvale, CA). To determine cell viability, PC-3 cells were incubated for 24 hours with or without the Cdc42 activator, ZCL278 or NSC23766. Using the trypan blue dye exclusion method, the numbers of live and dead cells were obtained using the Countess Automated Cell Counter (Invitrogen, Carlsbad, CA). The *p* values were assigned in each experiment. n= 5 independent experiments/ treatment group. Any null hypothesis with the probability level <95% was rejected.

C13. Primary neurons and time-lapse imaging

One-day old mouse pups were euthanized, and the brains were removed according to the animal use protocol approved by the East Carolina University Animal Use Committee. Dissociated neurons cultured on poly-L-lysine coated coverslips were treated at five days *in vitro* with DMSO (control) or ZCL278. Neurons were then fixed and stained with fluorescein-phalloidin to reveal actin-based structures. Neuronal morphology was observed using a Zeiss Axiovert S100 immunofluorescent microscope (Carl Zeiss, Thomwood, NY) and branch numbers were analyzed with MetaMorph™ 4.6 imaging software systems (Molecular Devices, Sunnyvale, CA). Results were averaged from 3 independent experiments (n=3/group). Any null hypothesis with the probability level <95% was rejected.

To determine growth cone dynamics, we applied time-lapse light microscopy according to a procedure described earlier (Jones et al., 2002; Jones et al., 2004). Briefly, neurons grown at 5 days *in vitro* were incubated with DMSO or ZCL278 and recorded for 10 minutes on 25 mm coverslips that were placed in an Attofluor cell chamber (Atto Instruments, Rockville, MD) on the heated stage of a Zeiss Axiovert S100 microscope (Carl Zeiss, Thomwood, NY). Differential interference contrast (DIC) images at 63X were captured by using a Hamamatsu Orca digital camera (Bridgewater, NJ). To minimize phototoxicity for the living cells, we used a computer-driven automatic shutter to achieve minimum illumination (300 msec/frame). Filopodia/microspike dynamics within growth cones of recorded images were then studied using MetaMorph™ 4.6 imaging software systems (Molecular Devices, Sunnyvale, CA).

C14. Statistical analysis

t-test analysis was performed using SigmaPlot 10.0 (Systat Software Inc., San Jose California) and p-values were designated for each experiment, each of which were repeated a minimum of three times. Any null hypothesis with probability level less than 95% was rejected.

D. Results

D1. Virtual screening for Cdc42 inhibitors

Analysis of the three-dimensional structure of Cdc42-ITSN complex (Protein Data Bank: 1KI1) revealed a main binding region between Cdc42 and ITSN (Synder et al., 2002). Residues Gln1380 and Arg1384 of ITSN were observed to form hydrogen bonds with Asn39 and Phe37 of Cdc42, respectively. Two clusters of hydrophobic interactions were found between Leu1376, Met1379 and Thr1383 of ITSN and Phe56, Tyr64, Leu67 and Leu70 of Cdc42. To screen for

Cdc42 inhibitors, the putative binding pocket on Cdc42 was created within 7 Å of the center of the above ITSN residues that interact with Cdc42. The binding pocket consists of 16 Cdc42 residues including Thr35, Val36, Asn39, Phe56 and Asp57 (Fig. 3.1A). The 197,000 compounds from SPECS were screened using HTVS (high-throughput virtual screening) and SP (standard precision) docking sequentially. The top ranked 100 molecules were subjected to manual inspection according to the following criteria: ITSN-like binding posture and occupation for the Leu1376, Gln1380, Arg1384, Met1379 and Thr1383 residue space of ITSN should be observed; at least three hydrogen bonds should be formed; a conserved hydrogen bond with Asn39 or Phe37 of Cdc42 should exist; diversity of scaffolds should be considered. A selection of 30 compounds was eventually tested for their ability to disrupt against Cdc42 activity and/or functions.

D2. Computed binding mode of ZCL278 in Cdc42

As shown in Fig. 3.1A, one small molecule, termed ZCL278, bound to a well-formed Cdc42 pocket lined by residues Thr35, Val36, Asp38, Asn39, Phe56, Tyr64, Leu67 and Leu70. Extensive favorable interactions were found between ZCL278 and Cdc42 residues. Five hydrogen bonds involving residues Thr35, Asn39 and Asp57, as well as hydrophobic interactions associated with residues Val36 and Phe56 were observed (Fig. 3.1B). The bromophenyl ring was inserted into the adjacent GTP/GDP binding pocket. The computed binding mode suggests that ZCL278 should be able to disrupt the Cdc42-ITSN interaction as well as GTP/GDP binding (Fig. 3.1C). Indeed, the competition between GTP and ZCL278 to influence Cdc42 GTPase activity was confirmed by using p50RhoGAP or Cdc42GAP assay (Fig. 3.2). Our results suggest that increasing GTP addition can compete with preloaded ZCL278 on Cdc42 and increase GTP

hydrolysis by purified recombinant Cdc42 protein *in vitro*. Thus, local GTP/GDP should have impact on the effective doses of ZCL278 in the cells.

D3. Synthesis of Cdc42 inhibitor ZCL278

In order to confirm the screening hits and provide high purity samples for biological exploitation, ZCL278 was synthesized, purified, and characterized. As illustrated in a scheme (Fig. 3.1D), after compound 2 was prepared from 4-bromo-2-chlorophenol and ethyl 2-bromoacetate in the presence of potassium carbonate, it was hydrolyzed in the alkali condition to provide acid 3. Treatment of compound 3 with refluxing thionyl chloride with DMF as a catalyst gave acyl chloride 4, which was converted to 4-(3-(2-(4-Bromo-2-chloro-phenoxy)-acetyl)-thioureido)-N-(4,6-dimethyl-pyrimidin-2-yl)-benzene-sulfonamide (compound 5, ZCL278) after treatment with sodium thiocyanate, followed by reaction with 4-amino-N-(4,6-dimethylpyrimidin-2-yl)-benzene-sulfonamide.

D4. Direct binding of ZCL278 and Cdc42 demonstrated by fluorescence titration and surface plasmon resonance

We assessed the binding affinity of ZCL278 and Cdc42 using two independent biophysical methods. First, fluorescence titration of purified Cdc42 by ZCL278 was carried out by monitoring the change of fluorescence intensity of a tryptophan residue on Cdc42 upon ZCL278 binding. Since ZCL278 has a weak absorption peak at 310 nm, in order to avoid any experimental error that might result from potential fluorescence quenching by ZCL278, the fluorescence emission of Cdc42 was monitored at 350 nm where ZCL278 has a negligible absorption. Thus, a K_d value of 6.4 μM was obtained as the binding affinity of ZCL278 for

Cdc42 (Fig. 3.3A). To further demonstrate the direct interaction between ZCL278 and Cdc42, a surface plasmon resonance (SPR) experiment was performed by covalently immobilizing purified Cdc42 on a CM5 chip and varying ZCL278 concentration. The SPR response was observed to increase along with elevated ZCL278 concentrations and eventually gave a K_d of 11.4 μM (Fig 3.3B and C). Discrepancies in K_d values obtained by fluorescent titration (Fig. 3.3A) and SPR experiments (Fig. 3.3B and C) can best be explained by decreased ZCL278 solubility in the titration buffer, whereas in SPR experiments, solubility is not a factor in ZCL278's ability to bind Cdc42 immobilized on the CM5 chip.

D5. ZCL278 inhibits Cdc42-mediated microspike formation

We assessed the 30 selected ZCL compounds for their ability to inhibit Cdc42-mediated microspike/filopodia formation in serum-starved Swiss 3T3 fibroblasts. Actin-based microspikes/filopodia are characteristic of Cdc42 activity in cultured fibroblastic cells (Kozma et al., 1995; Nobes and Hall, 1995). As shown in Fig. 3.4A, DMSO-treated (control) cells have few microspikes along its perimeter (arrows) as well as the characteristic presence of RhoA-mediated stress fibers (asterisk). When arrested fibroblasts were briefly stimulated with 1 unit/mL of a commercial Cdc42 activator (CN02, Cytoskeleton, Inc. Denver, CO), a dramatic increase in microspike number and decrease in stress fibers occurred (Fig. 3.4A, Activator). Compound ZCL278 was applied at 50 μM for either 15 minutes, or for 1 hour and then stimulated with the Cdc42 activator for 2 minute. After 15 minute incubation, the cell periphery of ZCL278-treated cells resembles control cells with few microspikes (Fig. 3.4A, ZCL278). Following 1 hour of ZCL278 treatment and Cdc42 stimulation, there is obvious inhibition of microspike formation (Fig. 3.4A, Activator+ZCL278) as compared to cells treated with only the

activator (Fig. 3.4A, Activator). ZCL197 and ZCL279, two other compounds with favorable predicted binding to Cdc42, either failed to inhibit microspike formation (Fig. 3.4A, Activator+ZCL197), or induced branched cellular processes resembling RhoA suppression (Fig. 3.4A, Activator+ZCL279). Therefore, ZCL278, but not ZCL197 or ZCL279, inhibits Cdc42-mediated microspike formation. Although ZCL278 displayed the most striking inhibitory effects on microspike formation among the 30 compounds tested, 4 other promising compounds identified from the virtual screening showed similar properties. The chemical structures of these 4 compounds, along with 6 other ZCL compounds, are described in Fig. 3.5.

In our in silica screening model, the Cdc42-ITSN interaction interface defines a binding pocket of 16 residues in Cdc42. We aligned the sequences of Cdc42 (P60953, from GenBank, http://www.uniprot.org/uniprot/), Rac1 (P63000) and RhoA (P61586) (Fig. 3.6). One of the 16 residues is different between Cdc42 and Rac1 (Phe56 (Cdc42)/Trp56 (Rac1)), while 3 residues are different between Cdc42 and RhoA (Asp38 (Cdc42)/Glu40 (RhoA), Phe56/Trp58, Gln74/Asp76). The determinant for the selectivity of these Rho GTPases toward their GEFs is Phe56 (Cdc42)/Trp56 (Rac1)/Trp58 (RhoA). We thus further performed studies to compare ZCL278 with Y-27632, a RhoA/Rho kinase inhibitor (Wennerber and Der, 2004; Fritz and Kaina, 2006), under the condition that RhoA is activated (Fig 3.4B, left). We also performed studies to compare ZCL278 with NSC23766, a Rac1 selective inhibitor (Kwon et al., 2000), under the condition that Rac1 is activated (Fig. 3.4B, right). These results demonstrated that ZCL278 inhibits Cdc42-mediated (Fig. 3.4A), but not RhoA- or Rac1-mediated phenotypes (Fig. 3.4B).

D6. ZCL278 inhibits Cdc42 activity

Since ZCL278 showed the direct binding to Cdc42 and displayed most inhibitory effects in a morphological assay of Cdc42 function, we analyzed its activity at a biochemical level. First, Cdc42 activation was investigated in human metastatic prostate cancer PC-3 cells that were treated with the Cdc42 activator or 50 μM ZCL278 for 5, 10, and 15 minutes. Serine 71 phosphorylation is known to negatively regulate Rac/Cdc42 activity (Uehata et al., 1997), thus an increase in phospho-Rac/Cdc42 expression is indicative of a decrease in active (GTP-bound) Rac/Cdc42. As depicted in Fig. 3.7A, activation of Cdc42 shows an expected decrease in phospho-Rac/Cdc42. However, the application of ZCL278 resulted in a time-dependent increase in Rac/Cdc42 phosphorylation.

Wiskott-Aldrich syndrome Protein (WASP) is a downstream effector of Cdc42 activation (Ridley, 2006). Tyrosine phosphorylation of WASP is linked to rapid Cdc42 degradation following its activation (Suzuki et al., 1999; Gao et al., 2004). As shown in Fig. 3.7A, the Cdc42 activator leads to a decreased expression of phospho-WASP by 15 minutes while ZCL278 does not suppress phospho-WASP activity. Thus, ZCL278 inhibits Rac/Cdc42 phosphorylation in a time-dependent manner and maintains tyrosine phosphorylation of WASP.

Serine 71 phosphorylation can occur on both Rac and Cdc42. To directly assess specific Cdc42 activation and inactivation, we utilized a G-LISA®, an ELISA-based assay that allows a quantitative determination of the levels of GTP-bound (active) Cdc42 in cellular lysates. Serum-starved Swiss 3T3 fibroblasts were incubated for 1 hour with 50 μM ZCL278 or 10 μM NSC23766 (Rac inhibitor), followed by 2 minutes of stimulation with 1 unit/mL Cdc42 activator. This analysis revealed a significant increase (70%) in GTP-bound Cdc42 in cells treated with the activator as compared to control (untreated) cells (Fig. 3.7B). Cells treated with

ZCL278 showed a dramatic (nearly 80%) decrease in GTP-Cdc42 content as compared with cells treated solely with the activator. Finally, we analyzed the ability of NSC23766 to cross-inhibit Cdc42 activation. NSC23766 was developed in a similar manner as ZCL278; however, it is specific to Rac and should therefore act as an additional negative control in this assay (Kwon et al., 2000). As expected, NSC23766 does not reduce GTP-Cdc42 content (Fig. 3.7B). These data establish that ZCL278 inhibits Cdc42 in two different cell types.

D7. ZCL278, but not NSC23766, disrupts the peri-nuclear distribution of active Cdc42

To confirm the ability of ZCL278 to selectively inhibit Cdc42 activation at the cellular level, serum starved Swiss 3T3 cells were treated with either 50 μM ZCL278 or 10 μM NSC23766 and were subsequently stimulated for 2 minutes with the Cdc42 activator (Fig. 3.8). Cells were probed with a mouse monoclonal antibody against active (GTP-bound) Cdc42 (Fig. 3.8A, represented in psuedocolor setting (MetaMorph™ 4.6 imaging software systems (Molecular Devices, Sunnyvale, CA) for clarity). Nuclei were visualized in dark blue by Hoechst staining. Control fibroblasts showed an organized peri-nuclear distribution of active Cdc42 (Fig. 3.8A). Cdc42 activation increased this distribution in the peri-nuclear region as well as in the nucleus (Fig. 3.8A), consistent with the established roles of Cdc42 in Golgi-based protein trafficking (Torres and Rosen, 2003). ZCL278 clearly disrupted this organization and reduced immunoreactivity of anti-active Cdc42 while NSC23766 did not have the same effects (see also the quantification of the percentage of cells showing organized perinuclear distribution in Fig. 3.8B). Additionally, application of the Cdc42 activator, ZCL278 or NSC23766 did not elicit significant changes in phospho-RhoA immunoreactivity (Fig. 3.8C). These results again indicate that ZCL278 selectively inhibits Cdc42.

D8. ZCL278, but not NSC23766, disrupts GM130 docked Golgi organization

To determine whether the ZCL278-induced disruption of peri-nuclear distribution of active Cdc42 reflected its effects on Golgi organization, we examined GM130, a peripheral cytoplasmic protein that is tightly bound to Golgi membranes and helps to maintain cis-Golgi structures (Torres and Rosen, 2006; Harris and Tepass, 2010). Control, serum-starved Swiss 3T3 cells showed well-developed stress fibers (Fig. 3.9, red) and GM130 immunoreactivity polarizing to one side of the nucleus (Fig. 3.9, green-asterisk). Treatment with the Cdc42 activator led to increased microspikes, as expected (Fig 3.9, red-arrows and insert, arrowheads), and intense peri-nuclear GM130 immuroreactivity (Fig. 3.9, green-asterisk). As depicted in Fig. 3.9 (also see Fig. 3.4A), ZCL278-treated cells show not only fewer microspikes but also a clear reduction of GM130 immunoreactivity as well as its dissipation to both sides of the nucleus (Fig. 3.9, green-asterisk). Rac inhibitor NSC23766 did not significantly alter GM130 expression or distribution (Fig. 3.9-green-asterisk). These results not only further confirm ZCL278 as a specific Cdc42 inhibitor, but also demonstrate the importance of Cdc42 in Golgi organization and protein trafficking.

D9. ZCL278 impedes wound healing without disruption of cell viability

Filopodia are dynamic structures that aid cells in pathfinding and migration (Erickson et al., 1996; Nakamura et al., 1995), and are largely controlled by Cdc42 activity (Gupton and Gertler, 2007). Using a metastatic line of human prostate cancer cells (PC-3), we employed a wound healing assay in order to elucidate the effects of ZCL278 on cellular migration. Quiescent PC-3 cells were wounded with a sterile pipette tip and treated with or without the Cdc42 activator, ZCL278, or the Rac inhibitor NSC23766 for 24 hours. As shown in Figure

3.10A and quantified in Fig. 3.10B, Cdc42 activation resulted in a significant increase (59%) in wound healing ability in comparison to controls (41%). Application of 50 μM and 5 μM ZCL278 inhibited PC-3 migration into the wound area. However, wound closure was less pronounced at 50 μM (8%) than 5 μM (30%) concentrations. Cellular migration was also significantly reduced with NSC23766 treatment. This result is to be expected since Rac regulates the formation of lamellipodia, which are well-described motile structures (Nemethova, 2008). These data, which are in agreement with our biochemical analysis, suggests that ZCL278 is not only a selective inhibitor of Cdc42 activation but also a potent suppressor of Cdc42-dependent cell motility.

In order to ensure that decreases in cellular migration seen with ZCL278 treatment was due to Cdc42 inhibition (or Rac inhibition when treated with NSC23766) rather than cell death, we tested cell viability using the trypan blue dye exclusion assay. PC-3 cells were arrested in G_0, and then 50 μM ZCL278 or 10 μM NSC23766 was applied for 24 hours. Fig. 3.10C demonstrates that there was no difference in viability between treated and non-treated (control) cells. Therefore, we conclude that the differences seen in migratory ability are due to ZCL278-mediated Cdc42 inhibition or NSC23766-mediated Rac inhibition and not cell death.

D10. ZCL278 inhibits neuronal branching and growth cone dynamics

Cdc42 plays a crucial role in the establishment of neuronal morphogenesis (Garvalov et al., 2007). Cdc42's absence in neurons resulted in a significantly reduced number of neurites and severely disrupted filopodia function (Yang et al., 2006). Therefore, we tested the ability of ZCL278 to inhibit neuronal branching in primary neonatal cortical neurons.

At 5 days cultured in *vitro*, cortical neurons extended neurites with multiple branches (Fig. 3.11A, Control). 50 μM of ZCL278 was applied for 5 and 10 minutes, while DMSO-treated

neurons were maintained as negative controls. As demonstrated in Fig. 3.11A, neuronal branching was suppressed in ZCL278-treated neurons over the time course in comparison to the highly branched neurites of control cells. Quantitative measurements found the branch number to be significantly reduced in ZCL278 treated neurons (Fig. 3.11B).

Cdc42 is also widely known to control filopodia and microspikes at the leading edge of migrating growth cones (Ridley and Hall, 1992). Time-lapse video light microscopy shows a control cortical neuron with multiple microspikes or filopodia extended from the growth cone (Fig. 3.11C). However, ZCL278 treatments resulted in rapid retraction of filopodia within 4 minutes (Fig. 3.11C). Thus, these studies further support ZCL278 as an effective small-molecule inhibitor of Cdc42-mediated neuronal branching and growth cone motility.

E. Discussion

Signaling through the Rho GTPase pathway allows cells to accomplish a myriad of cellular tasks including membrane trafficking, cell cycle control, and the regulation of cytoskeletal organization, which strongly influence cell morphology, motility, and cell fate (Brown et al., 2000; Govek et al., 2005, Hall, 1998). Currently, many pathological conditions have been attributed to Rho GTPase dysfunction or de-regulation, making them prime candidates for pharmaceutical intervention (Jaffe and Hall, 2005; Lu et al., 2009).

The available small molecule modulators of Rho GTPases have facilitated the exploitation of this important family of proteins. Notably, fasudil and Y-27632 are well-established and potent inhibitors of Rho kinase/p160^{ROCK}, one of the main downstream effectors of RhoA (Fritz and Kaina, 2006; Wennerberg and Der, 2005). Recent development of NSC23766 targeting Rac1-GEF interaction filled a gap in studies on Rac as a selective Rac1 inhibitor

(Kwon et al., 2000). However, there are few choices for effective small molecule inhibitors selective for Cdc42. Secramine, an analog of natural product galanthamine, was discovered recently by its ability to inhibit Cdc42-dependent Golgi to plasma membrane transport through RhoGDI1 (Pelish et al., 2006). Unlike the widely used Y-27632 (1903 publications) or NSC23766 (115 publications), secramine availability is very limited and few studies can be found in literature today (9 publications). Cdc42 de-regulation has been linked to various aspects of tumorigenesis, including transformation and metastasis (Boettner and Van Aelst, 2002; Stengel and Zheng, 2011). Additionally, neuronal development and maintenance relies heavily on appropriate Cdc42 activity (Auer et al., 2011). Given the urgent need to discover an effective tool to study Cdc42, we undertook the similar strategy in the discovery of NSC23766 and identified potential Cdc42 inhibitors by screening over 197,000 small molecules coupled with biochemical and cell-based verifications. Among the 30 potential leads that interfered with fibroblastic cell morphology related to Cdc42 function, ZCL278 emerged as the most effective and selective compound. ZCL278 synthesis involves few steps and is cell-permeable, therefore quite amenable for further exploitation as a pharmaceutical tool. In this study, we provide evidence for the characterization of the first effective Cdc42 small molecule inhibitor, which specifically and directly targets the binding site of its GEF, ITSN. This is yet another example of identification of small molecule modulator of biologically significant signaling pathways based on computer-assisted screening (Kwon et al., 2000; Massa et al., 2002).

Several studies have previously demonstrated the importance of Cdc42 activation for epithelial-to-mesenchymal transition (EMT) and resultant cellular movement that is necessary for cancer cell invasion (Chen et al., 2010; Johnson et al., 2010). Using a wound healing assay, we showed that treatment with a Cdc42 activator is capable of enhancing wound closure in

comparison to non-treated cells, bolstering evidence for Cdc42's ability to enhance the metastatic activity of cancer cells. Significantly, ZCL278 was able to inhibit the migratory ability of PC-3 cells in a concentration dependent manner. Furthermore, ZCL278 is not cytotoxic to cells, therefore cell death is not the reason for the significant reduction in migration. Our studies raised an exciting possibility that ZCL278 can be further investigated for its ability to inhibit cancer cell invasion and metastasis *in vivo*.

Our studies on primary cortical neurons also support the role of Cdc42 in neuronal development. As elegantly demonstrated by Garvalov et al. (2007), brain and neuronal development are severely disrupted in Cdc42 deficient mice (Garvalov et al., 2007). These mice exhibit a range of brain abnormalities including reduced axonal tracts, while neurons displayed a decrease in filopodial dynamics, increased growth cone size, and suppressed axon generation. Application of Cdc42 inhibitor ZCL278 to primary neurons reduced the number of branches formed and impeded growth cone dynamics. This is consistent with the notion that axon and dendrite motility is largely an actin-based process that is highly regulated by Cdc42 (Watabe-Uchida et al., 2006). Thus, ZCL278 is the first small molecule inhibitor of Cdc42-ITSN interaction and provides a powerful tool for further elucidation of Cdc42 function in human diseases including cancer and neurologic diseases.

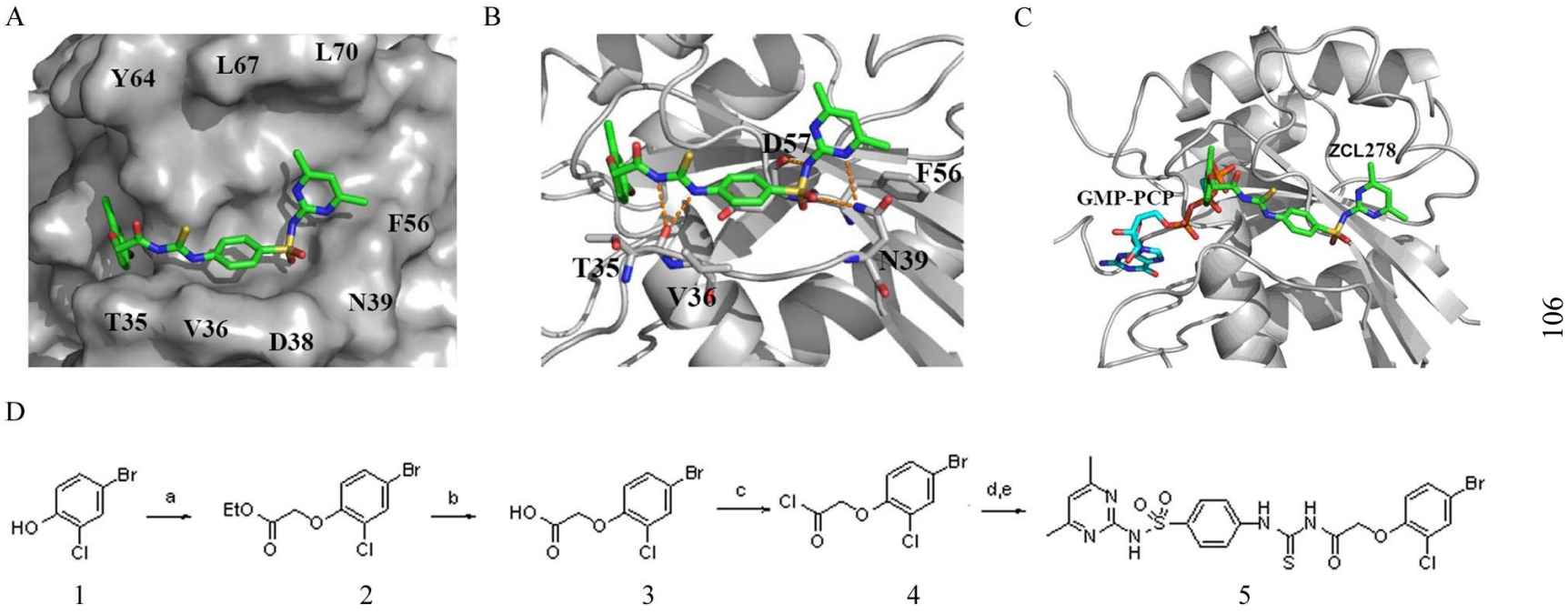
A
Y64
L67
L70
F56
N39
T35
V36
D38
B
D57
F56
T35
V36
N39
C
ZCL278
GMP-PCP
D
HO
Br
Cl
a
EtO
O
b
c
d,e
N
H
S
1
2
3
4
5

Figure 3.1 ***Identification of ZCL compounds targeting Cdc42-ITSN interaction.***

(A) Docked posture of ZCL278 in the Cdc42 binding pocket: protein is shown as gray surface; ligand is depicted by green sticks. (B) Proposed interactions between ZCL278 and Cdc42 residues: ZCL278 is in green; Cdc42 is shown as gray cartoon; residues of Cdc42 are in gray sticks; hydrogen bonds are represented as orange dash lines. (C). Superposition of GMP PCP (from Protein Data Bank: 2QRZ) and the docked Cdc42-ZCL278 complex. Cdc42: gray cartoon; ZCL278: green sticks; GMP-PCP: cyan sticks. (D). Synthesis of ZCL278. Reagents and conditions: (a) Ethyl 2-bromoacetate**,** K_2CO_3 , DMF, 70 °C; (b) NaOH, dioxane/H_2O; (c) SOCl2, DMF, reflux; (d) NaSCN, acetone, 0 °C to room temperature; (e) 4-amino-N-(4,6-dimethylpyrimidin-2-yl) benzenesulfonamide, 0 °C to room temperature. Note: GMP-PCP is GTP analog guanylyl beta, gamma-methylene diphosphonate (i.e. the presumed signaling-active state).

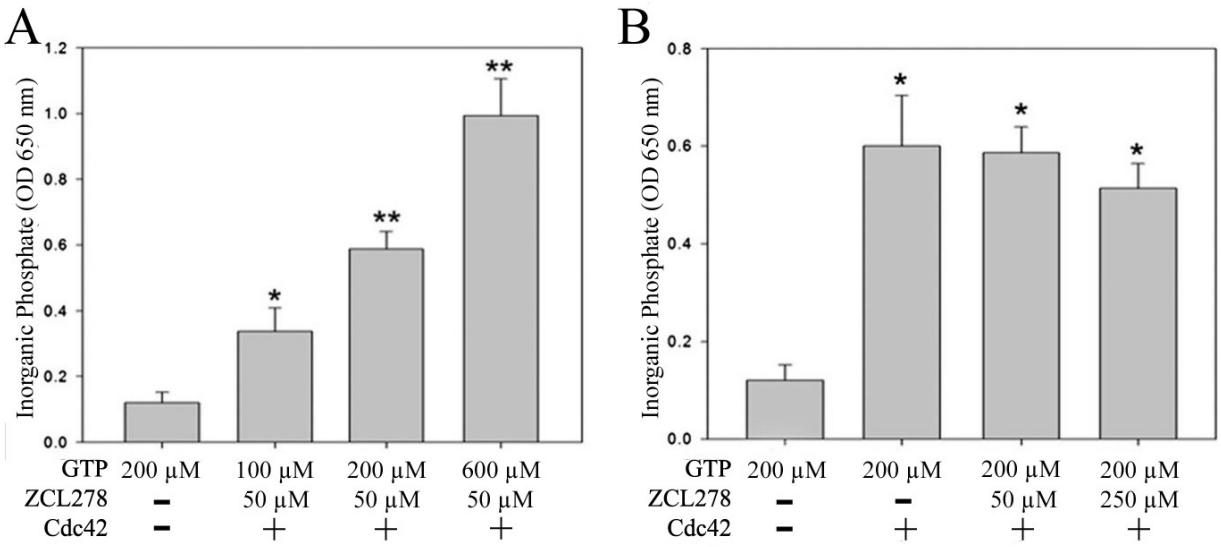
A
Inorganic Phosphate (OD 650 nm)
1.2
1.0
0.8
0.6
0.4
0.2
0.0
**
**
*
GTP 200 µM 100 µM 200 µM 600 µM
ZCL278 - 50 µM 50 µM 50 µM
Cdc42 - + + +
B
Inorganic Phosphate (OD 650 nm)
0.8
0.6
0.4
0.2
0.0
*
*
*
GTP 200 µM 200 µM 200 µM 200 µM
ZCL278 - - 50 µM 250 µM
Cdc42 - + + +

Figure 3.2 ***The competition between ZCL278 and GTP for Cdc42 interactions and the effect on GTPase activity.***

(A) Increasing GTP concentration competes with ZCL278 preloaded on Cdc42 and increases GTP hydrolysis by purified recombinant Cdc42 protein *in vitro* as depicted by increasing levels of inorganic phosphate. *: $p < 0.01$; **: $p < 0.00002$. (B) Increasing ZCL278 addition competes with preloaded GTP on Cdc42 and reduces GTP hydrolysis by purified recombinant Cdc42 protein *in vitro* as demonstrated by the decreased levels of inorganic phosphate. *: $p < 0.0006$.

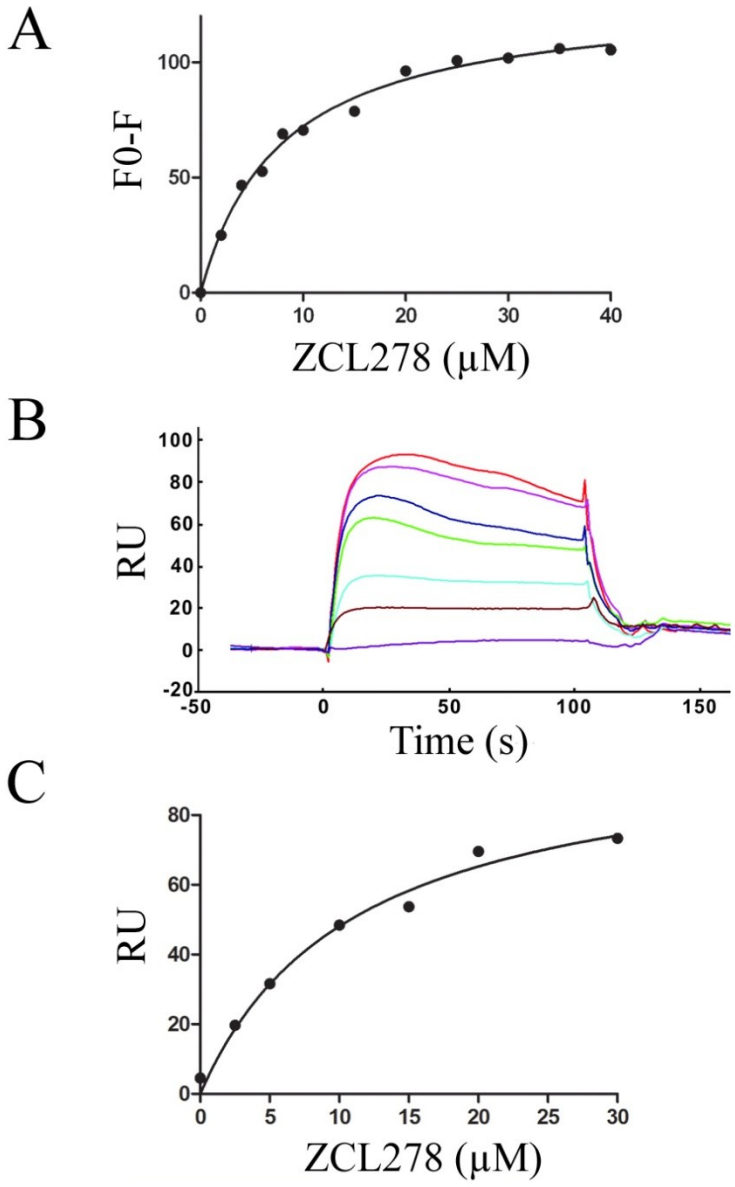
A
F0-F
100
50
0
0
10
20
30
40
ZCL278 (μM)
B
RU
100
80
60
40
20
0
-20
-50
0
50
100
150
Time (s)
C
RU
80
60
40
20
0
0
5
10
15
20
25
30
ZCL278 (μM)

Figure 3.3 ***Determination of ZCL278 and Cdc42 binding.***

(A). Fluorescence titration of Cdc42 with compound ZCL278. Fluorescence emission at 350 nm was monitored. *K*d = 6.4μM. (B). Surface plasmon resonance measurement of Cdc42-ZCL278 interaction. (C). Surface plasmon resonance determined a *K*d = 11.4 μM for Cdc42-ZCL278 affinity.

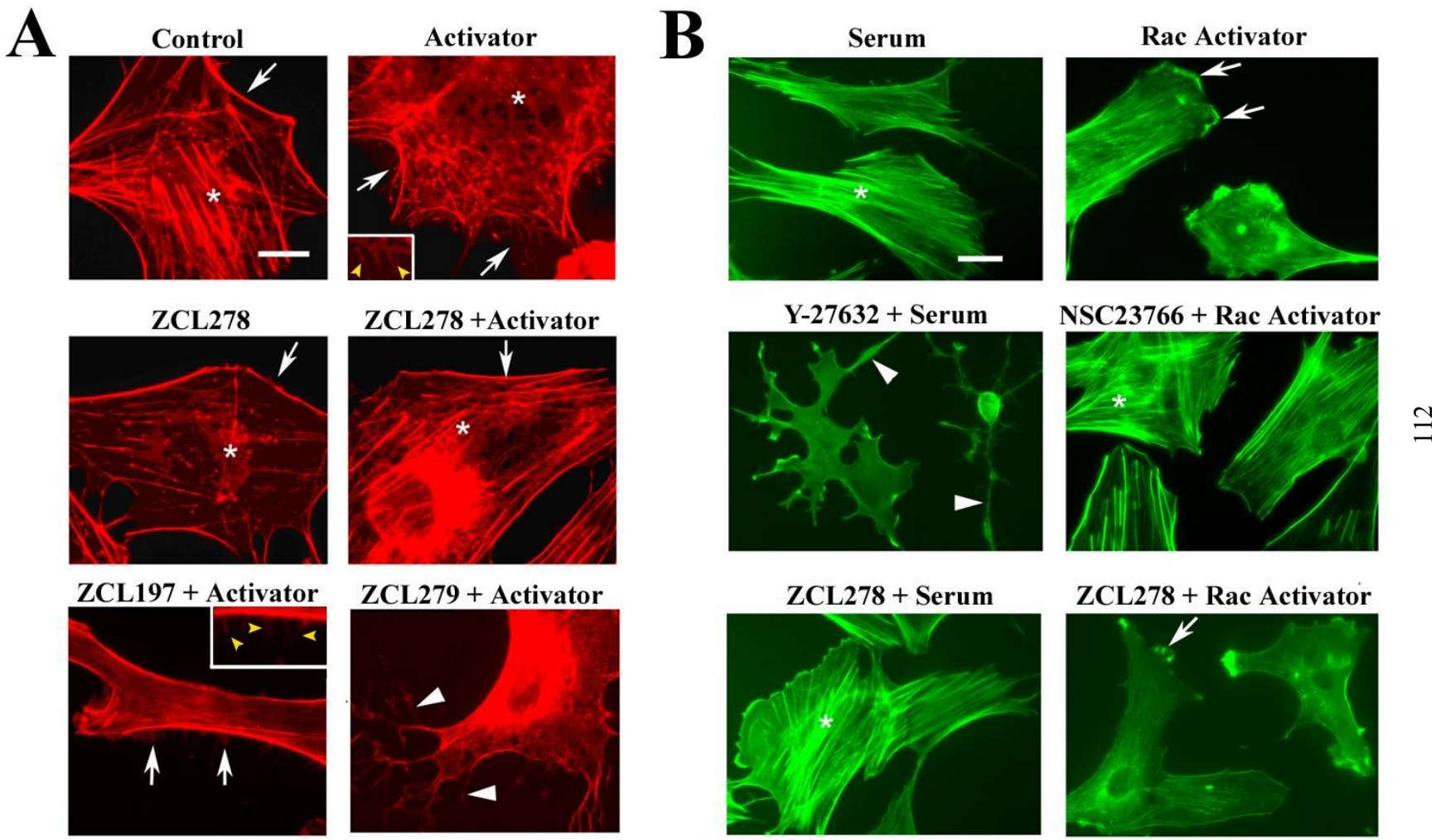
A
Control
Activator
ZCL278
ZCL278 +Activator
ZCL197 + Activator
ZCL279 + Activator
B
Serum
Rac Activator
Y-27632 + Serum
NSC23766 + Rac Activator
ZCL278 + Serum
ZCL278 + Rac Activator

Figure 3.4 ***ZCL278 inhibits Cdc42-mediated microspike formation***.

(A) ZCL278, but not ZCL197or ZCL279, inhibits Cdc42-mediated microspike formation. Swiss 3T3 cells were treated with or without Cdc42 ligands identified by the high-throughput in silico screening. While DMSO was used as a control, 1 unit/mL Cdc42 Activator was applied to stimulate Cdc42. 50 μM ZCL278, ZCL197, or ZCL279 was applied for either 15 minutes without activation of Cdc42, or for 1 hour and then stimulated with the Cdc42 activator for 2 minutes. Following treatments, cells were fixed and stained with rhodamine phalloidin to label filamentous actin. Arrows point to the cell periphery where microspikes may be seen. Insets show high magnification of microspikes (yellow arrowheads). Asterisks indicate the subcellular locations that normally show stress fiber distribution. Bar: 5 μm (B). ZCL278 does not induce RhoA inhibition mediated branching of cellular processes nor suppresses Rac1-mediated lamellipodia formation. Asterisks indicate stress fiber distribution while arrows point to lamellipodia and white arrowheads point to branched cellular processes. Bar: 5 μM.

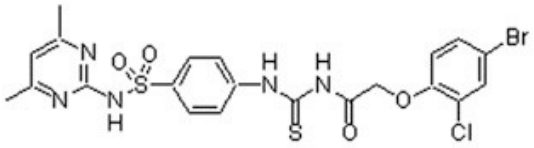

ZCL-278

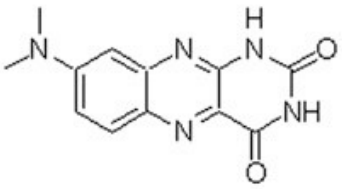

ZCL-369

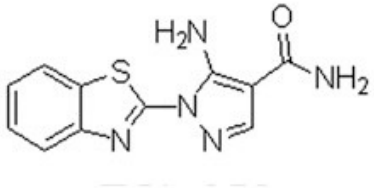

ZCL-358

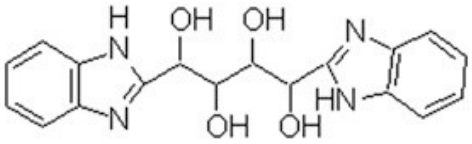

ZCL-193

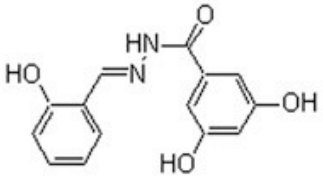

ZCL-367

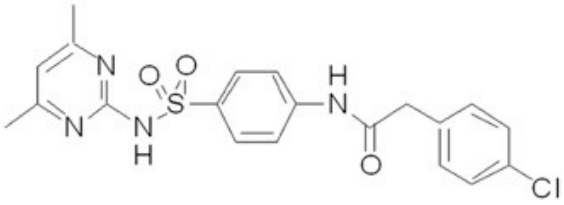

ZCL-197

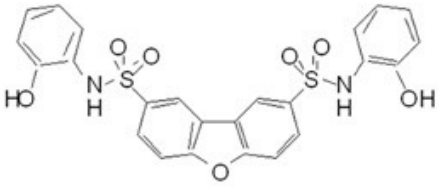

ZCL-279

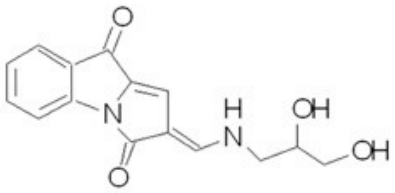

ZCL-357

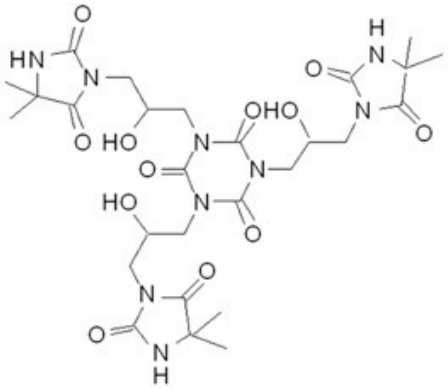

ZCL-351

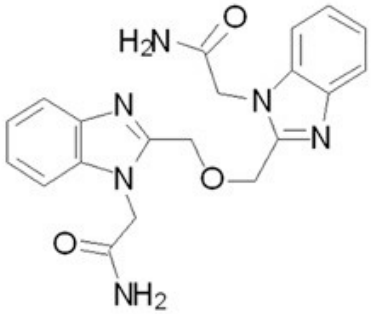

ZCL-354

Figure 3.5 ***Examples of ZCL series compounds identified from the in silica screening as targeting Cdc42-ITSN interaction.***

Most of these ZCL compounds showing favorable Cdc42-ITSN interaction display activities to suppress fibroblastic microspike formation with the exception of ZCL-279, which induced branched cellular processes resembling RhoA suppression and ZCL197, which did not suppress microspike formation.

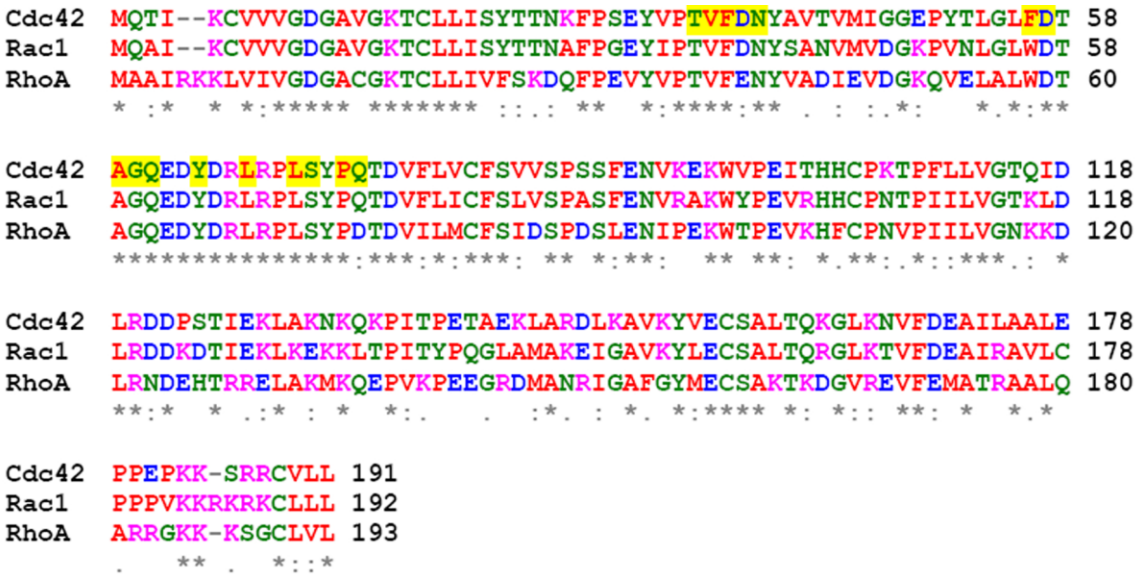
Cdc42 MQTI--KCVVVGDGAVGKTCLLISYTTNKFPSEYVPTVFDNYAVTVMIGGEPYTLGLFDT 58
Rac1 MQAI--KCVVVGDGAVGKTCLLISYTTNAFPGEYIPTVFDNYSANVMVDGKPVNLGLWDT 58
RhoA MAAIRKKLVIVGDGACGKTCLLIVFSKDQFPEVYVPTVFENYVADIEVDGKQVELALWDT 60
AGQEDYDRLRPLSYPQTDVFLVCFSVVSPSSFENVKEKWVPEITHHCPKTPFLLVGTQID 118
Rac1 AGQEDYDRLRPLSYPQTDVFLICFSLVSPASFENVRAKWYPEVRHHCPNTPIILVGTKLD 118
RhoA AGQEDYDRLRPLSYPDTDVILMCFSIDSPDSLENIPEKWTPEVKHFCPNVPIILVGNKKD 120
LRDDPSTIEKLAKNKQKPITPETAEKLARDLKAVKYVECSALTQKGLKNVFDEAILAALE 178
Rac1 LRDDKDTIEKLKEKKLTPITYPQGLAMAKEIGAVKYLECSALTQRGLKTVFDEAIRAVLC 178
RhoA LRNDEHTRRELAKMKQEPVKPEEGRDMANRIGAFGYMECSAKTKDGVREVFEMATRAALQ 180
PPEPKK-SRRCVLL 191
Rac1 PPPVKKRKRKCLLL 192
RhoA ARRGKK-KSGCLVL 193

Figure 3.6 ***Alignment of the sequences of Cdc42, Rac1, and RhoA highlighting the residues identified as part of the GTPase-ZCL compound binding pocket.***

We aligned the sequences of Cdc42 (P60953, from GenBank, http://www.uniprot.org/uniprot/), Rac1 (P63000) and RhoA (P61586). The 16 interacting Cdc42 residues, Thr35, Val36, Phe37, Asp38, Asn39, Phe56, Asp57, Ala59, Gly60, Gln61, Tyr64, Leu67, Leu70, Ser71, Pro73, and Gln74, are highlighted in the alignment. One of these 16 residues is different between Cdc42 and Rac1 (Phe56 (Cdc42)/Trp56 (Rac1)), while 3 residues are different between Cdc42 and RhoA (Asp38 (Cdc42)/Glu40 (RhoA), Phe56/Trp58, Gln74/Asp76). The determinant for the selectivity of these Rho GTPases toward their GEFs is Phe56 (Cdc42)/Trp56 (Rac1)/ Trp58 (RhoA) [22] which is also included in our defined binding pocket of Cdc42. Thus, this makes it feasible to identify selective inhibitors of Cdc42.

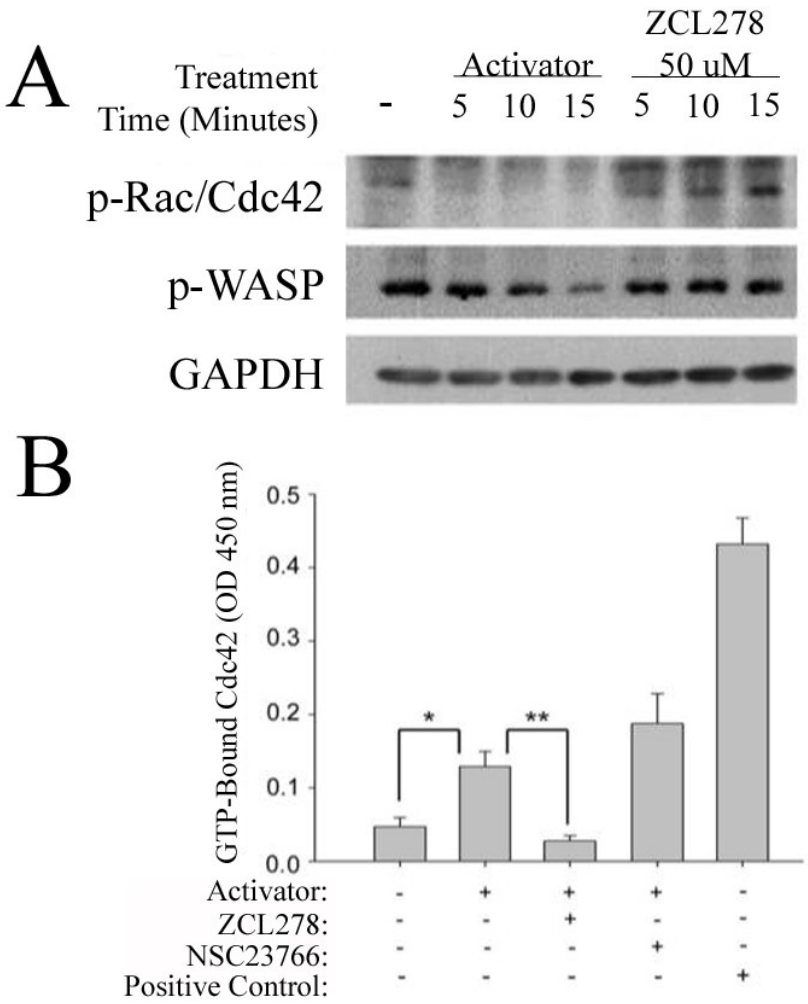
A
Treatment
Time (Minutes)
-
Activator
5 10 15
ZCL278
50 uM
5 10 15
p-Rac/Cdc42
p-WASP
GAPDH
B
GTP-Bound Cdc42 (OD 450 nm)
0.5
0.4
0.3
0.2
0.1
0.0
*
**
Activator:
ZCL278:
NSC23766:
Positive Control:

Figure 3.7 ***ZCL278 inhibits Cdc42 expression and activity.***

(A) ZCL278 inhibits endogenous Rac/Cdc42 activities. Serum-starved PC-3 cells were treated with either the Cdc42 activator at 1 unit/mL or 50 μM ZCL278 for the indicated time points. Cell lysates were subjected to Western blot analysis utilizing the following antibodies: phospho Rac1/cdc42 (upper), phospho-WASP (middle), and GAPDH (lower). (B) ZCL278, but not NSC23766, inhibits stimulated Cdc42 activity. Serum-starved Swiss 3T3 cells were incubated for 1 hour with either 50 μM ZCL278 or 10 μM NSC23766 and then stimulated for 2 minutes with a Cdc42 activator at 1 unit/mL. Cell lysates were then subjected to a colorimetric G-LISA® assay to measure GTP-bound Cdc42. A constitutively active Cdc42 was used as positive control. Negative controls included buffer only controls as well as untreated cellular lysates. Results shown are averaged from three independent experiments (n= 3/ group) ± S.E. (**, $p< 0.01$, *, $p<0.05$).

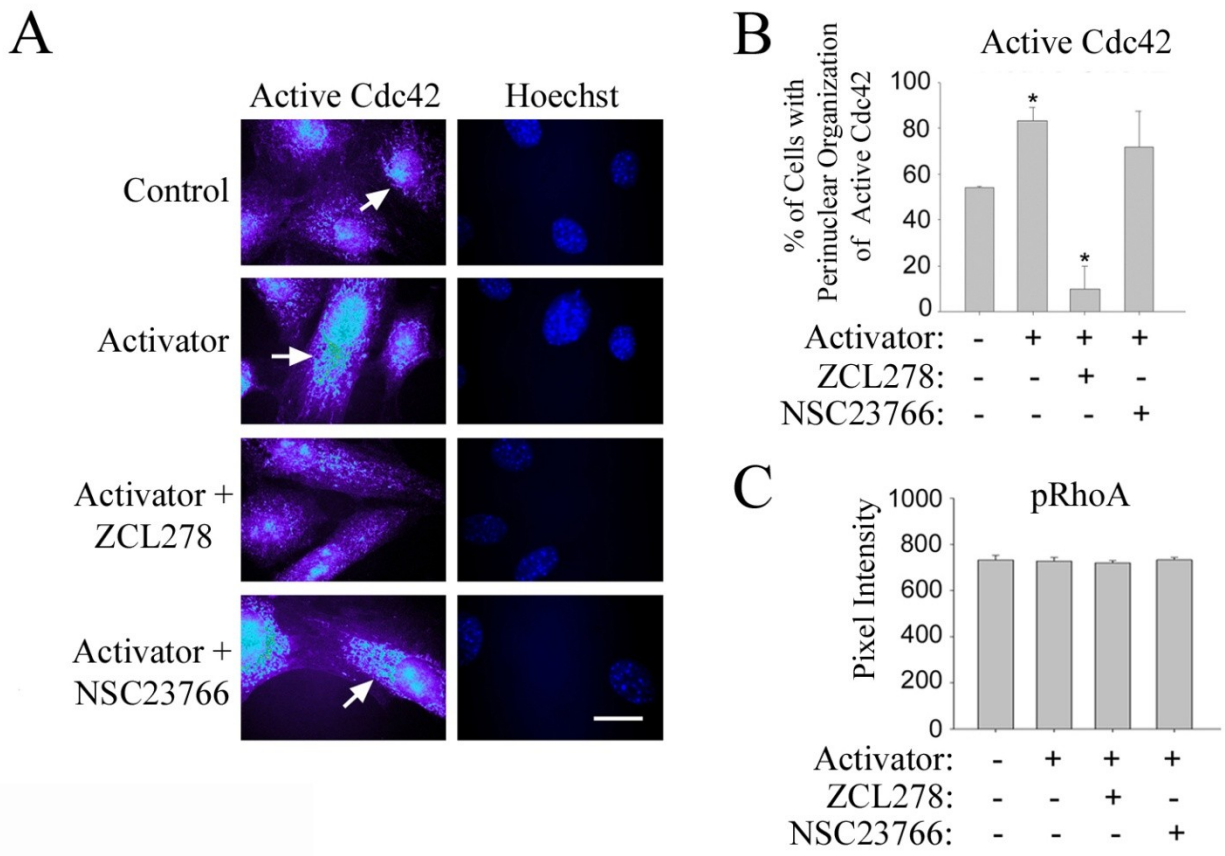
A
Active Cdc42
Hoechst
Control
Activator
Activator + ZCL278
Activator + NSC23766
B
Active Cdc42
% of Cells with Perinuclear Organization of Active Cdc42
100
80
60
40
20
0
*
*
Activator: - + + +
ZCL278: - - + -
NSC23766: - - - +
C
pRhoA
Pixel Intensity
1000
800
600
400
200
0
Activator: - + + +
ZCL278: - - + -
NSC23766: - - - +

Figure 3.8 ***Immunofluorescence light microscopy of active Cdc42 and phosphorylated RhoA***.

Serum starved Swiss 3T3 cells were treated with either DMSO as control, a Cdc42 activator, 50 μM ZCL278 or 10 μM NSC23766. Treatments with ZCL278 or NSC23766 were followed by stimulation for 2 minutes with a Cdc42 activator at 1 unit/mL. In order to determine if ZCL278 selectively inhibits Cdc42 but not RhoA activity, cells were probed with an active Cdc42 (A, and B) or phosphorylated RhoA (C) antibodies. Arrows: peri-nuclear organization of active Cdc42 possibly corresponding to the Golgi- ER network. In order to more clearly visualize staining intensity, active Cdc42 immunostaining is represented using the pseudocolor setting of the MetaMorph™ 4.6 imaging software systems (Molecular Devices, Sunnyvale, CA). Light blue indicates areas of higher intensity, whereas purple indicates areas of lower active Cdc42 intensity. Nuclei were visualized in dark blue by Hoechst staining. Bar: 15 μm. (B) Active Cdc42 associated with organized perinuclear Golgi-ER network was quantified. Organized Golgi-ER was quantified in five randomly selected regions of cells in each treatment group using the pseudocolor setting (*, $p< 0.05$). (C) Pixel intensity of phospho-RhoA in cells after treatments with Activator, ZCL278, or NSC23766 was quantified. Results reflect the averaged intensity generated at five random points in five independent cells (n= 5/ group) ± S.E. (*, $p< 0.03$).

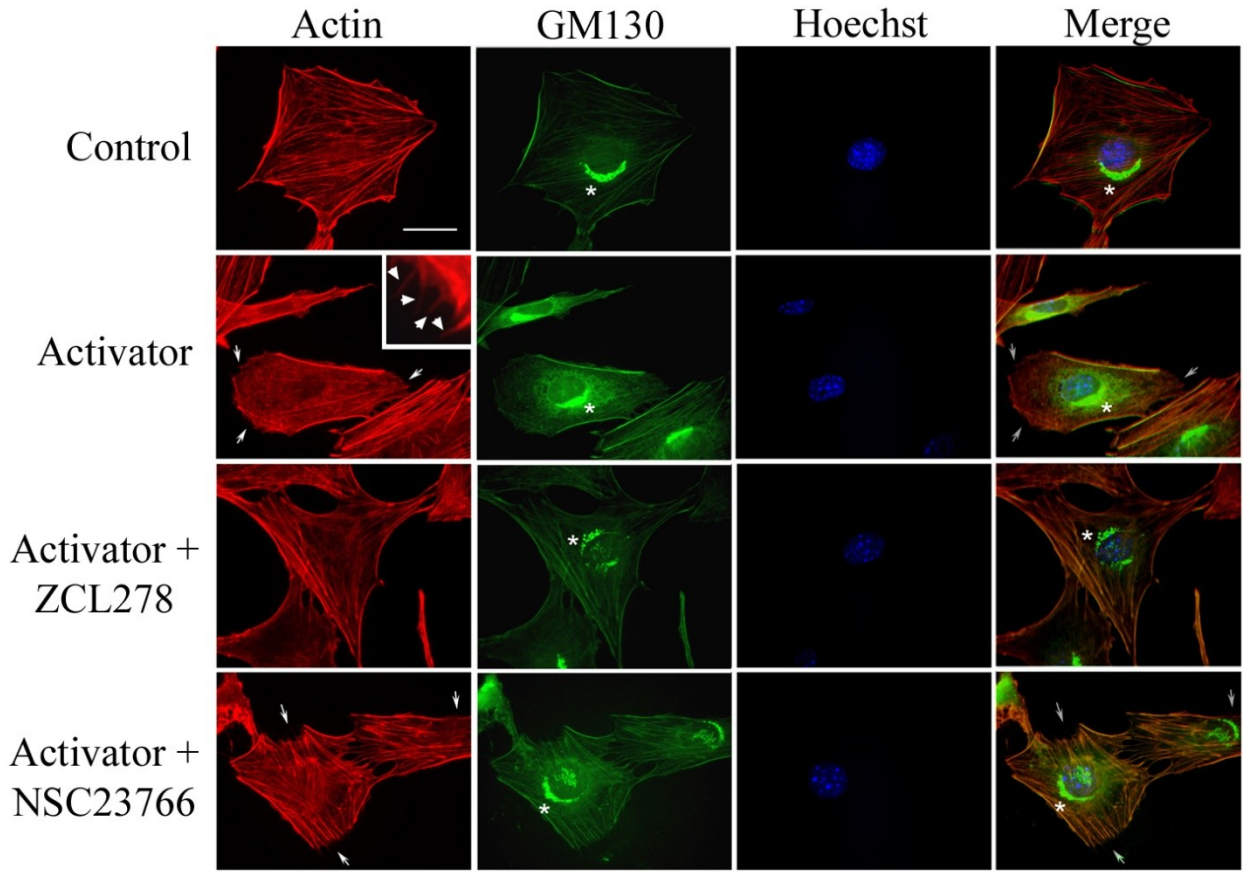
Actin
GM130
Hoechst
Merge
Control
Activator
Activator + ZCL278
Activator + NSC23766

Figure 3.9 ***ZCL278 disrupts GM130 docked Golgi organization*****.**

Serum-starved Swiss 3T3 cells were treated with DMSO as control, a Cdc42 activator, ZCL278, or NSC23766. Following the treatment, cells were stained by rhodamine phalloidin (Red), anti-GM130 (green), and Hoechst (blue). Arrows point to the cell edges where microspikes can be seen in phalloidin-stained cells (red). Insert shows the high magnification of the cells treated with the Cdc42 activator, where arrowheads point to microspikes. Asterisks in (green) point to the Golgi structure immunolabeled by anti-GM130. Cdc42 activation led to increased microspikes, as expected (Activator: red-arrows and insert: arrowheads), and intense peri-nuclear GM130 immuroreactivity (Activator: green-asterisk). Cells treated with ZCL278 showed fewer microspikes (ZCL278: red). GM130 immunoreactivity is clearly reduced and distributed to both sides of the nucleus (ZCL278: green-asterisk). Rac inhibitor NSC23766 did not significantly alter microspike formation (NSC23766: red-arrows) and GM130 expression or distribution (NSC23766: green-asterisk). Bar: 10 μm.

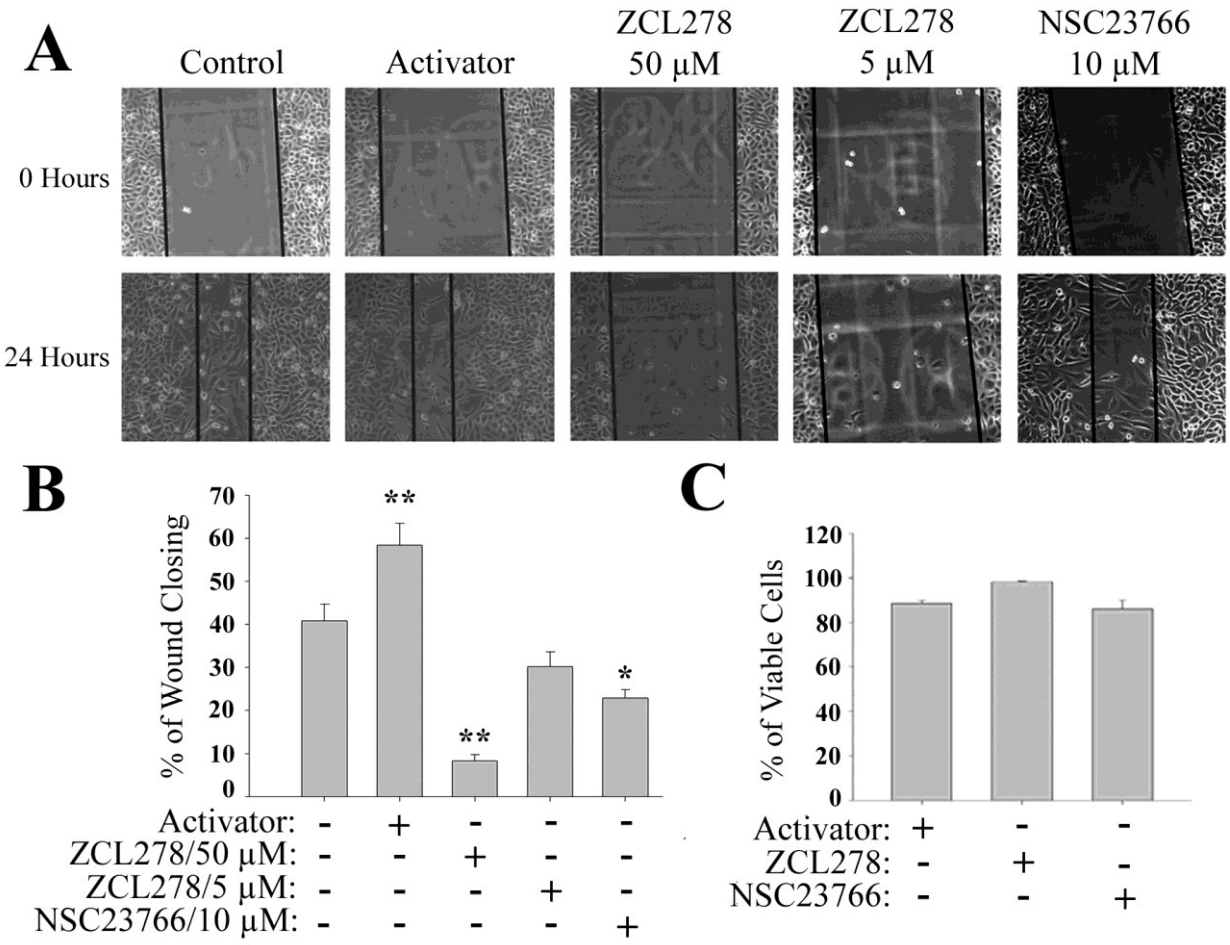
A
Control
Activator
ZCL278
50 µM
ZCL278
5 µM
NSC23766
10 µM
0 Hours
24 Hours
B
% of Wound Closing
70
60
50
40
30
20
10
0
**
**
*
Activator: - + - - -
ZCL278/50 µM: - - + - -
ZCL278/5 µM: - - - + -
NSC23766/10 µM: - - - - +
C
% of Viable Cells
120
100
80
60
40
20
0
Activator: + - -
ZCL278: - + -
NSC23766: - - +

Figure 3.10 ***ZCL278 impedes cellular migration without disruption of cell viability.***

(A) Serum starved PC-3 cells were grown to confluent monolayers, wounded using a sterile pipette tip, and incubated for 24 hours with a Cdc42 activator at 1 unit/mL, 50 μM ZCL278, 5 μM ZCL278, or 10 μM NSC23766. The distance of migration was then analyzed by phase contrast microscopy and MetaMorph™ 4.6 imaging software systems (Molecular Devices, Sunnyvale, CA). Black lines indicate the leading edge of the wound. (B) Wound healing was quantified at 0 and 24 hours by measuring the shortest distance between the edges of the scratch. Columns represent the wound healing as a percentage of the original wound distance. Results shown are averaged from three independent experiments (n= 3/ group) ± S.E. (**, $p< 0.01$, *, $p< 0.05$). (C) Serum-starved PC-3 cells were incubated for 24 hours with 50 uM ZCL278 or 10 uM NSC23766. Cell viability was determined using a Countess Automated Cell Counter (Invitrogen) combined with trypan blue dye staining of cells.

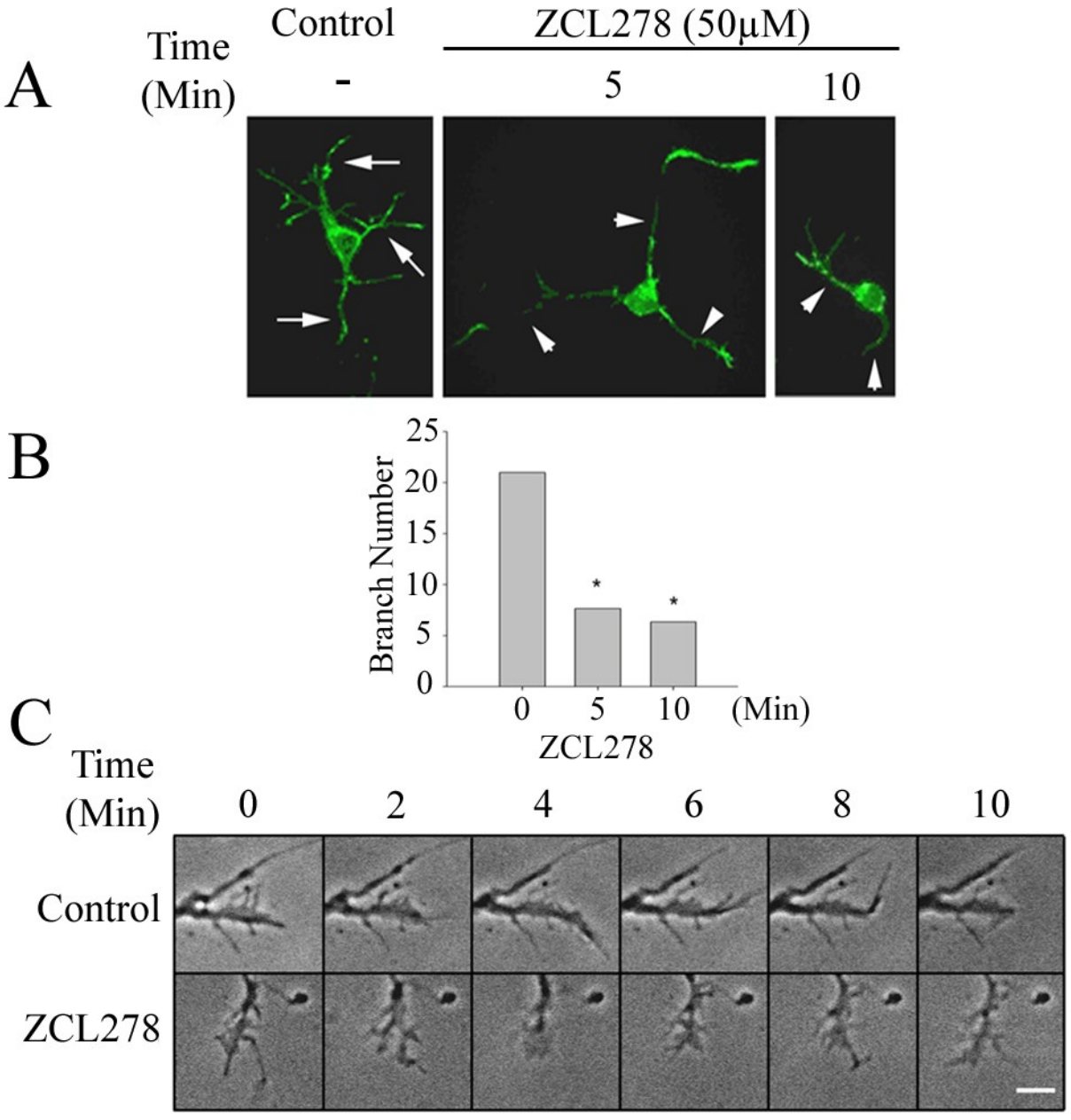
A
Time
(Min)
Control
ZCL278 (50μM)
-
5
10
B
Branch Number
25
20
15
10
5
0
*
*
0
5
10
(Min)
ZCL278
C
Time
(Min)
0
2
4
6
8
10
Control
ZCL278

Figure 3.11 ***ZCL278 inhibits neuronal branching and growth cone motility.***

Primary cortical neurons from postnatal day one mouse pups were cultured on poly-L-lysine coated coverslips. (A) Neurons were treated at 5 days *in vitro* with either DMSO (control) or 50 μM of ZCL278 for 5 and 10 minutes. Neurons were then fixed and actin based structures were identified with rhodamine phalloidin labeling. While control neurons showed multiple branches (arrows), ZCL278 treatment reduced the branch numbers (arrowheads). (B) The number of branches was counted on neurons treated with ZCL278. Results shown are averaged from 3 independent experiments (n= 3/ group) ± S.E. (*, $p< 0.01$). (C) Time-lapse imaging of cortical neuronal growth cone motility. While the control neuron maintains multiple microspikes or filapodia, ZCL278 treatment led to rapid retraction of microspikes or filopodia. Bar: 1 μm.

F. Acknowledgements

Chapter III was modified and reprinted from the Proceedings of the National Academy of Sciences of the United States of America. 110: 1261-1266. Amy Friesland, Yaxue Zhao, Yan-Hua Chen, Lie Wang, Huchen Zhou, and Qun Lu**.** Small molecule targeting Cdc42-intersectin interaction disrupts Golgi organization and suppresses cell motility. **Amy Friesland** is the lead first author with Yaxue Zhao as a co-first author. Copyright 2013, see Appendix B. Virtual Screening, synthesis, surface plasmon resonance, and determinations of pKa and solubility were performed by Yaxue Zhao, Lei Wang, and Huchen Zhou at Shanghai Jiao Tong University, Shanghai, China (Figures 3.1 and 3.3).

CHAPTER IV: Conclusions and General Discussion

It is abundantly clear through a variety of clinical and experimental studies that Rho proteins are critical regulators in many cellular functions which lead to their varied and important roles in pathological conditions ranging from cardiovascular and neurological dysfunction to cancer initiation and progression. Additionally, there are multiple lines of evidence supporting Rho pathway intervention as a viable treatment for several human disease conditions including cerebral vasospasm (Loirand et al., 2006; Shibuya et al., 1992) and pulmonary hypertension (Kishi et al., 2005). RhoA inhibitor LM11A-31 is currently in phase I human clinical trials as an Alzheimer's disease treatment, after marked success in mice (Knowles et al., 2013; Tep et al., 2013; Yang et al., 2008). For these reasons, Rho proteins are very attractive targets for drug development and therapeutic intervention (Lu et al., 2009). In the current study, we aim not only to understand the role of RhoA in chemotherapy induced neurotoxicity but to fill a substantial gap in Rho protein signaling by identifying and characterizing novel small molecules that specifically target Cdc42 activation.

In Chapter II, we confirmed that cisplatin induced RhoA activation in our *in vivo* CIPN model. In addition, this increase in RhoA activity was correlated with decreased peripheral nerve sensitivity and increased neuronal damage. Furthermore, application of upstream RhoA inhibitor LM11A-31 alleviated cisplatin-induced rise in RhoA activity and neurodegeneration. Importantly, our work expands on previous data supporting RhoA inhibition in CIPN recovery (James et al., 2010) and demonstrates that RhoA pathway suppression could be used in conjunction with clinically relevant doses of cisplatin chemotherapy to prevent CIPN development. This study, therefore, could have important clinical implications for patients undergoing chemotherapy. LM11A-31 is well tolerated in mice and capable of oral uptake and if

clinical trials are successful in human patients, this compound could be easily be transitioned clinically to an adjuvant therapy to cisplatin.

However, because the animals in our study are normal, healthy, young mice our results might be slightly skewed from what would be seen in a more clinically relevant tumor-bearing mouse model. Therefore, it will be very important to confirm the present results in a modified CIPN model. Currently our cisplatin doses are not only clinically relevant to human patients but have also been shown in mouse models of lung cancer (Oliver et al., 2010) and breast cancer (Shafee et al., 2008) to be effective and tolerable. Additionally, due to RhoA's known relevance to several types of cancer, application of Rho inhibitors may have a compound effect of decreasing tumor progression and preventing CIPN, which would make Rho suppression an even more valuable clinical target. In fact, studies support that pharmacological inhibition of Rho-kinase with Y-27632 could not only reduce melanoma tumor volumes (Routhier et al., 2010) but also decrease metastasis of breast cancer cells in C57/BL6 mouse models (Liu et al., 2009). Furthermore, recent work has indicated that Y-27632 and fasudil could also enhance the cytotoxic effects of cisplatin in *in vitro* models of ovarian cancer (Ohta et al., 2012).

Further study is needed to confirm the mechanism of cisplatin-induced neurodegeneration in the peripheral nerve. Although our study confirmed the involvement of the RhoA signaling pathway and implicated SHP2 phosphatase in the neurodegenerative mechanism, we still lack a clear understanding of cisplatin's direct target. Studies have suggested a preferential accumulation of cisplatin within the dorsal root ganglion (DRG) thereby increasing the likelihood of apoptosis (McDonald et al., 2005). However, this does not adequately explain the differences seen clinically from one patient to another, where their ability to recover varies from partial to full or they sustain permanent debilitation. It is more likely that cisplatin may also

target the nerve directly, due to its lack of protection by the blood brain barrier, thereby allowing cisplatin to affect the Schwann cell population and underlying axon with little interference. Additionally, it is unclear whether cisplatin may preferentially target smaller, more distal nerve fibers and endings, as opposed to larger more proximal nerves. Our studies suggest that cisplatin impacts nerve fiber morphology, especially in the level of myelination, which may explain the overall reduction in fiber size and subsequent reductions in axonal area. Interestingly, RhoA is known to be modulated by myelin-associated inhibitors Nogo (Chen et al., 2000b), myelin-associated glycoprotein (MAG; McKerracher et al., 1994) and oligodendrocyte-myelin glycoprotein (OMgp; Wang et al., 2002) which are well established in inflammatory-induced neuronal injuries.

Also of importance is the ability to understand how other Rho proteins (Rac1 and Cdc42) possibly contribute to CIPN generation. Many studies confirm signaling relationships between Rho proteins whereby they can antagonize or support each other. Although we have access to specific Rac1 inhibitor NSC23766, we were severely lacking small molecules that could be utilized to inhibit Cdc42 and be applied to our CIPN model. Therefore, in Chapter III we sought to develop and characterize small molecules that had the potential to fit into the GEF binding pocket of Cdc42 and specifically inhibit its activation. Our work identified compound ZCL278, which was able to bind and inhibit Cdc42-mediated functions such as microspike formation, Golgi organization, neuronal branching and cell motility. Importantly, ZCL278 was found to be cell permeable and quite easy to synthesize, making it an amenable option for use as a pharmaceutical lead. Moreover, ZCL278 did not alter Rac1 or RhoA-mediated activation or activity.

Identification of small molecule inhibitors of protein-protein interactions is becoming increasingly important due to the key roles they can play in many biological processes and their potential for therapeutic intervention. Small molecules can be highly specific for their molecular targets, and are thus of high interest to scientific investigators, pharmaceutical companies, and clinical researchers. Identification of ZCL278 has opened an important door to further understanding of Cdc42 signaling pathways. It will help determine how Cdc42 cooperates or antagonizes other Rho proteins, and the roles it plays in biological processes underlying human disease states. Additionally, ZCL278 identification will hopefully spur further screenings to identify more specific activators and inhibitors of Cdc42 as well as other Rho family members.

The next steps in order to utilize ZCL278 in our CIPN mouse model will be to elucidate its effects *in vivo* and determine proper dosage. First, determination of appropriate routes of *in vivo* administration, including method and vehicle are needed. Next, we will not only have to determine tolerability of the compound, but also ascertain appropriate dosage regimens. Furthermore, toxicity of ZCL278 will also have to be assessed by histological analysis of harvested tissue. Once characterized and determined to be safe for *in vivo* use, we can then modify our CIPN protocol to include ZCL278-mediated Cdc42 inhibition and investigate possible cross regulation of Cdc42 and RhoA.

Due to the described hierarchical relationships between Rho proteins (Nobes and Hall, 1995) it would be expected to see alteration in Rho proteins other than RhoA. As a mutually inhibitory antagonistic relationship exists between RhoA and Cdc42 (Nobes and Hall, 1995) results might show decreased Cdc42 activation as a result of cisplatin treatment. In fact, cisplatin and docetaxel were shown to suppress Cdc42 activity in a model of squamous cell carcinoma (Kogashiwa et al., 2010) and in a study of anticancer agents in human umbilical vein

endothelial cells (Bijman et al., 2006). In neurons, RhoA activation is also accompanied by the inhibition of Rac1 and Cdc42 (Yamaguchi et al., 2001; Wong et al., 2001). However, to date, there are no studies that have investigated Rac1 and Cdc42 in CIPN nerves. Understanding the totality of Rho GTPase function in cisplatin-induced neurotoxicity could allow us to more precisely target Rho-mediated neurodegenerative mechanisms that occur due to concurrent chemotherapeutic administration.

Overall, our studies further support Rho pathway intervention as a neuroprotective strategy that could be applied to a variety or human conditions, especially cisplatin-induced peripheral neuropathy. We confirm RhoA activity is increased due to cisplatin and correlate it to the neurodegeneration incurred through treatment. We established that LM11A-31, when co-administered with cisplatin, could not only reduce RhoA activity, but protect peripheral nerves from the detrimental effects of cisplatin. Additionally, by identification of ZCL278 we open a door for increased exploration of Cdc42 signaling *in vitro* that will hopefully one day allow us to assess Rho protein crosstalk *in vivo* in the CIPN mouse model. ZCL278 has the potential to become a powerful molecular tool that can enhance continued Rho protein exploration and development of targeted therapies that support not only treatments for CIPN, but also cancer, cardiovascular disease, and other neurological problems.

REFERENCES

Adam, L., Vadlamudi, R. K., McCrea, P., and Kumar, R. (2001). Tiam1 overexpression potentiates heregulin-induced lymphoid enhancer factor-1/beta-catenin nuclear signaling in breast cancer cells by modulating the intercellular stability. *J. Biol. Chem. 276*, 28443-50.

Adamson, P., Etienne, S., Couraud, P. O., Calder, V., and Greenwood, J. (1999). Lymphocyte migration through brain endothelial cell monolayers involves signaling through endothelial ICAM-1 via a rho-dependent pathway. *J. Immunol. 162*, 2964-73.

Ahmad, K. F., and Lim, W. A. (2010). The minimal autoinhibited unit of the guanine nucleotide exchange factor intersectin. *PLoS ONE 5*, e11291.

Ahnert-Hilger, G., Höltje, M., Grosse, G., Pickert, G., Mucke, C., Nixdorf-Bergweiler, B., Boquet, P., Hofmann, F., and Just, I. (2004). Differential effects of Rho GTPases on axonal and dendritic development in hippocampal neurones. *J. Neurochem. 90*, 9-18.

Aloe, L., Manni, L., Properzi, F., De Santis, S., and Fiore, M. (2000). Evidence that nerve growth factor promotes the recovery of peripheral neuropathy induced in mice by cisplatin: behavioral, structural and biochemical analysis. *Auton. Neurosci. 86*, 84-93.

Amano, M., Fukata, Y., and Kaibuchi, K. (2000). Regulation and functions of Rho-associated kinase. *Exp. Cell Res. 261*, 44-51.

Amano, M., Ito, M., Kimura, K., Fukata, Y., Chihara, K., Nakano, T., Matsuura, Y., and Kaibuchi, K. (1996). Phosphorylation and activation of myosin by Rho-associated kinase (Rho-kinase). *J. Biol. Chem. 271*, 20246-9.

Amano, T., Tanabe, K., Eto, T., Narumiya, S., and Mizuno, K. (2001). LIM-kinase 2 induces formation of stress fibres, focal adhesions and membrane blebs, dependent on its activation by Rho-associated kinase-catalysed phosphorylation at threonine-505. *Biochem. J. 354*, 149-59.

Auer, M., Hausott, B., and Klimaschewski, L. (2011). Rho GTPases as regulators of morphological neuroplasticity. *Ann. Anat. 193*, 259-66.

Authier, N., Balayssac, D., Marchand, F., Ling, B., Zangarelli, A., Descoeur, J., Coudore, F., Bourinet, E., and Eschalier, A. (2009). Animal models of chemotherapy-evoked painful peripheral neuropathies. *Neurotherapeutics 6*, 620-9.

Balasenthil, S., Sahin, A. A., Barnes, C. J., Wang, R. A., Pestell, R. G., Vadlamudi, R. K., and Kumar, R. (2004). p21-activated kinase-1 signaling mediates cyclin D1 expression in mammary epithelial and cancer cells. *J. Biol. Chem. 279*, 1422-8.

Bashour, A. M., Fullerton, A. T., Hart, M. J., and Bloom, G. S. (1997). IQGAP1, a Rac- and Cdc42-binding protein, directly binds and cross-links microfilaments. *J. Cell Biol. 137*, 1555-66.

Beijers, A. J., Jongen, J. L., and Vreugdenhil, G. (2012). Chemotherapy-induced neurotoxicity: the value of neuroprotective strategies. *Neth. J. Med. 70*, 18-25.

Benink, H. A., and Bement, W. M. (2005). Concentric zones of active RhoA and Cdc42 around single cell wounds. *J. Cell Biol. 168*, 429-39.

Benvenuti, F., Hugues, S., Walmsley, M., Ruf, S., Fetler, L., Popoff, M., Tybulewicz, V. L., and Amigorena, S. (2004). Requirement of Rac1 and Rac2 expression by mature dendritic cells for T cell priming. *Science 305*, 1150-3.

Bijman, M. N., van Nieuw Amerongen, G. P., Laurens, N., van Hinsbergh, V. W., and Boven, E. (2006). Microtubule-targeting agents inhibit angiogenesis at subtoxic concentrations, a process associated with inhibition of Rac1 and Cdc42 activity and changes in the endothelial cytoskeleton. *Mol. Cancer Ther. 5*, 2348-57.

Bito, H., Furuyashiki, T., Ishihara, H., Shibasaki, Y., Ohashi, K., Mizuno, K., Maekawa, M., Ishizaki, T., and Narumiya, S. (2000). A critical role for a Rho-associated kinase, p160ROCK, in determining axon outgrowth in mammalian CNS neurons. *Neuron 26*, 431-41.

Boettner, B., and Van Aelst, L. (2002). The role of Rho GTPases in disease development. *Gene 286,* 155-74.

Boo, J. H., Sohn, J. H., Kim, J. E., Song, H., and Mook-Jung, I. (2008). Rac1 changes the substrate specificity of gamma-secretase between amyloid precursor protein and Notch1. *Biochem. Biophys. Res. Commun. 372*, 913-7.

Boulikas, T., and Vougiouka, M. (2003). Cisplatin and platinum drugs at the molecular level. *Oncol. Rep. 10*, 1663-82.

Boulter, E., Garcia-Mata, R., Guilluy, C., Dubash, A., Rossi, G., Brennwald, P. J., and Burridge, K. (2010). Regulation of Rho GTPase crosstalk, degradation and activity by RhoGDI1. *Nat. Cell Biol. 12*, 477-83.

Boureux, A., Vignal, E., Faure, S., and Fort, P. (2007). Evolution of the Rho family of ras-like GTPases in eukaryotes. *Mol. Biol. Evol. 24*, 203-16.

Brabeck, C., Beschorner, R., Conrad, S., Mittelbronn, M., Bekure, K., Meyermann, R., Schluesener, H. J., and Schwab, J. M. (2004). Lesional expression of RhoA and RhoB following traumatic brain injury in humans. *J. Neurotrauma 21*, 697-706.

Broman, M. T., Kouklis, P., Gao, X., Ramchandran, R., Neamu, R. F., Minshall, R. D., and Malik, A. B. (2006). Cdc42 regulates adherens junction stability and endothelial permeability by inducing alpha-catenin interaction with the vascular endothelial cadherin complex. *Circ. Res. 98*, 73-80.

Brown, M. D., Cornejo, B. J., Kuhn, T. B., and Bamburg, J. R. (2000). Cdc42 stimulates neurite outgrowth and formation of growth cone filopodia and lamellipodia. *J. Neurobiol. 43*, 352-64.

Buhl, A. M., Johnson, N. L., Dhanasekaran, N., and Johnson, G. L. (1995). G alpha 12 and G alpha 13 stimulate Rho-dependent stress fiber formation and focal adhesion assembly. *J. Biol. Chem. 270*, 24631-4.

Bustelo, X. R., Sauzeau, V., and Berenjeno, I. M. (2007). GTP-binding proteins of the Rho/Rac family: regulation, effectors and functions in vivo. *Bioessays 29*, 356-70.

Cascinu, S., Cordella, L., Del Ferro, E., Fronzoni, M., and Catalano, G. (1995). Neuroprotective effect of reduced glutathione on cisplatin-based chemotherapy in advanced gastric cancer: a randomized double-blind placebo-controlled trial. *J. Clin. Oncol. 13*, 26-32.

Cataldo, A. M., Peterhoff, C. M., Troncoso, J. C., Gomez-Isla, T., Hyman, B. T., and Nixon, R. A. (2000). Endocytic pathway abnormalities precede amyloid beta deposition in sporadic Alzheimer's disease and Down syndrome: differential effects of APOE genotype and presenilin mutations. *Am. J. Pathol. 157*, 277-86.

Cerione, R. A. (2004). Cdc42: new roads to travel. *Trends Cell Biol. 14*, 127-32.

Chen, F., Ma, L., Parrini, M. C., Mao, X., Lopez, M., Wu, C., Marks, P. W., Davidson, L., Kwiatkowski, D. J., Kirchhausen, T., Orkin, S., Rosen, F., Mayer, B., Kirschner, M., and Alt, F. (2000a). Cdc42 is required for PIP(2)-induced actin polymerization and early development but not for cell viability. *Curr. Biol. 10*, 758-65.

Chen, M. S., Huber, A. B., van der Haar, M. E., Frank, M., Schnell, L., Spillmann, A. A., Christ, F., and Schwab, M. E. (2000b). Nogo-A is a myelin-associated neurite outgrowth inhibitor and an antigen for monoclonal antibody IN-1. *Nature 403*, 434-9.

Chen, L., Chan, T. H., Yuan, Y. F., Hu, L., Huang, J., Ma, S., Wang, J., Dong, S. S., Tang, K. H., Xie, D., Li, Y. and Guan, X. Y. (2010). CHD1L promotes hepatocellular carcinoma progression and metastasis in mice and is associated with these processes in human patients. *J. Clin. Invest. 120*, 1178-91.

Cheng, C., Webber, C. A., Wang, J., Xu, Y., Martinez, J. A., Liu, W. Q., McDonald, D., Guo, G. F., Nguyen, M. D., and Zochodne, D. W. (2008). Activated RHOA and peripheral axon regeneration. *Exp*. *Neurol. 212,* 358-69.

Cherfils, J., and Zeghouf, M. (2013). Regulation of Small GTPases by GEFs, GAPs, and GDIs. *Physiol. Rev. 93*, 269-309.

Ching, Y. P., Wong, C. M., Chan, S. F., Leung, T. H., Ng, D. C., Jin, D. Y., and Ng, I. O. (2003). Deleted in liver cancer (DLC) 2 encodes a RhoGAP protein with growth suppressor function and is underexpressed in hepatocellular carcinoma. *J. Biol. Chem. 278*, 10824-30.

Chitaley, K., Weber, D., and Webb, R. C. (2001). RhoA/Rho-kinase, vascular changes, and hypertension. *Curr. Hypertens. Rep. 3*, 139-44.

Chomiak, T., and Hu, B. (2009). What is the optimal value of the g-ratio for myelinated fibers in the rat CNS? A theoretical approach. *PLoS ONE 4*, e7754.

Chrostek, A., Wu, X., Quondamatteo, F., Hu, R., Sanecka, A., Niemann, C., Langbein, L., Haase, I., and Brakebusch, C. (2006). Rac1 is crucial for hair follicle integrity but is not essential for maintenance of the epidermis. *Mol. Cell. Biol. 26*, 6957-70.

Chuang, T. H., Xu, X., Kaartinen, V., Heisterkamp, N., Groffen, J., and Bokoch, G. M. (1995). Abr and Bcr are multifunctional regulators of the Rho GTP-binding protein family. *Proc. Natl. Acad. Sci. U.S.A. 92*, 10282-6.

Cosgaya, J. M., Chan, J. R., and Shooter, E. M. (2002). The neurotrophin receptor p75NTR as a positive modulator of myelination. *Science 298*, 1245-8.

Croft, D. R., and Olson, M. F. (2006). The Rho GTPase effector ROCK regulates cyclin A, cyclin D1, and p27Kip1 levels by distinct mechanisms. *Mol. Cell. Biol. 26*, 4612-27.

Da Silva, J. S., Medina, M., Zuliani, C., Di Nardo, A., Witke, W., and Dotti, C. G. (2003). RhoA/ROCK regulation of neuritogenesis via profilin IIa-mediated control of actin stability. *J. Cell Biol. 162*, 1267-79.

Debidda, M., Wang, L., Zang, H., Poli, V., and Zheng, Y. (2005). A role of STAT3 in Rho GTPase-regulated cell migration and proliferation. *J. Biol. Chem. 280*, 17275-85.

Dergham, P., Ellezam, B., Essagian, C., Avedissian, H., Lubell, W. D., and McKerracher, L. (2002). Rho signaling pathway targeted to promote spinal cord repair. *J. Neurosci. 22*, 6570-7.

Désiré, L., Bourdin, J., Loiseau, N., Peillon, H., Picard, V., De Oliveira, C., Bachelot, F., Leblond, B., Taverne, T., Beausoleil, E., Lacombe, S., and Domini, D. (2005). RAC1 inhibition targets amyloid precursor protein processing by gamma-secretase and decreases Abeta production in vitro and in vivo. *J. Biol. Chem. 280*, 37516-25.

Didsbury, J., Weber, R. F., Bokoch, G. M., Evans, T., and Snyderman, R. (1989). rac, a novel ras-related family of proteins that are botulinum toxin substrates. *J. Biol. Chem. 264*, 16378-82.

Dong, J. M., Leung, T., Manser, E., and Lim, L. (1998). cAMP-induced morphological changes are counteracted by the activated RhoA small GTPase and the Rho kinase ROKalpha. *J. Biol. Chem. 27*3, 22554-62.

Dotti, C. G., Sullivan, C. A., and Banker, G. A. (1988). The establishment of polarity by hippocampal neurons in culture. *J. Neurosci. 8*, 1454-68.

Dransart, E., Olofsson, B., and Cherfils, J. (2005). RhoGDIs revisited: novel roles in Rho regulation. *Traffic 6*, 957-66.

Dubreuil, C. I., Marklund, N., Deschamps, K., McIntosh, T. K., and McKerracher, L. (2006). Activation of Rho after traumatic brain injury and seizure in rats. *Exp. Neurol. 198*, 361-9.

Dubreuil, C. I., Winton, M. J., and McKerracher, L. (2003). Rho activation patterns after spinal cord injury and the role of activated Rho in apoptosis in the central nervous system. *J. Cell Biol. 162*, 233-43.

Durkin, M. E., Yuan, B. Z., Zhou, X., Zimonjic, D. B., Lowy, D. R., Thorgeirsson, S. S., and Popescu, N. C. (2007). DLC-1:a Rho GTPase-activating protein and tumour suppressor. *J. Cell. Mol. Med. 11*, 1185-207.

Eastman, A. (1990). Activation of programmed cell death by anticancer agents: cisplatin as a model system. *Cancer Cells 2*, 275-80.

Edwards, D. C., Sanders, L. C., Bokoch, G. M., and Gill, G. N. (1999). Activation of LIM-kinase by Pak1 couples Rac/Cdc42 GTPase signalling to actin cytoskeletal dynamics. *Nat. Cell Biol. 1*, 253-9.

Ellenbroek, S. I., and Collard, J. G. (2007). Rho GTPases: functions and association with cancer. *Clin. Exp. Metastasis 24*, 657-72.

Ellerbroek, S. M., Wennerberg, K., and Burridge, K. (2003). Serine phosphorylation negatively regulates RhoA in vivo. *J. Biol. Chem. 278*, 19023-31.

Erickson, J. W., Zhang, C. j., Kahn, R. A., Evans, T., and Cerione, R. A. (1996). Mammalian Cdc42 is a brefeldin A-sensitive component of the Golgi apparatus. *J. Biol. Chem. 271*, 26850-4.

Etienne, S., Adamson, P., Greenwood, J., Strosberg, A. D., Cazaubon, S., and Couraud, P. O. (1998). ICAM-1 signaling pathways associated with Rho activation in microvascular brain endothelial cells. *J. Immunol. 161*, 5755-61.

Etienne-Manneville, S., and Hall, A. (2003). Cdc42 regulates GSK-3beta and adenomatous polyposis coli to control cell polarity. *Nature 421*, 753-6.

Etienne-Manneville, S., and Hall, A. (2002). Rho GTPases in cell biology. *Nature 420*, 629-35.

Evangelista, M., Zigmond, S., and Boone, C. (2003). Formins: signaling effectors for assembly and polarization of actin filaments. *J. Cell. Sci. 116*, 2603-11.

Feng, Y., Schlösser, F. J., and Sumpio, B. E. (2009). The Semmes Weinstein monofilament examination as a screening tool for diabetic peripheral neuropathy. *J. Vasc. Surg. 50*, 675-82, 682.e1.

Fichtinger-Schepman, A. M., van der Veer, J. L., den Hartog, J. H., Lohman, P. H., and Reedijk, J. (1985). Adducts of the antitumor drug cis-diamminedichloroplatinum(II) with DNA: formation, identification, and quantitation. *Biochemistry 24*, 707-13.

Flatau, G., Lemichez, E., Gauthier, M., Chardin, P., Paris, S., Fiorentini, C., and Boquet, P. (1997). Toxin-induced activation of the G protein p21 Rho by deamidation of glutamine. *Nature 387*, 729-33.

Florea, A. M., and Büsselberg, D. (2011). Cisplatin as an anti-tumor drug: cellular mechanisms of activity, drug resistance and induced side effects. *Cancers 3,* 1351-1371.

Friesland, A., Zhao, Y., Chen, Y. H., Wang, L., Zhou, H., and Lu, Q. (2013). Small molecule targeting Cdc42-intersectin interaction disrupts Golgi organization and suppresses cell motility. *Proc. Natl. Acad. Sci. U.S.A. 110,* 1261-6.

Fritz, G., Brachetti, C., Bahlmann, F., Schmidt, M., and Kaina, B. (2002). Rho GTPases in human breast tumours: expression and mutation analyses and correlation with clinical parameters. *Br. J. Cancer 87*, 635-44.

Fritz, G., Just, I., and Kaina, B. (1999). Rho GTPases are over-expressed in human tumors. *Int. J. Cancer 81*, 682-7.

Fritz, G., and Kaina, B. (2006). Rho GTPases: promising cellular targets for novel anticancer drugs. *Curr. Cancer Drug Targets 6*, 1-14.

Fromm, C., Coso, O. A., Montaner, S., Xu, N., and Gutkind, J. S. (1997). The small GTP-binding protein Rho links G protein-coupled receptors and Galpha12 to the serum response element and to cellular transformation. *Proc. Natl. Acad. Sci. U.S.A. 9*4, 10098-103.

Frost, J. A., Xu, S., Hutchison, M. R., Marcus, S., and Cobb, M. H. (1996). Actions of Rho family small G proteins and p21-activated protein kinases on mitogen-activated protein kinase family members. *Mol. Cell. Biol. 16*, 3707-13.

Fukata, M., Watanabe, T., Noritake, J., Nakagawa, M., Yamaga, M., Kuroda, S., Matsuura, Y., Iwamatsu, A., Perez, F., and Kaibuchi, K. (2002). Rac1 and Cdc42 capture microtubules through IQGAP1 and CLIP-170. *Cell 109*, 873-85.

Funakoshi, Y., Ichiki, T., Shimokawa, H., Egashira, K., Takeda, K., Kaibuchi, K., Takeya, M., Yoshimura, T., and Takeshita, A. (2001). Rho-kinase mediates angiotensin II-induced monocyte chemoattractant protein-1 expression in rat vascular smooth muscle cells. *Hypertension 38*, 100-4.

Gao, Y., Dickerson, J. B., Guo, F., Zheng, J., and Zheng, Y. (2004). Rational design and characterization of a Rac GTPase-specific small molecule inhibitor. *Proc. Natl. Acad. Sci. U.S.A. 101*, 7618-23.

Garvalov, B. K., Flynn, K. C., Neukirchen, D., Meyn, L., Teusch, N., Wu, X., Brakebusch, C., Bamburg, J. R., and Bradke, F. (2007). Cdc42 regulates cofilin during the establishment of neuronal polarity. *J. Neurosci. 27*, 13117-29.

Gianni, D., Zambrano, N., Bimonte, M., Minopoli, G., Mercken, L., Talamo, F., Scaloni, A., and Russo, T. (2003). Platelet-derived growth factor induces the beta-gamma-secretase-mediated cleavage of Alzheimer's amyloid precursor protein through a Src-Rac-dependent pathway. *J. Biol. Chem. 278*, 9290-7.

Giniger, E. (2002). How do Rho family GTPases direct axon growth and guidance? A proposal relating signaling pathways to growth cone mechanics. *Differentiation 70*, 385-96.

Gjoerup, O., Lukas, J., Bartek, J., and Willumsen, B. M. (1998). Rac and Cdc42 are potent stimulators of E2F-dependent transcription capable of promoting retinoblastoma susceptibility gene product hyperphosphorylation. *J. Biol. Chem. 273*, 18812-8.

Gohla, A., Harhammer, R., and Schultz, G. (1998). The G-protein G13 but not G12 mediates signaling from lysophosphatidic acid receptor via epidermal growth factor receptor to Rho. *J. Biol. Chem. 273*, 4653-9.

Golden, S. A., Christoffel, D. J., Heshmati, M., Hodes, G. E., Magida, J., Davis, K., Cahill, M. E., Dias, C., Ribeiro, E., Ables, J. L., Kennedy, P. J., Robison, A. J., and Robison, A. J. (2013). Epigenetic regulation of RAC1 induces synaptic remodeling in stress disorders and depression. *Nat. Med. 19*, 337-44.

Gómez Del Pulgar, T., Valdés-Mora, F., Bandrés, E., Pérez-Palacios, R., Espina, C., Cejas, P., García-Cabezas, M. A., Nistal, M., Casado, E., González-Barón, M., and González-Barón, M. (2008). Cdc42 is highly expressed in colorectal adenocarcinoma and downregulates ID4 through an epigenetic mechanism. *Int. J. Oncol. 33*, 185-93.

Goode, B. L., and Eck, M. J. (2007). Mechanism and function of formins in the control of actin assembly. *Annu. Rev. Biochem. 76*, 593-627.

Gopalakrishnan, S. M., Teusch, N., Imhof, C., Bakker, M. H., Schurdak, M., Burns, D. J., and Warrior, U. (2008). Role of Rho kinase pathway in chondroitin sulfate proteoglycan-mediated inhibition of neurite outgrowth in PC12 cells. *J. Neurosci. Res. 86*, 2214-26.

Goreshnik, I., and Maly, D. J. (2010). A small molecule-regulated guanine nucleotide exchange factor. *J. Am. Chem. Soc. 132*, 938-40.

Gotta, M., Abraham, M. C., and Ahringer, J. (2001). CDC-42 controls early cell polarity and spindle orientation in C. elegans. *Curr. Biol. 11*, 482-8.

Govek, E. E., Newey, S. E., Akerman, C. J., Cross, J. R., Van der Veken, L., and Van Aelst, L. (2004). The X-linked mental retardation protein oligophrenin-1 is required for dendritic spine morphogenesis. *Nat. Neurosci. 7*, 364-72.

Govek, E. E., Newey, S. E., and Van Aelst, L. (2005). The role of the Rho GTPases in neuronal development. *Genes Dev. 19*, 1-49.

Gregg, R. W., Molepo, J. M., Monpetit, V. J., Mikael, N. Z., Redmond, D., Gadia, M., and Stewart, D. J. (1992). Cisplatin neurotoxicity: the relationship between dosage, time, and platinum concentration in neurologic tissues, and morphologic evidence of toxicity. *J. Clin. Oncol. 10*, 795-803.

Grisold, W., Cavaletti, G., and Windebank, A. J. (2012). Peripheral neuropathies from chemotherapeutics and targeted agents: diagnosis, treatment, and prevention. *Neuro-oncology 14* Suppl 4, iv45-iv54.

Guilluy, C., Brégeon, J., Toumaniantz, G., Rolli-Derkinderen, M., Retailleau, K., Loufrani, L., Henrion, D., Scalbert, E., Bril, A., Torres, R. M., and Offermanns, S. (2010). The Rho exchange factor Arhgef1 mediates the effects of angiotensin II on vascular tone and blood pressure. *Nat. Med. 16*, 183-90.

Guilluy, C., Garcia-Mata, R., and Burridge, K. (2011). Rho protein crosstalk: another social network? *Trends Cell Biol. 21*, 718-26.

Guipponi, M., Scott, H. S., Hattori, M., Ishii, K., Sakaki, Y., and Antonarakis, S. E. (1998). Genomic structure, sequence, and refined mapping of the human intersectin gene (ITSN), which encompasses 250 kb on chromosome 21q22.1-->q22.2. *Cytogenet. Cell Genet. 83*, 218-20.

Gupton, S. L., and Gertler, F. B. (2007). Filopodia: the fingers that do the walking. Sci. STKE 2007, re5.

Gutiérrez-Gutiérrez, G., Sereno, M., Miralles, A., Casado-Sáenz, E., and Gutiérrez-Rivas, E. (2010). Chemotherapy-induced peripheral neuropathy: clinical features, diagnosis, prevention and treatment strategies. *Clin. Transl. Oncol. 12*, 81-91.

Hall, A. (1998). Rho GTPases and the actin cytoskeleton. *Science 279*, 509-14.

Hara, M., Takayasu, M., Watanabe, K., Noda, A., Takagi, T., Suzuki, Y., and Yoshida, J. (2000). Protein kinase inhibition by fasudil hydrochloride promotes neurological recovery after spinal cord injury in rats. *J. Neurosurg. 93*, 94-101.

Harris, K. P., and Tepass, U. (2010). Cdc42 and vesicle trafficking in polarized cells. *Traffic 11*, 1272-9.

Higby, D. J., Wallace, H. J., Albert, D. J., and Holland, J. F. (1974). Diaminodichloroplatinum: a phase I study showing responses in testicular and other tumors. *Cancer 33*, 1*21*9-5.

Hill, C. S., Wynne, J., and Treisman, R. (1995). The Rho family GTPases RhoA, Rac1, and CDC42Hs regulate transcriptional activation by SRF. *Cell 81*, 1159-70.

Honing, H., van den Berg, T. K., van der Pol, S. M., Dijkstra, C. D., van der Kammen, R. A., Collard, J. G., and de Vries, H. E. (2004). RhoA activation promotes transendothelial migration of monocytes via ROCK. *J. Leukoc. Biol. 75*, 523-8.

Hordijk, P. L., ten Klooster, J. P., van der Kammen, R. A., Michiels, F., Oomen, L. C., and Collard, J. G. (1997). Inhibition of invasion of epithelial cells by Tiam1-Rac signaling. *Science 278*, 1464-6.

Huang, H., Zhu, L., Reid, B. R., Drobny, G. P., and Hopkins, P. B. (1995). Solution structure of a cisplatin-induced DNA interstrand cross-link. *Science 270*, 1842-5.

Hussain, N. K., Jenna, S., Glogauer, M., Quinn, C. C., Wasiak, S., Guipponi, M., Antonarakis, S. E., Kay, B. K., Stossel, T. P., Lamarche-Vane, N., and McPherson, P. S. (2001). Endocytic protein intersectin-l regulates actin assembly via Cdc42 and N-WASP. *Nat. Cell Biol. 3*, 927-32.

Ide, M., and Lewis, D. A. (2010). Altered cortical CDC42 signaling pathways in schizophrenia: implications for dendritic spine deficits. *Biol. Psychiatry 68*, 25-32.

Ishizaki, T., Maekawa, M., Fujisawa, K., Okawa, K., Iwamatsu, A., Fujita, A., Watanabe, N., Saito, Y., Kakizuka, A., Morii, N., and Narumiya, S. (1996). The small GTP-binding protein Rho binds to and activates a 160 kDa Ser/Thr protein kinase homologous to myotonic dystrophy kinase. *EMBO J. 15*, 1885-93.

Ishizaki, T., Uehata, M., Tamechika, I., Keel, J., Nonomura, K., Maekawa, M., and Narumiya, S. (2000). Pharmacological properties of Y-27632, a specific inhibitor of rho-associated kinases. *Mol. Pharmacol. 57*, 976-83.

Jaffe, A. B., and Hall, A. (2005). Rho GTPases: biochemistry and biology. *Annu. Rev. Cell Dev. Biol. 21*, 247-69.

Jaggi, A. S., and Singh, N. (2012). Mechanisms in cancer-chemotherapeutic drugs-induced peripheral neuropathy. *Toxicology 291*, 1-9.

James, S. E., Burden, H., Burgess, R., Xie, Y., Yang, T., Massa, S. M., Longo, F. M., and Lu, Q. (2008). Anti-cancer drug induced neurotoxicity and identification of Rho pathway signaling modulators as potential neuroprotectants. *Neurotoxicology 29*, 605-12.

James, S. E., Dunham, M., Carrion-Jones, M., Murashov, A., and Lu, Q. (2010). Rho kinase inhibitor Y-27632 facilitates recovery from experimental peripheral neuropathy induced by anti-cancer drug cisplatin. *Neurotoxicology 31*, 188-94.

Joberty, G., Petersen, C., Gao, L., and Macara, I. G. (2000). The cell-polarity protein Par6 links Par3 and atypical protein kinase C to Cdc42. *Nat. Cell Biol. 2,* 531-9.

Johnson, D. I., and Pringle, J. R. (1990). Molecular characterization of CDC42, a Saccharomyces cerevisiae gene involved in the development of cell polarity. *J. Cell Biol. 111*, 143-52.

Johnson, D. I. (1999). Cdc42: An essential Rho-type GTPase controlling eukaryotic cell polarity. *Microbiol. Mol. Biol. Rev. 63*, 54-105.

Johnson, E., Seachrist, D. D., DeLeon-Rodriguez, C. M., Lozada, K. L., Miedler, J., Abdul-Karim, F. W., and Keri, R. A. (2010). HER2/ErbB2-induced breast cancer cell migration and invasion require p120 catenin activation of Rac1 and Cdc42. *J. Biol. Chem. 285*, 29491-501.

Jones, S. B., Lu, H. Y., and Lu, Q. (2004). Abl tyrosine kinase promotes dendrogenesis by inducing actin cytoskeletal rearrangements in cooperation with Rho family small GTPases in hippocampal neurons. *J. Neurosci. 24*, 8510-21.

Kaley, T. J., and Deangelis, L. M. (2009). Therapy of chemotherapy-induced peripheral neuropathy. *Br. J. Haematol. 145*, 3-14.

Kamai, T., Tsujii, T., Arai, K., Takagi, K., Asami, H., Ito, Y., and Oshima, H. (2003). Significant association of Rho/ROCK pathway with invasion and metastasis of bladder cancer. *Clin. Cancer Res. 9*, 2632-41.

Kamai, T., Yamanishi, T., Shirataki, H., Takagi, K., Asami, H., Ito, Y., and Yoshida, K. (2004). Overexpression of RhoA, Rac1, and Cdc42 GTPases is associated with progression in testicular cancer. *Clin. Cancer Res. 10*, 4799-805.

Karpushev, A. V., Levchenko, V., Ilatovskaya, D. V., Pavlov, T. S., and Staruschenko, A. (2011). Novel role of Rac1/WAVE signaling mechanism in regulation of the epithelial Na+ channel. *Hypertension 57*, 996-1002.

Kataoka, C., Egashira, K., Inoue, S., Takemoto, M., Ni, W., Koyanagi, M., Kitamoto, S., Usui, M., Kaibuchi, K., Shimokawa, H., and Takeshita, A. (2002). Important role of Rho-kinase in the pathogenesis of cardiovascular inflammation and remodeling induced by long-term blockade of nitric oxide synthesis in rats. *Hypertension 39*, 245-50.

Kawano, Y., Fukata, Y., Oshiro, N., Amano, M., Nakamura, T., Ito, M., Matsumura, F., Inagaki, M., and Kaibuchi, K. (1999). Phosphorylation of myosin-binding subunit (MBS) of myosin phosphatase by Rho-kinase in vivo. *J. Cell Biol. 147*, 1023-38.

Kay, A. J., and Hunter, C. P. (2001). CDC-42 regulates PAR protein localization and function to control cellular and embryonic polarity in C. elegans. *Curr. Biol. 11*, 474-81.

Kelland, L. R. (1993). New platinum antitumor complexes. *Crit. Rev. Oncol. Hematol. 15*, 1*91*-219.

Kimura, K., Ito, M., Amano, M., Chihara, K., Fukata, Y., Nakafuku, M., Yamamori, B., Feng, J., Nakano, T., Okawa, K., Iwamatsu, A., and Kaibuchi, K. (1996). Regulation of myosin phosphatase by Rho and Rho-associated kinase (Rho-kinase). *Science 273*, 245-8.

Kishi, T., Hirooka, Y., Masumoto, A., Ito, K., Kimura, Y., Inokuchi, K., Tagawa, T., Shimokawa, H., Takeshita, A., and Sunagawa, K. (2005). Rho-kinase inhibitor improves increased vascular resistance and impaired vasodilation of the forearm in patients with heart failure. *Circulation 111*, 2741-7.

Knowles, J. K., Simmons, D. A., Nguyen, T. V., Vander Griend, L., Xie, Y., Zhang, H., Yang, T., Pollak, J., Chang, T., Arancio, O., Buckwalter, M. S., and Wyss-Coray, T. (2013). A small molecule p75(NTR) ligand prevents cognitive deficits and neurite degeneration in an Alzheimer's mouse model. *Neurobiol. Aging 34*, 2052-63.

Koeppen, S., Verstappen, C. C. P., and Körte, R. (2004). Lack of neuroprotection by an ACTH (4–9) analogue. A randomized trial in patients treated with vincristine for Hodgkin's or non-Hodgkin's lymphoma. *J. Cancer Res. Clin. Oncol. 130*:153-60.

Kogashiwa, Y., Sakurai, H., Kimura, T., and Kohno, N. (2010). Docetaxel suppresses invasiveness of head and neck cancer cells in vitro. *Cancer Sci. 101*, 1382-6.

Kontaridis, M. I., Eminaga, S., Fornaro, M., Zito, C. I., Sordella, R., Settleman, J., and Bennett, A. M. (2004). SHP2 positively regulates myogenesis by coupling to the Rho GTPase signaling pathway. *Mol. Cell. Biol. 24*, 5340-52.

Kouklis, P., Konstantoulaki, M., Vogel, S., Broman, M., and Malik, A. B. (2004). Cdc42 regulates the restoration of endothelial barrier function. *Circ. Res. 94*, 159-66.

Kourlas, P. J., Strout, M. P., Becknell, B., Veronese, M. L., Croce, C. M., Theil, K. S., Krahe, R., Ruutu, T., Knuutila, S., Bloomfield, C. D., Bloomfield, C. D., and Caligiuri, M. A. (2000). Identification of a gene at 11q23 encoding a guanine nucleotide exchange factor: evidence for its fusion with MLL in acute myeloid leukemia. *Proc. Natl. Acad. Sci. U.S.A. 97*, 2145-50.

Kozma, R., Ahmed, S., Best, A., and Lim, L. (1995). The Ras-related protein Cdc42Hs and bradykinin promote formation of peripheral actin microspikes and filopodia in Swiss 3T3 fibroblasts. *Mol. Cell. Biol. 15*, 1942-52.

Kozma, R., Sarner, S., Ahmed, S., and Lim, L. (1997). Rho family GTPases and neuronal growth cone remodelling: relationship between increased complexity induced by Cdc42Hs, Rac1, and acetylcholine and collapse induced by RhoA and lysophosphatidic acid. *Mol. Cell. Biol. 17*, 1201-11.

Kranenburg, O., Poland, M., Gebbink, M., Oomen, L., and Moolenaar, W. H. (1997). Dissociation of LPA-induced cytoskeletal contraction from stress fiber formation by differential localization of RhoA. *J. Cell Sci. 110*, 2417-27.

Kranenburg, O., Poland, M., van Horck, F. P., Drechsel, D., Hall, A., and Moolenaar, W. H. (1999). Activation of RhoA by lysophosphatidic acid and Galpha12/13 subunits in neuronal cells: induction of neurite retraction. *Mol. Biol. Cell 10*, 1851-7.

Kumagai, N., Morii, N., Fujisawa, K., Nemoto, Y., and Narumiya, S. (1993). ADP-ribosylation of rho p21 inhibits lysophosphatidic acid-induced protein tyrosine phosphorylation and phosphatidylinositol 3-kinase activation in cultured Swiss 3T3 cells. *J. Biol. Chem. 268*, 24535-8.

Kwon, T., Kwon, D. Y., Chun, J., Kim, J. H., and Kang, S. S. (2000). Akt protein kinase inhibits Rac1-GTP binding through phosphorylation at serine 71 of Rac1. *J. Biol. Chem. 275*, 423-8

Lamarche, N., Tapon, N., Stowers, L., Burbelo, P. D., Aspenström, P., Bridges, T., Chant, J., and Hall, A. (1996). Rac and Cdc42 induce actin polymerization and G1 cell cycle progression independently of p65PAK and the JNK/SAPK MAP kinase cascade. *Cell 87*, 519-29.

Lammers, M., Meyer, S., Kühlmann, D., and Wittinghofer, A. (2008). Specificity of interactions between mDia isoforms and Rho proteins. *J. Biol. Chem. 283*, 35236-46.

Lane, J., Martin, T. A., Watkins, G., Mansel, R. E., and Jiang, W. G. (2008). The expression and prognostic value of ROCK I and ROCK II and their role in human breast cancer. *Int. J. Oncol. 33*, 585-93.

Laufs, U., and Liao, J. K. (1998). Post-transcriptional regulation of endothelial nitric oxide synthase mRNA stability by Rho GTPase. *J. Biol. Chem. 273*, 24266-71.

Lee, M., You, H. J., Cho, S. H., Woo, C. H., Yoo, M. H., Joe, E. H., and Kim, J. H. (2002). Implication of the small GTPase Rac1 in the generation of reactive oxygen species in response to beta-amyloid in C6 astroglioma cells. *Biochem.. J 366*, 937-43.

Lee, M. J., Van Brocklyn, J. R., Thangada, S., Liu, C. H., Hand, A. R., Menzeleev, R., Spiegel, S., and Hla, T. (1998). Sphingosine-1-phosphate as a ligand for the G protein-coupled receptor EDG-1. *Science 279,* 1552-5.

Lim, L., Manser, E., Leung, T., and Hall, C. (1996). Regulation of phosphorylation pathways by p21 GTPases. The p21 Ras-related Rho subfamily and its role in phosphorylation signalling pathways. *Eur. J. Biochem. 242*, 171-85.

Lin, D., Edwards, A. S., Fawcett, J. P., Mbamalu, G., Scott, J. D., and Pawson, T. (2000). A mammalian PAR-3-PAR-6 complex implicated in Cdc42/Rac1 and aPKC signalling and cell polarity. *Nat. Cell Biol.* 2, 540-7.

Lin, R., Cerione, R. A., and Manor, D. (1999). Specific contributions of the small GTPases Rho, Rac, and Cdc42 to Dbl transformation. *J. Biol. Chem. 27*4, 23633-41.

Liu, S., Goldstein, R. H., Scepansky, E. M., and Rosenblatt, M. (2009). Inhibition of rho-associated kinase signaling prevents breast cancer metastasis to human bone. *Cancer Res. 69*, 8742-51.

Liu, X., Choy, E., Hornicek, F. J., Yang, S., Yang, C., Harmon, D., Mankin, H., and Duan, Z. (2011). ROCK1 as a potential therapeutic target in osteosarcoma. *J. Orthop. Res. 29*, 1259-66.

Liu, Y., Wang, Y., Zhang, Y., Miao, Y., Zhao, Y., Zhang, P. X., Jiang, G. Y., Zhang, J. Y., Han, Y., Lin, X. Y., Yang, L. H., Li, Q. C., Zhao, C., and Wang, E. H. (2009). Abnormal expression of p120-catenin, E-cadherin, and small GTPases is significantly associated with malignant phenotype of human lung cancer. *Lung Cancer 63*, 375-82.

Loirand, G., Guérin, P., and Pacaud, P. (2006). Rho kinases in cardiovascular physiology and pathophysiology. *Circ. Res. 98*, 322-34.

Lozano, E., Frasa, M. A., Smolarczyk, K., Knaus, U. G., and Braga, V. M. (2008). PAK is required for the disruption of E-cadherin adhesion by the small GTPase Rac. *J. Cell. Sci. 121*, 933-8.

Longo, F. M., and Massa, S. M. (2008). Small molecule modulation of p75 neurotrophin receptor functions. *CNS Neurol. Disord. Drug Targets 7*, 63-70.

Lu, Q., Longo, F. M., Zhou, H., Massa, S. M., and Chen, Y. H. (2009). Signaling through Rho GTPase pathway as viable drug target. *Curr. Med. Chem. 16*, 1355-65.

Ma, L., Rohatgi, R., and Kirschner, M. W. (1998). The Arp2/3 complex mediates actin polymerization induced by the small GTP-binding protein Cdc42. *Proc. Natl. Acad. Sci. U.S.A. 95,* 15362-7.

Machesky, L. M., and Insall, R. H. (1998). Scar1 and the related Wiskott-Aldrich syndrome protein, WASP, regulate the actin cytoskeleton through the Arp2/3 complex. *Curr. Biol. 8*, 1347-56.

Madaule, P., and Axel, R. (1985). A novel ras-related gene family. *Cell 41*, 31-40.

Maekawa, M., Ishizaki, T., Boku, S., Watanabe, N., Fujita, A., Iwamatsu, A., Obinata, T., Ohashi, K., Mizuno, K., and Narumiya, S. (1999). Signaling from Rho to the actin cytoskeleton through protein kinases ROCK and LIM-kinase. *Science 285*, 895-8.

Maillet, M., Lynch, J. M., Sanna, B., York, A. J., Zheng, Y., and Molkentin, J. D. (2009). Cdc42 is an antihypertrophic molecular switch in the mouse heart. *J. Clin. Invest. 119*, 3079-88.

Mallat, Z., Gojova, A., Sauzeau, V., Brun, V., Silvestre, J. S., Esposito, B., Merval, R., Groux, H., Loirand, G., and Tedgui, A. (2003). Rho-associated protein kinase contributes to early atherosclerotic lesion formation in mice. *Circ. Res. 93*, 884-8.

Malosio, M. L., Gilardelli, D., Paris, S., Albertinazzi, C., and de Curtis, I. (1997). Differential expression of distinct members of Rho family GTP-binding proteins during neuronal development: identification of Rac1B, a new neural-specific member of the family. *J. Neurosci. 17*, 6717-28.

Massa, S. M., Xie, Y., and Longo, F. M. (2002). Alzheimer's therapeutics: neurotrophin small molecule mimetics. *J. Mol. Neurosci. 19*, 107-11.

Massa, S. M., Xie, Y., Yang, T., Harrington, A. W., Kim, M. L., Yoon, S. O., Kraemer, R., Moore, L. A., Hempstead, B. L., and Longo, F. M. (2006). Small, nonpeptide p75NTR ligands induce survival signaling and inhibit proNGF-induced death. *J. Neurosci. 26*, 5288-300.

Masumoto, A., Hirooka, Y., Shimokawa, H., Hironaga, K., Setoguchi, S., and Takeshita, A. (2001). Possible involvement of Rho-kinase in the pathogenesis of hypertension in humans. *Hypertension 38*, 1307-10.

Matsui, T., Amano, M., Yamamoto, T., Chihara, K., Nakafuku, M., Ito, M., Nakano, T., Okawa, K., Iwamatsu, A., and Kaibuchi, K. (1996). Rho-associated kinase, a novel serine/threonine kinase, as a putative target for small GTP binding protein Rho. *EMBO J. 15*, 2208-16.

Matsui, T., Maeda, M., Doi, Y., Yonemura, S., Amano, M., Kaibuchi, K., Tsukita, S., and Tsukita, S. (1998). Rho-kinase phosphorylates COOH-terminal threonines of ezrin/radixin/moesin (ERM) proteins and regulates their head-to-tail association. *J. Cell Biol. 140*, 647-57.

McDonald, E. S., Randon, K. R., Knight, A., and Windebank, A. J. (2005). Cisplatin preferentially binds to DNA in dorsal root ganglion neurons in vitro and in vivo: a potential mechanism for neurotoxicity. *Neurobiol. Dis. 18*, 305-13.

McKerracher, L., David, S., Jackson, D. L., Kottis, V., Dunn, R. J., and Braun, P. E. (1994). Identification of myelin-associated glycoprotein as a major myelin-derived inhibitor of neurite growth. *Neuron 13*, 805-11.

McWhinney, S. R., Goldberg, R. M., and McLeod, H. L. (2009). Platinum neurotoxicity pharmacogenetics. *Mol. Cancer Ther. 8*, 10-16.

Michaelson, D., Silletti, J., Murphy, G., D'Eustachio, P., Rush, M., and Philips, M. R. (2001a). Differential localization of Rho GTPases in live cells: regulation by hypervariable regions and RhoGDI binding. *J. Cell Biol. 152*, 111-26.

Miki, H., Yamaguchi, H., Suetsugu, S., and Takenawa, T. (2000). IRSp53 is an essential intermediate between Rac and WAVE in the regulation of membrane ruffling. *Nature 408*, 732-5.

Minard, M. E., Kim, L. S., Price, J. E., and Gallick, G. E. (2004). The role of the guanine nucleotide exchange factor Tiam1 in cellular migration, invasion, adhesion and tumor progression. *Breast Cancer Res. Treat. 84*, 21-32.

Mizuarai, S., Yamanaka, K., and Kotani, H. (2006). Mutant p53 induces the GEF-H1 oncogene, a guanine nucleotide exchange factor-H1 for RhoA, resulting in accelerated cell proliferation in tumor cells. *Cancer Res. 66*, 6319-26.

Moriki, N., Ito, M., Seko, T., Kureishi, Y., Okamoto, R., Nakakuki, T., Kongo, M., Isaka, N., Kaibuchi, K., and Nakano, T. (2004). RhoA activation in vascular smooth muscle cells from stroke-prone spontaneously hypertensive rats. *Hypertens. Res. 27*, 263-70.

Moskwa, P., Paclet, M. H., Dagher, M. C., and Ligeti, E. (2005). Autoinhibition of p50 Rho GTPase-activating protein (GAP) is released by prenylated small GTPases. *J. Biol. Chem. 280*, 6716-20.

Mukai, Y., Shimokawa, H., Matoba, T., Kandabashi, T., Satoh, S., Hiroki, J., Kaibuchi, K., and Takeshita, A. (2001). Involvement of Rho-kinase in hypertensive vascular disease: a novel therapeutic target in hypertension. *FASEB J. 15*, 1062-4.

Nagumo, H., Sasaki, Y., Ono, Y., Okamoto, H., Seto, M., and Takuwa, Y. (2000). Rho kinase inhibitor HA-1077 prevents Rho-mediated myosin phosphatase inhibition in smooth muscle cells. *Am. J. Physiol., Cell Physiol. 278*, C57-65.

Nakamura, N., Rabouille, C., Watson, R., Nilsson, T., Hui, N., Slusarewicz, P., Kreis, T. E., and Warren, G. (1995). Characterization of a cis-Golgi matrix protein, GM130. *J. Cell Biol. 131*, 1715-26.

Nakayama, A. Y., Harms, M. B., and Luo, L. (2000). Small GTPases Rac and Rho in the maintenance of dendritic spines and branches in hippocampal pyramidal neurons. *J. Neurosci. 20*, 5329-38.

Narumiya, S., Ishizaki, T., and Uehata, M. (2000). Use and properties of ROCK-specific inhibitor Y-27632. *Meth. Enzymol. 325*, 273-84.

Nemethova, M., Auinger, S., and Small, J. V. (2008). Building the actin cytoskeleton: filopodia contribute to the construction of contractile bundles in the lamella. *J. Cell Biol. 180*, 1233-44.

Nimnual, A. S., Taylor, L. J., and Bar-Sagi, D. (2003). Redox-dependent downregulation of Rho by Rac. *Nat. Cell Biol. 5*, 236-41.

Nobes, C. D., and Hall, A. (1995). Rho, rac and cdc42 GTPases: regulators of actin structures, cell adhesion and motility. *Biochem. Soc. Trans. 23*, 456-9.

Nohria, A., Grunert, M. E., Rikitake, Y., Noma, K., Prsic, A., Ganz, P., Liao, J. K., and Creager, M. A. (2006). Rho kinase inhibition improves endothelial function in human subjects with coronary artery disease. *Circ. Res. 99*, 1426-32.

Noritake, J., Fukata, M., Sato, K., Nakagawa, M., Watanabe, T., Izumi, N., Wang, S., Fukata, Y., and Kaibuchi, K. (2004). Positive role of IQGAP1, an effector of Rac1, in actin-meshwork formation at sites of cell-cell contact. *Mol. Biol. Cell 15*, 1065-76.

Ohta, Y., Hartwig, J. H., and Stossel, T. P. (2006). FilGAP, a Rho- and ROCK-regulated GAP for Rac binds filamin A to control actin remodelling. *Nat. Cell Biol. 8*, 803-14.

Ohta, T., Takahashi, T., Shibuya, T., Amita, M., Henmi, N., Takahashi, K., and Kurachi, H. (2012). Inhibition of the Rho/ROCK pathway enhances the efficacy of cisplatin through the blockage of hypoxia-inducible factor-1a in human ovarian cancer cells. *Cancer Biol. Ther. 13*, 25-33.

Oliver, T. G., Mercer, K. L., Sayles, L. C., Burke, J. R., Mendus, D., Lovejoy, K. S., Cheng, M. H., Subramanian, A., Mu, D., Powers, S., et al. (2010). Chronic cisplatin treatment promotes enhanced damage repair and tumor progression in a mouse model of lung cancer. *Genes Dev. 24*, 837-52.

Pace, A., Carpano, S., and Galie, E. (2007). Vitamin E in the neuroprotection of cisplatin induced peripheral neurotoxicity and ototoxicity. *J. Clin. Oncol. 25*, 9114.

Pace, A., Giannarelli, D., Galiè, E., Savarese, A., Carpano, S., Della Giulia, M., Pozzi, A., Silvani, A., Gaviani, P., Scaioli, V., Jandolo, B., Bove, L., and Cognetti, F (2010). Vitamin E neuroprotection for cisplatin neuropathy: a randomized, placebo-controlled trial. *Neurology 74*, 762-6.

Pace, A., Savarese, A., Picardo, M., Maresca, V., Pacetti, U., Del Monte, G., Biroccio, A., Leonetti, C., Jandolo, B., Cognetti, F., Jandolo, B., Bove, L., and Cognetti, F. (2003). Neuroprotective effect of vitamin E supplementation in patients treated with cisplatin chemotherapy. *J. Clin. Oncol. 21*, 927-31.

Pachman, D. R., Barton, D. L., Watson, J. C., and Loprinzi, C. L. (2011). Chemotherapy-induced peripheral neuropathy: prevention and treatment. *Clin. Pharmacol. Ther. 90*, 377-87.

Park, S. B., Krishnan, A. V., Lin, C. S., Goldstein, D., Friedlander, M., and Kiernan, M. C. (2008). Mechanisms underlying chemotherapy-induced neurotoxicity and the potential for neuroprotective strategies. *Curr. Med. Chem. 15,* 3081-94.

Pasteris, N. G., Cadle, A., Logie, L. J., Porteous, M. E., Schwartz, C. E., Stevenson, R. E., Glover, T. W., Wilroy, R. S., and Gorski, J. L. (1994). Isolation and characterization of the faciogenital dysplasia (Aarskog-Scott syndrome) gene: a putative Rho/Rac guanine nucleotide exchange factor. *Cell 79*, 669-78.

Pelish, H. E., Ciesla, W., Tanaka, N., Reddy, K., Shair, M. D., Kirchhausen, T., and Lencer, W. I. (2006). The Cdc42 inhibitor secramine B prevents cAMP-induced K+ conductance in intestinal epithelial cells. *Biochem. Pharmacol. 71*, 1720-6.

Pelish, H. E., Peterson, J. R., Salvarezza, S. B., Rodriguez-Boulan, E., Chen, J. L., Stamnes, M., Macia, E., Feng, Y., Shair, M. D., and Kirchhausen, T. (2006). Secramine inhibits Cdc42-dependent functions in cells and Cdc42 activation in vitro. *Nat. Chem. Biol. 2*, 39-46.

Peterson, J. R., Lebensohn, A. M., Pelish, H. E., and Kirschner, M. W. (2006). Biochemical suppression of small-molecule inhibitors: a strategy to identify inhibitor targets and signaling pathway components. *Chem. Biol. 13*, 443-52.

Qiu, R. G., Abo, A., and Steven Martin, G. (2000). A human homolog of the C. elegans polarity determinant Par-6 links Rac and Cdc42 to PKCzeta signaling and cell transformation. *Curr. Biol. 10*, 697-707.

Redowicz, M. J. (1999). Rho-associated kinase: involvement in the cytoskeleton regulation. *Arch. Biochem. Biophys. 364*, 122-4.

Rekhter, M., Chandrasekhar, K., Gifford-Moore, D., Huang, X. D., Rutherford, P., Hanson, J., and Kauffman, R. (2007). Immunohistochemical analysis of target proteins of Rho-kinase in a mouse model of accelerated atherosclerosis. *Exp. Clin. Cardiol. 12*, 169-74.

Reuther, G. W., Lambert, Q. T., Booden, M. A., Wennerberg, K., Becknell, B., Marcucci, G., Sondek, J., Caligiuri, M. A., and Der, C. J. (2001). Leukemia-associated Rho guanine nucleotide exchange factor, a Dbl family protein found mutated in leukemia, causes transformation by activation of RhoA. *J. Biol. Chem. 276*, 27145-51.

Ridley, A. J. (2006). Rho GTPases and actin dynamics in membrane protrusions and vesicle trafficking. *Trends Cell Biol. 16*, 522-9.

Ridley, A. J., and Hall, A. (1992). The small GTP-binding protein rho regulates the assembly of focal adhesions and actin stress fibers in response to growth factors. *Cell 70*, 389-99.

Ridley, A. J., Paterson, H. F., Johnston, C. L., Diekmann, D., and Hall, A. (1992). The small GTP-binding protein rac regulates growth factor-induced membrane ruffling. *Cell 70*, 401-10.

Ridley, A. J., Schwartz, M. A., Burridge, K., Firtel, R. A., Ginsberg, M. H., Borisy, G., Parsons, J. T., and Horwitz, A. R. (2003). Cell migration: integrating signals from front to back. *Science 302*, 1704-9.

Rihet, S., Vielh, P., Camonis, J., Goud, B., Chevillard, S., and de Gunzburg, J. (2001). Mutation status of genes encoding RhoA, Rac1, and Cdc42 GTPases in a panel of invasive human colorectal and breast tumors. *J. Cancer Res. Clin. Oncol. 127*, 733-8.

Rohatgi, R., Ma, L., Miki, H., Lopez, M., Kirchhausen, T., Takenawa, T., and Kirschner, M. W. (1999). The interaction between N-WASP and the Arp2/3 complex links Cdc42-dependent signals to actin assembly. *Cell 97*, 221-31.

Rosenberg, B., VanCamp, L., and Krigas, T. (1965). Inhibition of cell division is Escherichia Coli by electrolysis products from a platinum electrode. *Nature 205*, 698-9.

Rosenfeldt, H., Castellone, M. D., Randazzo, P. A., and Gutkind, J. S. (2006). Rac inhibits thrombin-induced Rho activation: evidence of a Pak-dependent GTPase crosstalk. *J. Mol. Signal. 1*, 8.

Routhier, A., Astuccio, M., Lahey, D., Monfredo, N., Johnson, A., Callahan, W., Partington, A., Fellows, K., Ouellette, L., Zhidro, S., Goodrow, C., Smith, A., and Ka, S. (2010). Pharmacological inhibition of Rho-kinase signaling with Y-27632 blocks melanoma tumor growth. *Oncol. Rep. 23,* 861-7.

Rushton, W. A. (1951). A theory of the effects of fibre size in medullated nerve. *J. Physiol. (Lond.) 115*, 101-22.

Sander, E. E., ten Klooster, J. P., van Delft, S., van der Kammen, R. A., and Collard, J. G. (1999). Rac downregulates Rho activity: reciprocal balance between both GTPases determines cellular morphology and migratory behavior. *J. Cell Biol. 147*, 1009-22.

Sawada, N., Itoh, H., Yamashita, J., Doi, K., Inoue, M., Masatsugu, K., Fukunaga, Y., Sakaguchi, S., Sone, M., Yamahara, K., Yurugi, T., and Nakao, K. (2001). cGMP-dependent protein kinase phosphorylates and inactivates RhoA. *Biochem. Biophys. Res. Commun. 280*, 798-805.

Schloss, J. M., Colosimo, M., Airey, C., Masci, P. P., Linnane, A. W., and Vitetta, L. (2013). Nutraceuticals and chemotherapy induced peripheral neuropathy (CIPN): A systematic review. *Clin. Nutr.* In Press, http://dx.doi.org/10.1016/j.clnu.2013.04.007.

Schnelzer, A., Prechtel, D., Knaus, U., Dehne, K., Gerhard, M., Graeff, H., Harbeck, N., Schmitt, M., and Lengyel, E. (2000). Rac1 in human breast cancer: overexpression, mutation analysis, and characterization of a new isoform, Rac1b. *Oncogene 19*, 3013-20.

Schoenwaelder, S. M., Petch, L. A., Williamson, D., Shen, R., Feng, G. S., and Burridge, K. (2000). The protein tyrosine phosphatase SHP2 regulates RhoA activity. *Curr. Biol. 10*, 1523-6.

Shafee, N., Smith, C. R., Wei, S., Kim, Y., Mills, G. B., Hortobagyi, G. N., Stanbridge, E. J., and Lee, E. Y. (2008). Cancer stem cells contribute to cisplatin resistance in Brca1/p53-mediated mouse mammary tumors. *Cancer Res. 68*, 3243-50.

Shibata, S., Mu, S., Kawarazaki, H., Muraoka, K., Ishizawa, K., Yoshida, S., Kawarazaki, W., Takeuchi, M., Ayuzawa, N., Miyoshi, J., Takai, Y., and Ishikawa, A. (2011). Rac1 GTPase in rodent kidneys is essential for salt-sensitive hypertension via a mineralocorticoid receptor-dependent pathway. *J. Clin. Invest. 121*, 3233-43.

Shibuya, M., Suzuki, Y., Sugita, K., Saito, I., Sasaki, T., Takakura, K., Nagata, I., Kikuchi, H., Takemae, T., and Hidaka, H. (1992). Effect of AT877 on cerebral vasospasm after aneurysmal subarachnoid hemorrhage. Results of a prospective placebo-controlled double-blind trial. *J. Neurosurg. 76*, 571-7.

Shimizu, Y., Thumkeo, D., Keel, J., Ishizaki, T., Oshima, H., Oshima, M., Noda, Y., Matsumura, F., Taketo, M. M., and Narumiya, S. (2005). ROCK-I regulates closure of the eyelids and ventral body wall by inducing assembly of actomyosin bundles. *J. Cell Biol. 168*, 941-53.

Shimokawa, H., Morishige, K., Miyata, K., Kandabashi, T., Eto, Y., Ikegaki, I., Asano, T., Kaibuchi, K., and Takeshita, A. (2001). Long-term inhibition of Rho-kinase induces a regression of arteriosclerotic coronary lesions in a porcine model in vivo. *Cardiovasc. Res. 51*, 169-77.

Singh, A., Karnoub, A. E., Palmby, T. R., Lengyel, E., Sondek, J., and Der, C. J. (2004). Rac1b, a tumor associated, constitutively active Rac1 splice variant, promotes cellular transformation. *Oncogene 23*, 9369-80.

Sinha, S., and Yang, W. (2008). Cellular signaling for activation of Rho GTPase Cdc42. *Cell. Signal. 20*, 1927-34.

Smith, W. J., Hamel, B., Yohe, M. E., Sondek, J., Cerione, R. A., and Snyder, J. T. (2005). A Cdc42 mutant specifically activated by intersectin. *Biochemistry 44*, 13282-90.

Smyth, J. F., Bowman, A., and Perren, T. (1997). Glutathione reduces the toxicity and improves quality of life of women diagnosed with ovarian cancer treated with cisplatin: results of a double-blind, randomised trial. *Ann. Oncol. 8,* 569-73.

Snyder, J. T., Worthylake, D. K., Rossman, K. L., Betts, L., Pruitt, W. M., Siderovski, D. P., Der, C. J., and Sondek, J. (2002). Structural basis for the selective activation of Rho GTPases by Dbl exchange factors. *Nat. Struct. Biol. 9*, 468-75.

Song, X. Y., Zhou, F. H., Zhong, J. H., Wu, L. L., and Zhou, X. F. (2006). Knockout of p75(NTR) impairs re-myelination of injured sciatic nerve in mice. *J. Neurochem. 96,* 833-42.

Sordella, R., Jiang, W., Chen, G. C., Curto, M., and Settleman, J. (2003). Modulation of Rho GTPase signaling regulates a switch between adipogenesis and myogenesis. *Cell 113*, 147-58.

Stengel, K., and Zheng, Y. (2011). Cdc42 in oncogenic transformation, invasion, and tumorigenesis. *Cell. Signal. 23*, 1415-1423.

Strumberg, D., Brügge, S., Korn, M. W., Koeppen, S., Ranft, J., Scheiber, G., Reiners, C., Möckel, C., Seeber, S., and Scheulen, M. E. (2002). Evaluation of long-term toxicity in patients after cisplatin-based chemotherapy for non-seminomatous testicular cancer. *Ann. Oncol. 13*, 229-36.

Suetsugu, S., Kurisu, S., Oikawa, T., Yamazaki, D., Oda, A., and Takenawa, T. (2006). Optimization of WAVE2 complex-induced actin polymerization by membrane-bound IRSp53, PIP(3), and Rac. *J. Cell Biol. 173*, 571-85.

Sugihara, K., Nakatsuji, N., Nakamura, K., Nakao, K., Hashimoto, R., Otani, H., Sakagami, H., Kondo, H., Nozawa, S., Aiba, A., Katsuki, M. (1998). Rac1 is required for the formation of three germ layers during gastrulation. O*ncogene 17*, 3427-33.

Suidan, H. S., Nobes, C. D., Hall, A., and Monard, D. (1997). Astrocyte spreading in response to thrombin and lysophosphatidic acid is dependent on the Rho GTPase. *Glia 21*, 244-52.

Sung, J. K., Miao, L., Calvert, J. W., Huang, L., Louis Harkey, H., and Zhang, J. H. (2003). A possible role of RhoA/Rho-kinase in experimental spinal cord injury in rat. *Brain Res. 959*, 29-38.

Suzuki, Y., Yamamoto, M., Wada, H., Ito, M., Nakano, T., Sasaki, Y., Narumiya, S., Shiku, H., and Nishikawa, M. (1999). Agonist-induced regulation of myosin phosphatase activity in human platelets through activation of Rho-kinase. *Blood 93*, 3408-17.

Ta, L. E., Low, P. A., and Windebank, A. J. (2009). Mice with cisplatin and oxaliplatin-induced painful neuropathy develop distinct early responses to thermal stimuli. *Mol. Pain 5*, 9.

Takabe, K., Paugh, S. W., Milstien, S., and Spiegel, S. (2008). "Inside-out" signaling of sphingosine-1-phosphate: therapeutic targets. *Pharmacol. Rev. 60*, 181-95.

Takemoto, M., Sun, J., Hiroki, J., Shimokawa, H., and Liao, J. K. (2002). Rho-kinase mediates hypoxia-induced downregulation of endothelial nitric oxide synthase. *Circulation 106,* 57-62.

Tanenburg, R. J. (2009). Diabetic peripheral neuropathy: Painful or painless. *Hospital Physician 45,* 1-8.

Tatsumi, S., Mabuchi, T., Katano, T., Matsumura, S., Abe, T., Hidaka, H., Suzuki, M., Sasaki, Y., Minami, T., and Ito, S. (2005). Involvement of Rho-kinase in inflammatory and neuropathic pain through phosphorylation of myristoylated alanine-rich C-kinase substrate (MARCKS). *Neuroscience 131*, 491-8.

Tep, C., Lim, T. H., Ko, P. O., Getahun, S., Ryu, J. C., Goettl, V. M., Massa, S. M., Basso, M., Longo, F. M., and Yoon, S. O. (2013). Oral administration of a small molecule targeted to block proNGF binding to p75 promotes myelin sparing and functional recovery after spinal cord injury. *J. Neurosci. 33*, 397-410.

Threadgill, R., Bobb, K., and Ghosh, A. (1997). Regulation of dendritic growth and remodeling by Rho, Rac, and Cdc42. *Neuron 19*, 625-34.

Thumkeo, D., Keel, J., Ishizaki, T., Hirose, M., Nonomura, K., Oshima, H., Oshima, M., Taketo, M. M., and Narumiya, S. (2003). Targeted disruption of the mouse rho-associated kinase 2 gene results in intrauterine growth retardation and fetal death. *Mol. Cell. Biol. 23*, 5043-55.

Thurnherr, T., Benninger, Y., Wu, X., Chrostek, A., Krause, S. M., Nave, K. A., Franklin, R. J., Brakebusch, C., Suter, U., and Relvas, J. B. (2006). Cdc42 and Rac1 signaling are both required for and act synergistically in the correct formation of myelin sheaths in the CNS. *J. Neurosci. 26,* 10110-9.

Torres, E., and Rosen, M. K. (2003). Contingent phosphorylation/dephosphorylation provides a mechanism of molecular memory in WASP. *Mol. Cell 11*, 1215-27.

Torres, E., and Rosen, M. K. (2006). Protein-tyrosine kinase and GTPase signals cooperate to phosphorylate and activate Wiskott-Aldrich syndrome protein (WASP)/neuronal WASP. *J. Biol. Chem. 281,* 3513-20.

Tsang, R. Y., Al-Fayea, T., and Au, H. J. (2009). Cisplatin overdose: toxicities and management. *Drug Safety 32*, 1109-22.

Tucci, M. G., Lucarini, G., Brancorsini, D., Zizzi, A., Pugnaloni, A., Giacchetti, A., Ricotti, G., and Biagini, G. (2007). Involvement of E-cadherin, beta-catenin, Cdc42 and CXCR4 in the progression and prognosis of cutaneous melanoma. *Br. J. Dermatol. 157*, 1212-6.

Uehata, M., Ishizaki, T., Satoh, H., Ono, T., Kawahara, T., Morishita, T., Tamakawa, H., Yamagami, K., Inui, J., Maekawa, M., Narumiya, S. (1997). Calcium sensitization of smooth muscle mediated by a Rho-associated protein kinase in hypertension. *Nature 389*, 990-4.

Vadlamudi, R. K., Adam, L., Wang, R. A., Mandal, M., Nguyen, D., Sahin, A., Chernoff, J., Hung, M. C., and Kumar, R. (2000). Regulatable expression of p21-activated kinase-1 promotes anchorage-independent growth and abnormal organization of mitotic spindles in human epithelial breast cancer cells. *J. Biol. Chem. 275*, 36238-44.

Vadlamudi, R. K., Li, F., Barnes, C. J., Bagheri-Yarmand, R., and Kumar, R. (2004). p41-Arc subunit of human Arp2/3 complex is a p21-activated kinase-1-interacting substrate. *EMBO Rep. 5*, 154-60.

Van Aelst, L., and Cline, H. T. (2004). Rho GTPases and activity-dependent dendrite development. *Curr. Opin. Neurobiol. 14*, 297-304.

van der Hoop, R. G., Vecht, C. J., van der Burg, M. E., Elderson, A., Boogerd, W., Heimans, J. J., Vries, E. P., van Houwelingen, J. C., Jennekens, F. G., and Gispen, W. H. (1990). Prevention of cisplatin neurotoxicity with an ACTH(4-9) analogue in patients with ovarian cancer. *N. Engl. J. Med. 322,* 89-94.

van der Hoop, R. G., van der Burg, M. E., ten Bokkel Huinink, W. W., van Houwelingen, C., and Neijt, J. P. (1990). Incidence of neuropathy in 395 patients with ovarian cancer treated with or without cisplatin. *Cancer 66*, 1697-702

Vaughan, E. M., Miller, A. L., Yu, H. Y., and Bement, W. M. (2011). Control of local Rho GTPase crosstalk by Abr. *Curr. Biol. 21,* 270-7.

Verdú, E., Vilches, J. J., Rodríguez, F. J., Ceballos, D., Valero, A., and Navarro, X. (1999). Physiological and immunohistochemical characterization of cisplatin-induced neuropathy in mice. *Muscle Nerve 22*, 329-40.

Vega, F. M., and Ridley, A. J. (2008). Rho GTPases in cancer cell biology. *FEBS Lett. 582*, 2093-101.

Vishnubhotla, R., Sun, S., Huq, J., Bulic, M., Ramesh, A., Guzman, G., Cho, M., and Glover, S. C. (2007). ROCK-II mediates colon cancer invasion via regulation of MMP-2 and MMP-13 at the site of invadopodia as revealed by multiphoton imaging. *Lab. Invest. 87*, 1149-58.

Walters, C. E., Pryce, G., Hankey, D. J., Sebti, S. M., Hamilton, A. D., Baker, D., Greenwood, J., and Adamson, P. (2002). Inhibition of Rho GTPases with protein prenyltransferase inhibitors prevents leukocyte recruitment to the central nervous system and attenuates clinical signs of disease in an animal model of multiple sclerosis. *J. Immunol. 168*, 4087-94.

Wang, K. C., Koprivica, V., Kim, J. A., Sivasankaran, R., Guo, Y., Neve, R. L., and He, Z. (2002). Oligodendrocyte-myelin glycoprotein is a Nogo receptor ligand that inhibits neurite outgrowth. *Nature 417*, 941-4.

Wang, L., Yang, L., Filippi, M. D., Williams, D. A., and Zheng, Y. (2006). Genetic deletion of Cdc42GAP reveals a role of Cdc42 in erythropoiesis and hematopoietic stem/progenitor cell survival, adhesion, and engraftment. *Blood 107*, 98-105.

Wang, P. L., Niidome, T., Akaike, A., Kihara, T., and Sugimoto, H. (2009). Rac1 inhibition negatively regulates transcriptional activity of the amyloid precursor protein gene. *J. Neurosci. Res. 87*, 2105-14.

Watabe-Uchida, M., Govek, E. E., and Van Aelst, L. (2006). Regulators of Rho GTPases in neuronal development. *J. Neurosci. 26*, 10633-5.

Wen, Y., Eng, C. H., Schmoranzer, J., Cabrera-Poch, N., Morris, E. J., Chen, M., Wallar, B. J., Alberts, A. S., and Gundersen, G. G. (2004). EB1 and APC bind to mDia to stabilize microtubules downstream of Rho and promote cell migration. *Nat. Cell Biol. 6*, 820-30.

Wennerberg, K., and Der, C. J. (2004). Rho-family GTPases: it's not only Rac and Rho (and I like it). *J. Cell Sci. 117*, 1301-12.

Wong, C. C., Wong, C. M., Tung, E. K., Man, K., and Ng, I. O. (2009). Rho-kinase 2 is frequently overexpressed in hepatocellular carcinoma and involved in tumor invasion. *Hepatology 49*, 1583-94.

Wong, K., Ren, X. R., Huang, Y. Z., Xie, Y., Liu, G., Saito, H., Tang, H., Wen, L., Brady-Kalnay, S. M., Mei, L., Wu, J. Y., Xiong, W. C., and Rao, Y. (2001). Signal transduction in neuronal migration: roles of GTPase activating proteins and the small GTPase Cdc42 in the Slit-Robo pathway. *Cell 107*, 209-21.

Wozniak, K., and Blasiak, J. (2002). Recognition and repair of DNA-cisplatin adducts. *Acta Biochim. Pol. 49*, 583-96.

Wu, D. J., Xu, J. Z., Wu, Y. J., Jean-Charles, L., Xiao, B., Gao, P. J., and Zhu, D. L. (2009). Effects of fasudil on early atherosclerotic plaque formation and established lesion progression in apolipoprotein E-knockout mice. *Atherosclerosis 207*, 68-73.

Yamaguchi, Y., Katoh, H., Yasui, H., Mori, K., and Negishi, M. (2001). RhoA inhibits the nerve growth factor-induced Rac1 activation through Rho-associated kinase-dependent pathway. *J. Biol. Chem. 276*, 18977-83.

Yamashita, T., and Tohyama, M. (2003). The p75 receptor acts as a displacement factor that releases Rho from Rho-GDI. *Nat. Neurosci. 6*, 461-7.

Yang, T., Knowles, J. K., Lu, Q., Zhang, H., Arancio, O., Moore, L. A., Chang, T., Wang, Q., Andreasson, K., Rajadas, J., Fuller, G. G., Xie, Y.,Massa, S. M. and Longo, F. (2008). Small molecule, non-peptide p75 ligands inhibit Abeta-induced neurodegeneration and synaptic impairment. *PLoS ONE 3*, e3604

Yang, L., Wang, L., and Zheng, Y. (2006). Gene targeting of Cdc42 and Cdc42GAP affirms the critical involvement of Cdc42 in filopodia induction, directed migration, and proliferation in primary mouse embryonic fibroblasts. *Mol. Biol. Cell 17*, 4675-85.

Yasuda, S., Taniguchi, H., Oceguera-Yanez, F., Ando, Y., Watanabe, S., Monypenny, J., and Narumiya, S. (2006). An essential role of Cdc42-like GTPases in mitosis of HeLa cells. *FEBS Lett. 580*, 3375-80.

Yoshida, T., Zhang, Y., Rivera Rosado, L. A., Chen, J., Khan, T., Moon, S. Y., and Zhang, B. (2010). Blockade of Rac1 activity induces G1 cell cycle arrest or apoptosis in breast cancer cells through downregulation of cyclin D1, survivin, and X-linked inhibitor of apoptosis protein. *Mol. Cancer Ther. 9,* 1657-68.

Yuan, B. Z., Zhou, X., Durkin, M. E., Zimonjic, D. B., Gumundsdottir, K., Eyfjord, J. E., Thorgeirsson, S. S., and Popescu, N. C. (2003). DLC-1 gene inhibits human breast cancer cell growth and in vivo tumorigenicity. *Oncogene 22*, 445-50.

Zheng, Y., Fischer, D. J., Santos, M. F., Tigyi, G., Pasteris, N. G., Gorski, J. L., and Xu, Y. (1996). The faciogenital dysplasia gene product FGD1 functions as a Cdc42Hs-specific guanine-nucleotide exchange factor. *J. Biol. Chem. 271,* 33169-72.

Zhou, H., Wang, D. A., Baldini, L., Ennis, E., Jain, R., Carie, A., Sebti, S. M., and Hamilton, A. D. (2006). Structure-activity studies on a library of potent calix[4]arene-based PDGF antagonists that inhibit PDGF-stimulated PDGFR tyrosine phosphorylation. *Org. Biomol. Chem. 4*, 2376-86.

Zhou, Y., Su, Y., Li, B., Liu, F., Ryder, J. W., Wu, X., Gonzalez-DeWhitt, P. A., Gelfanova, V., Hale, J. E., May, P. C., Paul, S. M., and Ni, B. (2003). Nonsteroidal anti-inflammatory drugs can lower amyloidogenic Abeta42 by inhibiting Rho. *Science 302*, 1215-7.

Zhu, X., Raina, A. K., Boux, H., Simmons, Z. L., Takeda, A., and Smith, M. A. (2000). Activation of oncogenic pathways in degenerating neurons in Alzheimer disease. *Int. J. Dev. Neurosci. 18*, 433-7.

Zigmond, S. H. (2004). Formin-induced nucleation of actin filaments. *Curr. Opin. Cell Biol. 16*, 99-105.

Zuo, Y., Shields, S. K., and Chakraborty, C. (2006). Enhanced intrinsic migration of aggressive breast cancer cells by inhibition of Rac1 GTPase. *Biochem. Biophys. Res. Commun. 351*, 361-7.

Zwelling, L. A., and Kohn, K. W. (1979). Mechanism of action of cis-dichlorodiammineplatinum(II). *Cancer Treat. Rep. 63*, 1439-44.

APPENDIX A : ANIMAL USE PROTOCOL

East Carolina University

1907-2007 CENTENNIAL

Animal Care and Use Committee
212 Ed Warren Life Sciences Building
East Carolina University
Greenville, NC 27834

252-744-2436 office
252-744-2355 fax

April 26, 2010

Qun Lu, Ph.D.
Department of Anatomy
Brody Building
ECU Brody School of Medicine

Dear Dr. Lu:

Your Animal Use Protocol entitled, "Chemotherapy-Induced Peripheral Neuropathy," (AUP #A174a) was reviewed by this institution's Animal Care and Use Committee on 4/26/10. The following action was taken by the Committee:

"Approved as submitted"

Please contact Dale Aycock at 744-2997 prior to biohazard use

A copy is enclosed for your laboratory files. Please be reminded that all animal procedures must be conducted as described in the approved Animal Use Protocol. Modifications of these procedures cannot be performed without prior approval of the ACUC. The Animal Welfare Act and Public Health Service Guidelines require the ACUC to suspend activities not in accordance with approved procedures and report such activities to the responsible University Official (Vice Chancellor for Health Sciences or Vice Chancellor for Academic Affairs) and appropriate federal Agencies.

Sincerely yours,

Robert G. Carroll, Ph.D.
Chairman, Animal Care and Use Committee

RGC/jd

enclosure

APPENDIX B: PNAS LICENCE TO PUBLISH

PNAS License to Publish

Please complete both sections of this form and fax it to PNAS (202-334-2739). Failure to return the form will delay or prevent publication.

Ms. No. 2011-16051RRR

License to Publish

1. In consideration of publication of the WORK (including but not limited to figures, tables, artwork, abstracts, cover images, or summaries submitted with the WORK) in the Proceedings of the National Academy of Sciences USA (PNAS), the author(s) hereby grants to the National Academy of Sciences (USA) for the full term of copyright and any extensions thereto the sole and exclusive, irrevocable license to publish, reproduce, distribute, transmit, display, store, translate, create derivative works from and otherwise use the Work in any language or in any form, manner, format, or medium now known or hereafter developed without limitation throughout the world, and to permit and/or license others to do any or all of the above. In the event that PNAS decides not to publish the WORK, this license shall be terminated and all rights revert to the author(s).
2. In consideration of publication of the WORK in PNAS, the author(s) also grants to the National Academy of Sciences for the full term of copyright and any extensions thereto all of the same rights provided for in clause 1 above, for the Supplemental Information, but on a nonexclusive basis.
3. Ownership of copyright in the WORK remains with the author(s), and provided that, when reproducing the WORK or extracts from it, the author(s) credit first publication of the WORK in PNAS, the author(s) retains the following nonexclusive rights:
   a. The author(s) reserves the right after publication of the WORK by PNAS, to use all or part of the WORK in compilations or other publications of the author's own works, to use figures and tables created by them and contained in the WORK, and to make copies of all or part of the WORK for the author's use for lectures, classroom instruction, or similar uses.
   b. The author(s) reserves the right to post the WORK (including the PNAS-formatted PDF) after publication in PNAS on the author's web page provided that a link to the article in PNAS Online is included.
   c. The author(s) reserves the right to post and update the WORK on pre-print services such as arXiv provided that PNAS-formatted files (HTML and PDF) are not used and that a link to the WORK in PNAS Online is included.
   d. The author(s) reserves the right to deposit his or her final manuscript in the author(s)'s funding body's archive or designated repository on acceptance for publication by PNAS, provided that a link to the WORK in PNAS Online is included; and, the right to request public access 6 months after print publication or immediately upon publication by PNAS if the author(s) has paid the PNAS open access fee. PNAS automatically deposits the PNAS-formatted version of all papers in PubMed Central.
4. The exclusive license granted to PNAS permits the following: after publication of the WORK by PNAS, third parties are automatically granted permission to use figures and tables created by the author(s) and contained in the WORK for noncommercial use (e.g., not for sale or for commercial advantage).
5. The author(s) warrants that the WORK is original, that it has not been published, that all the facts it contains are true and accurate, that it does not infringe upon any copyright, proprietary, or personal right of any third party, and that permissions have been obtained and are attached for any portions of the WORK owned or controlled by a third party. Each author identified on the manuscript must sign this form. If any author's signature does not appear below, the signing author(s) represents and warrants that he or she signs this license as authorized agent(s) for and on behalf of all the authors and that this license is made on behalf of all the authors. The author(s) shall indemnify the Academy and/or its successors and assigns for any and all claims, costs, and expenses, including attorney's fees, arising out of any breach of this warranty or other representations contained herein.
6. The Author(s) authorize(s) PNAS to take such steps as it considers necessary at its own expense in the Author(s)'s name and on their behalf if it believes that a third party is infringing or is likely to infringe the copyright in the WORK.
7. If the WORK has been prepared by an employee within the scope of his or her employment, the employer reserves the right to make copies of the WORK for its own internal use.

A Small Molecule Targeting Cdc42-Intersectin Interaction Disrupts Golgi Organization and Suppresses Cell Motility
Title of WORK

Amy Friesland 11/28/12
Author's Signature Date

Amy Friesland
Print Name

11/29/12
Author's Signature Date

QUN LU
Print Name

11/29/12
Author's Signature Date

YAN-HUA CHEN
Print Name

Documentation Report:

If any of the following items are pertinent to your paper, we must receive the appropriate documentation or statements before we can publish your paper.

Please check the appropriate boxes and sign below:

- ☐ None of the 3 items below applies to this paper.
- ☐ Structural Coordinate Deposition and Release. Authors of papers reporting new or revised structures must deposit their coordinates in the Protein Data Bank or an equivalent public archive, and the accession numbers must be supplied for publication. You agree, by signing below, that the coordinates will be released when the article is published. A footnote reporting the accession numbers will be added to your paper. You must provide the accession numbers on the page proof.
- ☐ Sequence Database Deposition. Authors of papers reporting new sequences must submit these data to an appropriate database, and the accession numbers must be supplied for publication. A footnote reporting the accession numbers will be added to your paper. You must provide the accession numbers on the page proof.
- ☐ Permission to Print Previously Published Material. If your paper includes material (e.g., figures or tables) that were published previously, whether or not you are an author of the earlier publication, you must provide the previous publisher's permission to republish this material in print and online. We acknowledge that copyright is held by the original publisher. Please state which items were published previously and where:

Author's Signature Date

Print Name

If WORK is a Work Made for Hire and the employer of the author(s) owns the copyright, this license to publish must be signed by an author and an authorized representative of the employer.

Name of Employer

Authorized Signature Date

Title

Name(s) of Employee(s)

Authorized Signature Date

Title

If all authors are U.S. Government employees: I certify that the WORK was written as part of the official duties of the authors as employees of the U.S. Government. On behalf of all authors, I authorize publication of the WORK in PNAS under terms equivalent to those provided for in the license and agree to all of the warranties specified in the license.

Author's Signature Date

Print Name

Author's Signature Date

Print Name